

Conformal Inference for Counterfactuals and Individual Treatment Effects with Experiment Attrition

Xiangyu Song*

April 2, 2026

Abstract

Attrition in survey and field experiments presents a challenge for social science research. Common approaches to deal with this problem – such as complete case analysis, multiple imputation, and weighting methods – rely on strong assumptions that may not hold in practice. This paper introduces a new method that combines recent advances in statistical inference with established tools for handling missing data. The approach produces prediction intervals for treatment effects that are both robust and precise. Evidence from simulation studies shows that the method achieves better coverage and produces narrower intervals than common alternatives. The reanalysis of two recently published experiment studies illustrates how this framework allows researchers to compare treatment effects across participants who remain in the study, those who drop out, and the full sample. Taken together, these results highlight how the proposed approach provides a stronger foundation for causal inference in the presence of attrition.

Keywords: conformal inference, missing data, experiment attrition, causal inference

*Ph.D. student, Department of Political Science, Washington University in St. Louis. xiangyusong@wustl.edu.

1 Introduction

Since the seminal contributions by Neyman and Fisher in the 1920s (Fisher, 1937; Splawa-Neyman, 1990(1923)), the use of randomized experiments (randomized controlled trials) has become a cornerstone for estimating causal effects (Huber, 2012; Imbens, 2024). While rare in the 1970s and 1980s (e.g., LaLonde, 1986), experimental studies have expanded rapidly in the social sciences over the past two decades (Imbens, 2024). Political scientists now routinely employ survey and field experiments, often alongside survey instruments, to evaluate theories and estimate causal effects (e.g., Imai and Strauss, 2011; Kalla and Broockman, 2018). Yet, like all empirical strategies, experiments face threats to validity, particularly attrition (Hausman and Wise, 1979), which complicates inference (Gerber and Green, 2012). In survey experiments, non-response due to attrition prevents observation of outcomes for all participants, while in field experiments attrition reduces sample size and statistical power. When attrition is non-random, it introduces selection bias that undermines theoretical claims. Ignoring attrition and restricting analysis to observed samples generally yields biased and inconsistent estimators (Coppock et al., 2017).

Existing approaches to address attrition each have their own limitations. Some rely on unverifiable assumptions about model specification or data structure, such as sample selection models (Heckman, 1979), instrumental variables (Huber, 2012), and imputation or complete case methods (e.g., Fukumoto, 2022; King et al., 2001; Rubin, 1976). Some reweighting methods, like inverse propensity weighting (IPW) (Horvitz and and Thompson, 1952; Huber, 2012), adjust for missingness using observed observations but do not leverage information from attrited observations and can yield biased estimates when missingness depends on treatment and covariates. Other bounding approaches, like partial identification (Horowitz and Manski, 1998, 2000; Lee, 2009; Coppock et al., 2017), relax these parametric assumptions but are not designed to address the covariate shift problem, where the covariate distribution differs between observed and attrited groups.

In this paper, I propose to leverage conformal inference, a nonparametric and distribution-free method for uncertainty quantification on individual predictions, to construct valid prediction intervals for treatment effects in the presence of attrition. Conformal inference provides a way to quantify uncertainty without relying on strong parametric assumptions on the data generating process (DGP). Intuitively, the method works by comparing the model's predictions to the actual observed outcomes. By assessing how well the model's predictions align with the observed values, it determines a range (or interval) around each prediction that will contain the true value with

a user-specified level of confidence (e.g., 90% or 95%). The advantage of conformal inference is that, regardless of the complexity of the model or the distribution of the data, it guarantees coverage: if we ask for 95% coverage, then, on average, about 95% of the prediction intervals will indeed contain the true outcome. This property makes conformal inference particularly appealing for causal inference, where we often want reliable, distribution-free uncertainty quantification for treatment effects at the individual or subgroup level.

Recent advances in the conformal inference literature have demonstrated its potential in addressing causal inference problems under attrition. [Lei and Candès \(2021\)](#) provide a theoretical framework for using conformal inference to construct prediction intervals for counterfactuals and individual treatment effect (ITE). However, their method is not designed specifically to handle missing data problems induced by attrition, as it relies on relatively strong missing data assumptions, and the resulting prediction intervals can be overly wide (non-informative) in practice. Building on this work, [Yang et al. \(2024\)](#) and [Gao et al. \(2025\)](#) introduce approaches that lead to more accurate and efficient prediction intervals. Rather than using the potential outcome framework, [Yang et al. \(2024\)](#) reformulate the covariate shift problem as a missing data problem, and provide a doubly robust and computationally efficient method for constructing prediction intervals for estimands of interest. However, they do not directly tackle the issue of missing data due to attrition. This is why one of the core motivations of this paper is to formally address missing data problems induced by experimental attrition.

This paper makes three contributions to the literature. First, it introduces conformal inference as a useful framework for political science research, demonstrating how it can provide reliable measures of uncertainty for causal estimands such as treatment effects and counterfactuals. By focusing on distribution-free and model-agnostic inference, this approach helps researchers quantify uncertainty even when conventional statistical assumptions may not hold. Second, building on [Lei and Candès \(2021\)](#) and [Gao et al. \(2025\)](#), this paper combines conformal inference with flexible estimators to construct prediction intervals for treatment effects among participants who drop out of experiments. It offers a general and practical way to handle missing data problems caused by experimental attrition under the potential outcome framework. Third, this paper presents one of the most comprehensive evaluations of how conformal inference performs across different predictive models, underscoring both its strengths and its potential limitations for empirical applications in social science researches.

I demonstrate the advantages of my proposed approach to deal with experimental attrition

in two ways. First, through extensive Monte Carlo (MC) simulations, this paper shows that the proposed method can construct prediction intervals for the treatment effects in the attrition group with both valid coverage and narrower interval length. It also outperforms existing parametric and nonparametric methods in terms of empirical coverage and average interval length. Second, by reanalyzing two recently published experimental studies, this paper demonstrates how the proposed method can be applied in practice to compare treatment effects across participants who remain in the study, those who drop out, and the full sample. In addition, it enables researchers to aggregate individual-level treatment effects to estimate average treatment effects for different subpopulations. Overall, compared with current methods, the proposed approach produces more precise and robust prediction intervals for the causal estimands of interest.

The rest of the paper is organized as follows. Section 2 goes over the current approaches to deal with missing data problem. Section 3 introduces the problem setup. Section 4 provides a brief review of conformal inference and covariate shift problem. Section 5 discusses the conformal inference method for missing data problem induced by experimental attrition. Section 6 presents the proposed method for constructing prediction intervals for counterfactuals and ITE in the presence of experimental attrition. Section 7 evaluates the performance of the proposed method through extensive MC simulations. Section 8 illustrates the application of the proposed method by the reanalysis of two recently published experimental studies. Section 9 concludes.

2 Current Approaches to Deal with Attrition in Experimental Settings

Researchers have proposed several remedies to deal with the prevalence of missing data as a result of experimental attrition. The first set of solutions addresses missingness problems due to attrition in the outcome by introducing parametric assumptions (Coppock et al., 2017). For example, sample selection models Heckman (1979), in which outcomes are observed only for a non-randomly subset of units, rely on strong assumptions, including correct specification of the selection process, distribution functions, and exclusion restrictions. Similarly, proponents of instrumental variable approaches as a way to deal with attrition assume that there exists a variable that is related to the missingness but has no direct effect on the outcome Huber (2012). However, such assumptions are hard to verify on theoretical grounds, and valid instruments are hard to find in practice.

A second family of approaches employs (multiple) imputation methods or complete case anal-

ysis (e.g., listwise or pairwise deletion) to correct for potential bias due to missing data (e.g., [Fukumoto, 2022](#); [King et al., 2001](#); [Rubin, 1976](#)). Although not designed to handle causal inference problems directly, we can manipulate these imputation methods to impute the missing potential outcomes and attrited observations. Nevertheless, these methods are also limited to strong assumptions. For example, multiple imputation using Amelia II assumes that the complete data (that is, both observed and unobserved) are multivariate normal and the missingness to be missing at random (MAR). Complete case analysis can cause bias estimates when the missingness does not satisfy missing completely at random (MCAR) or missing at random ([Shin, 2024](#)). Imputation methods are also problematic under missing not at random (MNAR), which violates the ignorability of missingness, or when the covariates are themselves missing ([Coppock et al., 2017](#); [Shin, 2024](#)).

The third line of approach leverages inverse propensity weighting (IPW) to reweight the observations based on observed covariates ([Horvitz and and Thompson, 1952](#); [Huber, 2012](#)). However, IPW only provides treatment effect on the observed group, but as social scientists, we want ATE for all observations, including observed and attrited groups. Also, this IPW approach alone does not resolve the issue of making valid inference on the attrition group - particularly when the attrition is induced by treatment or other covariates. In that case, although IPW can give unbiased treatment effect for observed group, it could still be biased for all observations. Finally, the fourth line of approach tackles the missing data problem through partial identification, for example, nonparametric bounds ([Horowitz and Manski, 1998, 2000](#); [Lee, 2009](#)) and double sampling with worst-case bounds ([Coppock et al., 2017](#)). Although these nonparametric approaches make fewer assumptions, they overlook the potential covariate shift problems, where the covariate distribution differs across attrited and observed groups.

In this paper, I propose to leverage conformal inference, a nonparametric and distribution-free method for uncertainty quantification on individual predictions, to construct valid prediction intervals for treatment effects in the presence of attrition. Compared to current approaches, conformal inference does not rely on parametric assumptions on the data distribution, thus offering a more robust and flexible framework for handling missing data problems induced by experimental attrition. The next two sections provide the problem setup, a brief introduction to conformal inference, and why it can be used to deal with experimental attrition.

3 Problem Setup and Notation

Consider the following setup for a randomized experiment with attrition induced by survey non-response or experiment dropout. We adopt the potential outcome framework (Splawa-Neyman, 1990(1923); Rubin, 1974). Let $D_i \in \{0, 1\}$ be a binary treatment indicator, where $D_i = 1$ if unit i is treated and equals 0 otherwise (control), let $(Y_i(1), Y_i(0))$ be the potential outcomes for unit i , and X_i the vector including k pretreatment covariates. In a similar way, we define $D, Y(d)$, and X without subscripts to be the population counterparts. We first assume that the data are independently and identically distributed (i.i.d.):

$$(Y_i(0), Y_i(1), D_i, X_i) \stackrel{\text{i.i.d.}}{\sim} (Y(1), Y(0), D, X).$$

In addition, we make the stable unit treatment value assumption (SUTVA). Then, the observed triples $Y_i^{\text{obs}}, D_i, X_i$ are comprised by

$$Y_i^{\text{obs}} = D_i Y_i(1) + (1 - D_i) Y_i(0).$$

We define individual treatment effect (ITE) τ_i as follows

$$\tau_i := Y_i(1) - Y_i(0).$$

We denote $R \in \{0, 1\}$ the binary indicator of response, with $R = 1$ representing observations without attrition and $R = 0$ representing those with attrition. Following the literature on covariate shift, external validity, and missing data (Athey et al., 2020; Egami and Hartman, 2023; Gao et al., 2025; Lei and Candès, 2021), we call the sample with observed outcome ($R = 1$) as the source data and those with missing outcomes as target data ($R = 0$). Assume we observe the triples (Y, D, X) from the source data, but only observe the pair (D, X) from the target group. Table 1 summarizes problem setup. From the table, we can see that there are two missing data problems. First, due to the fundamental problem of causal inference (Holland, 1986), only one of the potential outcomes is observed for each unit (first four rows of Table 1). Second, due to experiment attrition, both potential outcomes are missing for the attrited units (last two rows of Table 1).

We make the following additional assumptions for the problem setup throughout the paper:

TABLE 1: RANDOMIZED EXPERIMENT WITH ATTRITION

$Y(1)$	$Y(0)$	D	X	R
✓	?	1	✓	1
?	✓	0	✓	1
?	✓	0	✓	1
✓	?	1	✓	1
⋮	⋮	⋮	⋮	⋮
?	?	0	✓	0
?	?	1	✓	0

Note: This table summarizes the setup of randomized experiment with attrition. $Y_i(1)$ and $Y_i(0)$ denote the potential outcome. D denotes the treatment, X denotes the covariates, and R denotes the indicator of attrition with $R = 1$ as the complete sample and $R = 0$ as the attrition sample. ✓ stands for observed quantity while ? stands for unobserved quantity.

Assumption 1 (Unconfoundedness).

$$(Y(1), Y(0)) \perp\!\!\!\perp D \mid X.$$

The unconfoundedness assumption of treatment assignment requires that conditional on the covariates, the treatment assignment is independent of the potential outcomes. Similarly, we assume a version of unconfoundedness for the response indicator R :

Assumption 2 (Unconfoundedness of Attrition/MAR).

$$(Y(1), Y(0)) \perp\!\!\!\perp R \mid X, D.$$

In the framework of missing data problem, Assumption 2 can be referred to as missing at random (MAR). This assumption allows us to use the observed data from the source group to make inference about the target group, without assuming the covariate distribution remains the same across groups. In other words, the missing data induced by the attrition is independent of the potential outcomes, conditional on the observed covariates.¹

¹When we tackle the missingness pattern as missing completely at random (MCAR), we do not necessarily need Assumption 2. As discussed by Gerber and Green (2012, 221), under MCAR, we only need to assume that

$$(Y(1), Y(0)) \perp\!\!\!\perp R \mid X.$$

Oftentimes this kind of missingness is relatively innocuous as the difference-in-means estimator remains an unbiased estimator of the average treatment effect (ATE).

Assumption 3 (Overlap). We assume the overlap condition for both the propensity score of treatment and experiment attrition: for $c > 0$,

$$c < e_D(X) \equiv \mathbb{P}(D = 1 | X) < 1 - c$$

$$c < e_R(X, D) \equiv \mathbb{P}(R = 1 | X, D) < 1 - c.$$

The overlap assumption is common in the causal inference and missing data literature (Imbens and Rubin, 2015; Rosenbaum and Rubin, 1983). It requires that the probability of receiving treatment and the probability of response are both bounded away from 0 and 1, conditional on the covariates (and treatment). This assumption is crucial for the identification of ITE in the presence of experiment attrition. It ensures that there is a non-negligible probability of observing both treatment and control groups across all levels of covariates, as well as a non-negligible probability of response for both groups, which enables the comparisons across subpopulations.

To make the following analysis more concrete, we define the following notation throughout the paper. Let $\mathcal{C}_d(X)$ be the prediction interval for the potential outcome $Y(d)$, where $d \in \{0, 1\}$. Similarly, let $\mathcal{C}_{\text{ITE}}(X)$ be the prediction interval for the ITE. Denote $\check{\mathcal{C}}_{\text{ITE}}(X)$ as the extrapolated prediction interval for the ITE in the attrition group.

4 Conformal Inference with Covariate Shift

This section presents an introduction to conformal inference and covariate shift problems.

4.1 Conformal Inference

In this study, the primary estimands of interest are counterfactual potential outcomes and the ITE.² Rather than generating point predictions, I propose using conformal inference to construct valid prediction intervals that cover these random variables.

Conformal inference provides a practical way to quantify uncertainty in modern prediction settings, especially when we rely on flexible machine-learning models (Angelopoulos et al., 2024). In political science research, we can train a model to predict an outcome based on observed characteristics. For example, Gohdes (2020) tries to predict regime violence based on death records and Mueller (2024) tries to predict crowd cohesion score from survey responses collected at every

²While political scientists often focus on aggregate effects such as the ATE or the average treatment effect on the treated (ATT), these quantities can be obtained by taking expectations over the ITE.

protest. While a model produces a single predicted value, it does not automatically tell us how reliable that prediction is. Some predictions are based on abundant, stable patterns in the data, while others may be much more uncertain.

Conformal inference addresses this challenge by taking any prediction model as an input and adding a calibrated bound around each prediction, namely a prediction interval, that is designed to include the true outcome with a pre-specified probability (for instance, 95%).³ The intuition here is to assess how well the model’s predictions align with the actual observed values in a held-out calibration set. We first use a training data to fit a prediction model, which can be any off-the-shelf machine learning algorithm, such as random forests, gradient boosting machines, or neural networks. Next, we apply this trained model to a separate calibration dataset to generate predictions. We then compare these predictions to the actual observed outcomes in the calibration dataset. The discrepancy between the predicted and observed value is called the nonconformity score.⁴ By permuting the nonconformity scores and selecting a pre-specified quantile of the permuted distribution, we can determine a margin of error around each prediction. This margin of error is then used to construct the prediction interval. Then, given any new data point drawn from the same population, we can use the pre-trained model to generate a prediction and use the calibrated margin of error to construct a prediction interval.

Introduced and developed by Vladimir Vovk and collaborators (Vovk et al., 1999, 2009, 2019), conformal inference has gained significant attention from the statistics community for regression problems (e.g., Lei et al., 2013; Lei and Wasserman, 2014; Lei et al., 2018) and classification problems (e.g., Romano et al., 2020; Sadinle et al., 2019). As noted by Angelopoulos and Bates (2022), these prediction intervals are valid in a distribution-free sense: they possess explicit, non-asymptotic guarantees even without distributional or model assumptions. In other words, this coverage guarantee holds without requiring strong assumptions about how the data are generated or whether the underlying model is perfectly specified. Instead, conformal inference only relies on the idea that the observed data points come from a similar underlying process. Under this condition, the method ensures that, on average, the intervals will contain the true value with the desired probability. In addition to the interval coverage, we are also interested in the interval size, which

³This prediction interval is different from confidence interval. The confidence interval is a frequentist approach, in which we assume the knowledge of the true DGP, or at least the conditional distribution of the estimand given covariates. Also, it comes from repeated sampling and the Central Limit Theorem, which guarantees the coverage in limit. However, prediction intervals constructed by conformal inference only assumes exchangeability of the DGP and guarantees the finite-sample coverage without any reliance on asymptotic approximations.

⁴There are many different measures of this discrepancy. One can imagine the most intuitive ones as the residual or softmax score.

reflects the model’s uncertainty in a transparent way. Narrower intervals imply more confidence in the prediction, while wider intervals signal greater uncertainty. This feature allows researchers to understand not only what the model predicts, but also how stable or reliable that prediction appears to be.

In the context of the missing data problem induced by experimental attrition, we are interested in two kinds of predictions, as indicated by two types of missingness mentioned in Table 1. First, we want to predict the potential outcome under treated (control) that is not observed for each non-attrited control (treatment) unit. Second, we want to predict both the potential outcomes (or the combined ITE) for each attrited unit. In both cases, instead of simply providing a point estimate with unknown uncertainty, we will use conformal inference to construct prediction intervals that quantify the uncertainty around these predictions. However, when making these two kinds of predictions, we face a challenge called covariate shift at both steps.

4.2 Covariate Shift

A key appeal of conformal inference is its nonparametric nature. It generates prediction intervals with guaranteed marginal coverage for data drawn i.i.d. from any distribution, without requiring parametric assumptions. This property makes conformal inference a fully distribution-free approach. Importantly, the i.i.d. assumption, while sufficient, is not strictly necessary. Conformal inference also applies under the weaker assumption of exchangeability, which allows observations to exhibit some dependence as long as their joint distribution is unchanged by permuting their order. In effect, the data can be dependent but must still be identically distributed in the sense that no observation is “special” or carries extra information simply because of when it appears.⁵ Thus, conformal inference retains theoretical robustness even beyond the standard i.i.d. framework.

In our setting, however, these assumptions must be relaxed further. Our goal is two-fold: first, to construct valid prediction intervals for the counterfactuals \mathcal{C}_d and ITE \mathcal{C}_{ITE} for the observed group; and second, to extrapolate these prediction intervals to the attrition group, yielding interval estimates of the ITE $\check{\mathcal{C}}_{ITE}$. In this context, the exchangeability assumption no longer holds across groups. To account for this violation, we must address the covariate shift problem, defined as a distribution shift for the covariates (Shimodaira, 2000; Tibshirani et al., 2019), at both stages of the inference procedure.

⁵See A.1 for a formal definition. Exchangeability is *the* crucial condition underpinning the validity of conformal inference: it ensures that the nonconformity scores can be meaningfully ranked to construct prediction intervals.

Ideally, in a randomized experiment without attrition, the joint distribution of covariates and outcomes can be written as $P_X \times P_{Y|X}$ for all observations. However, due to the attrition, the joint distribution changes to $Q_X \times P_{Y|X}$, with potentially different covariate distribution Q_X across groups. Under the shift from P_X to Q_X , our goal is to construct the prediction interval \mathcal{C}_d for the counterfactual $Y(d)$ with desired coverage:

$$\mathbb{P}_{(X, Y(d)) \sim Q_X \times P_{Y(d)|X}} (Y(d) \in \mathcal{C}_d(X)) \geq 1 - \alpha, \quad d \in \{0, 1\}, \quad (1)$$

and then extrapolate the prediction intervals to the attrition group:

$$\mathbb{P}_{(X, \mathcal{C}_{\text{ITE}}) \sim Q_X \times P_{\mathcal{C}_{\text{ITE}}|X}} \left(\mathcal{C}_{\text{ITE}} \subset \check{\mathcal{C}}_{\text{ITE}}(X) \right) \geq 1 - \gamma. \quad (2)$$

Under the ideal randomized experiment with i.i.d. data, these complications would not arise. Random assignment ensures that treatment is independent of covariates, yielding constant propensity scores across all covariate strata. Moreover, with no attrition, the covariate distribution remains identical across groups. In such a setting, covariate shift is not a concern.

With attrition, the situation changes significantly. The covariate distribution may differ across groups in two distinct ways. First, covariates differ between the observed and attrition groups: $\mathbb{P}(X | D, R = 0) \neq \mathbb{P}(X | D, R = 1)$. Under the MAR assumption, attrition depends on observed covariates, generating a shift from $P_{X|D, R=1}$ to $P_{X|D, R=0}$. When constructing prediction intervals for the attrition group, only observations with \mathcal{C}_{ITE} from the observed group are informative for constructing $\check{\mathcal{C}}_{\text{ITE}}(X)$ for the attrition group, making it necessary to correct for this distributional difference.

Second, attrition also induces covariate shift between treatment and control units within the observed group: $\mathbb{P}(X | D = 0, R = 1) \neq \mathbb{P}(X | D = 1, R = 1)$. Even with random assignment of treatment, missingness correlated with covariates can distort the covariate balance originally ensured by randomization. Thus, when constructing prediction intervals for counterfactuals within the observed group, we still need to account for the covariate shift problem.

4.3 Weighted Conformal Inference

To tackle the covariate shift problem for interval estimates, one solution is to rely on the weighted conformal inference developed by [Tibshirani et al. \(2019\)](#).⁶ Conformalized quantile regression (CQR), introduced by [Romano et al. \(2019\)](#), is designed to produce the interval estimate in the form of

$$\mathcal{C}(x) = [\hat{q}_{\alpha_{lo}}(x) - \eta, \hat{q}_{\alpha_{hi}}(x) + \eta], \quad (3)$$

where $\hat{q}_{\alpha_{lo}}(x)$ and $\hat{q}_{\alpha_{hi}}(x)$ are the estimates of the pre-specified error margin α_{lo} -th and α_{hi} -th conditional quantiles of $Y | X = x$. η is the constant computed after ranking the nonconformity scores. To compute the conditional quantile, we can simply change the loss function of a specific machine learning algorithm to a quantile loss, or use quantile regression (e.g., [Koenker and Bassett, 1978](#); [Koenker and Hallock, 2001](#)). As proved by [Romano et al. \(2019\)](#), CQR has finite sample coverage guarantee.

The intuition to solve the covariate shift problem is reweighting. By reweighting each nonconformity score by a probability that is proportional to the likelihood ratio

$$w(x) = \frac{dQ_X(x)}{dP_X(x)},$$

weighted conformal inference can achieve the desired coverage ([Tibshirani et al., 2019](#)). This weighting scheme resembles the nonconformity score computed on the target population, which makes the nonconformity scores “look exchangeable” at the test point ([Tibshirani et al., 2019](#)). In terms of the CQR, we are still constructing intervals like the one in Equation (3), η is computed to incorporate the weights for a weighted interval estimate.

To estimate the weight $w(x)$, [Lei and Candès \(2021\)](#) leverage the propensity score of the treatment $e_D(x)$, which resembles the logic of inverse propensity weighting (IPW) ([Imbens and Rubin, 2015](#)). Under the overlap assumption, we are essentially calibrating the source covariate distribution to the target one. For example, if we are trying to construct prediction intervals of $Y(1)$ for the control group and $Y(0)$ for the treatment group, the weights are estimated as the following:

$$w_1(x) \propto \frac{1 - e_D(x)}{e_D(x)}, \quad w_0(x) \propto \frac{e_D(x)}{1 - e_D(x)}.$$

⁶[Lei and Candès \(2021\)](#) provide a version of split conformalized quantile regression, which combines the weighted conformal inference with conformalized quantile regression (CQR) for regression problems.

5 Conformal Inference with Attrition

The logic of reweighting the nonconformity score in weighted conformal inference offers a principled solution to the covariate shift problem. This paper aims to construct prediction intervals for ITE in the attrition group with guaranteed coverage. Achieving this goal requires addressing two key challenges. First, we need to construct prediction intervals for the counterfactuals and ITE within the observed group with guaranteed coverage. Second, we need to extrapolate these prediction intervals to the attrition group. Covariate shift problem arises in both stages.

Lei and Candès (2021) propose a two-step approach for constructing prediction intervals of treatment effects for observations with both potential outcomes missing. Firstly, they construct the prediction intervals for the counterfactuals and ITE within the group with observed outcome using the weighted split-CQR, by which they refer to as the nested approach.⁷ Secondly, they conduct a second conformal inference on these prediction intervals of ITE to extrapolate the intervals to the unit with both potential outcomes missing.

While this two-step method offers finite-sample coverage guarantees, it faces three important limitations. First, this method is not designed to address attrition problems in randomized experiments. Second, even reframing the prediction on the ITE for units with both potential outcomes missing as a missing data problem, the method addresses covariate shift only in the first step. The second step employs an unweighted conformal inference, which implicitly requires a stronger assumption of missingness pattern as MCAR. Under MCAR, the distribution of covariates between source group and target group remains the same, justifying the use of unweighted conformal inference. Nevertheless, when the missingness pattern is MAR, their proposed method has less satisfying performance. Third, the prediction intervals are too conservative, in the sense that the coverage is mostly 1 with an interval that is too wide to be useful in practice.⁸

This paper follows a similar two-step approach. Consider the following condition:

$$\mathbb{P}(Y_i(1) - Y_i(0) \in \mathcal{C}_i) = \underbrace{\mathbb{P}(Y_i(1) - Y_i(0) \in \mathcal{C}_i \mid R_i = 1)P(R_i = 1)}_I + \underbrace{\mathbb{P}(Y_i(1) - Y_i(0) \in \mathcal{C}_i \mid R_i = 0)P(R_i = 0)}_{II},$$

⁷Lei and Candès (2021) define the nested approach by splitting the data into two folds: using the first fold to construct prediction intervals for counterfactuals and using the second fold to compute the prediction intervals for ITEs.

⁸Algorithm D.2, D.3, and D.4 sketches the conformal inference strategy proposed by Lei and Candès (2021). Figure E.1 shows the performance of their method in a Monte Carlo simulation.

where $\mathcal{C}_i = \mathcal{C}_{\text{ITE}}(X_i; D_i, Y_i^{\text{obs}})$. Since only one of the potential outcomes is missing for $R = 1$, term I can be reduced to

$$\begin{aligned} \mathbb{P}(Y_i(1) - Y_i(0) \in \mathcal{C}_i \mid R_i = 1)P(R_i = 1) = \\ \mathbb{P}(Y_i(0) \in \mathcal{C}_0(X_i) \mid D_i = 1, R_i = 1)P(D_i = 1 \mid R_i = 1) \\ + \mathbb{P}(Y_i(1) \in \mathcal{C}_1(X_i) \mid D_i = 0, R_i = 1)P(D_i = 0 \mid R_i = 1). \end{aligned} \quad (4)$$

If we are able to construct prediction intervals such that

$$\mathbb{P}(Y_i(0) \in \mathcal{C}_0(X_i) \mid D_i = 1, R_i = 1) \geq 1 - \alpha \quad \text{and} \quad \mathbb{P}(Y_i(1) \in \mathcal{C}_1(X_i) \mid D_i = 0, R_i = 1) \geq 1 - \alpha,$$

we can guarantee that

$$\mathbb{P}(Y_i(1) - Y_i(0) \in \mathcal{C}_i \mid R_i = 1) \geq 1 - \alpha \quad (5)$$

is satisfied by the following decomposition:

$$\mathcal{C}_{\text{ITE}}(X; D, Y^{\text{obs}}) = \begin{cases} Y^{\text{obs}} - \mathcal{C}_0(X) & \text{if } D = 1 \\ \mathcal{C}_1(X) - Y^{\text{obs}} & \text{if } D = 0 \end{cases}, \quad (6)$$

where the intervals \mathcal{C}_{ITE} can be perceived as the surrogate intervals or pseudo outcomes for ITE.

For term II, to extrapolate these intervals to the target group with attrition, we follow [Lei and Candès \(2021\)](#) to find an interval expansion function $\check{\mathcal{C}}(\cdot)$ that maps a covariate value to an interval such that

$$\mathbb{P}\left(\mathcal{C}_{\text{ITE}} \subset \check{\mathcal{C}}_{\text{ITE}}(X) \mid R = 0\right) \geq 1 - \gamma, \quad (7)$$

By Bonferroni correction, we can construct the prediction intervals that satisfy the condition (7).

$$\begin{aligned} \mathbb{P}\left(Y(1) - Y(0) \notin \check{\mathcal{C}}_{\text{ITE}}(X) \mid R = 0\right) \leq \\ \mathbb{P}(Y(1) - Y(0) \notin \mathcal{C}_{\text{ITE}} \mid R = 0) + \mathbb{P}\left(\mathcal{C}_{\text{ITE}} \not\subset \check{\mathcal{C}}_{\text{ITE}}(X) \mid R = 0\right) \leq \alpha + \gamma. \end{aligned}$$

As mentioned above, we need to account for the covariate shift problems in both steps: (1) from treatment (control) units to the control (treatment) units inside the observed group, and (2)

from the observed group ($R = 1$) to the attrition group ($R = 0$). Although weighted conformal inference provides a principled solution to covariate shift, it still relies on the empirical distribution of nonconformity scores and therefore can produce relatively wide prediction intervals in finite samples. Moreover, because our framework requires addressing two covariate shift problems sequentially, estimation error from the two propensity score models may compound, leading to further efficiency losses in the resulting intervals. Finally, our goal is to construct prediction intervals that attain valid asymptotic coverage under some regularity conditions. Therefore, following [Yang et al. \(2024\)](#) and [Gao et al. \(2025\)](#), instead of deriving the threshold of nonconformity score from the empirical distribution which produces overly wide prediction intervals with only finite sample coverage, we leverage the semiparametric efficiency theory for identification. Specifically, as it will be explain in detail in the next section, we identify the threshold of nonconformity score by deriving the efficient influence function (EIF). We adopt the following notations for simplicity:

$$\begin{aligned}\mathbb{P}(Y(d) \in \mathcal{C}_d \mid D = 1 - d, R = 1) &= \mathbb{P}(V_d < \eta_{\alpha,d} \mid D = 1 - d, R = 1) \\ \mathbb{P}(\mathcal{C}_{\text{ITE}} \subset \check{\mathcal{C}}_{\text{ITE}} \mid R = 0) &= \mathbb{P}(V_{\mathcal{E}} < \eta_{\gamma,\mathcal{E}} \mid R = 0),\end{aligned}$$

where V_d and $V_{\mathcal{E}}$ are the nonconformity scores for the counterfactuals and ITE, respectively, $\eta_{\alpha,d}$ and $\eta_{\gamma,\mathcal{E}}$ are the thresholds of the nonconformity scores for the counterfactuals and ITE, respectively. Our goal is to identify $\eta_{\alpha,d}$ as $(1 - \alpha)$ quantile of V_d and $\eta_{\gamma,\mathcal{E}}$ as $(1 - \gamma)$ quantile of $V_{\mathcal{E}}$.

6 Conformal Inference with Semiparametric Efficient Estimator

In this section, I first derive the EIF for identifying the semiparametric efficient estimator used to construct prediction intervals: $\eta_{\alpha,d}$ for the observed group and $\eta_{\gamma,\mathcal{E}}$ for the attrition group. Next, I present the details for implementing the identification algorithm.

6.1 Conformal Inference for Counterfactuals and ITE on Observed Group

As outlined above, we adopt a two-step approach to construct prediction intervals for the ITE in the attrition group. In the first step, we construct prediction intervals for the counterfactuals $Y(d)$ for those with $D = 1 - d$ for $d \in \{0, 1\}$ and then prediction intervals for ITE within the observed group using the semiparametric efficient estimator of the quantile of interest $\eta_{\alpha,d}$. In other words, to do so, it is important to extrapolate the information from units with $D = d$ to the group with

$D = 1 - d$, for $d \in \{0, 1\}$. Therefore, given a desired coverage level $(1 - \alpha)$, we identify $\eta_{\alpha, d}$ by linking the observed distribution of nonconformity score, $V_d \mid D = d, R = 1$, to the target distribution, $V_d \mid D = 1 - d, R = 1$.

Lemma 1 (Setting 1 in Theorem 1 of Gao et al. (2025)). *Under Assumption 1, we have*

$$\begin{aligned} 1 - \alpha &= \mathbb{P}(V_d < \eta_{\alpha, d} \mid D = 1 - d, R = 1) \\ &= \mathbb{E}_X \left[\mathbb{P}(V_d < \eta_{\alpha, d} \mid D = d, R = 1, X) \mid D = 1 - d, R = 1 \right]. \end{aligned}$$

Proof. See Section C.1 for the proof of Lemma 1. □

This identification formula is the foundation for estimating $\eta_{\alpha, d}$ and ensures the constructed prediction intervals \mathcal{C}_d and \mathcal{C}_{ITE} achieve desired coverage in the target data. We now derive the EIF for $\eta_{\alpha, d}$ under some regularity conditions following Yang et al. (2024) and setting 1 of Gao et al. (2025).

Theorem 1 (Lemma 1 of Yang et al. (2024)). *Suppose $\mathbb{E} \left[\frac{(\mathbb{P}(D=1-d, R=1|X))^2}{\mathbb{P}(D=d, R=1|X)} \right]$ is finite and that the density of the conditional distribution of $V_d \mid D = d, R = 1$ at $\eta_{\alpha, d}$ is bounded away from zero. Then under Assumption 1 and 3, the efficient influence function of the conditional quantile $\eta_{\alpha, d}$ under $D = 1$ for constructing prediction interval of $Y(1)$ is given up to a proportionality constant by*

$$\begin{aligned} \psi_1(\eta_{\alpha, 1}, X; m, e_R, \pi_D) &= R(1 - D) \left[m_1(\eta_{\alpha, 1}, X) - (1 - \alpha) \right] \\ &\quad + \frac{D R e_R(X, 0)}{\pi_D(X) e_R(X, 1)} \left[\mathbb{1}_{\{V_1 < \eta_{\alpha, 1}\}} - m_1(\eta_{\alpha, 1}, X) \right], \end{aligned} \tag{8}$$

and the one under $D = 0$ for constructing prediction interval of $Y(0)$ is given up to a proportionality constant by

$$\begin{aligned} \psi_0(\eta_{\alpha, 0}, X; m, e_R, \pi_D) &= R D \left[m_0(\eta_{\alpha, 0}, X) - (1 - \alpha) \right] \\ &\quad + \frac{(1 - D) R e_R(X, 1) \pi_D(X)}{e_R(X, 0)} \left[\mathbb{1}_{\{V_0 < \eta_{\alpha, 0}\}} - m_0(\eta_{\alpha, 0}, X) \right], \end{aligned} \tag{9}$$

where

$$\begin{aligned} m_d(\eta_{\alpha, d}, X) &:= \mathbb{E} \left[\mathbb{1}_{\{V_d < \eta_{\alpha, d}\}} \mid X, D = d, R = 1 \right] \\ \pi_D(X) &:= \frac{e_D(X)}{1 - e_D(X)} \quad \text{and} \quad e_R(X, d) := \mathbb{P}(R = 1 \mid D = d, X). \end{aligned}$$

Proof. See Section C.2 for the proof of Theorem 1. □

In practice, by finding the smallest value that satisfies the sample moment conditions for the EIFs

$$\frac{1}{N} \sum_{i=1}^N \psi_d(\hat{\eta}_{\alpha,d}, X_i; \hat{m}, \hat{e}_R, \hat{\pi}_D) \geq 0,$$

we can identify $\eta_{\alpha,d}$ and construct the prediction intervals for the counterfactuals, and then the ITE as in Equation (6).

Now we have been able to identify $\eta_{\alpha,d}$ for the observed group. We need to similarly identify $\eta_{\gamma,\mathcal{E}}$ to extrapolate the prediction intervals of ITE to the attrition group.

6.2 Conformal Inference for ITE with Attrition

The second step is to extrapolate the prediction intervals of ITE from the observed group to the attrition group with attrition. Intuitively, we are constructing intervals that cover the prediction intervals of ITE constructed in the first step. We build on the interval expansion approach proposed by [Lei and Candès \(2021\)](#) to construct the prediction intervals for ITE in the attrition group. Specifically, we treat the prediction intervals obtained in the first step as surrogates for the ITE intervals in the attrition group and jointly calibrate the left and right endpoints of \mathcal{C}_{ITE} to construct the prediction interval $\check{\mathcal{C}}_{\text{ITE}}(X)$ for the attrition group. Unlike the unweighted conformal inference that fails to account for the covariate shift problem, we again derive the EIF for this secondary conformal inference step ([Gao et al., 2025](#); [Yang et al., 2024](#)).

Analogous to Lemma 1, we extend the information from the observed group in the first step to the attrition group by relating the study distribution of nonconformity score $V_{\mathcal{E}} | R = 1$ to the target distribution $V_{\mathcal{E}} | R = 0$. This yields the following identification formula for the quantile of interest $\eta_{\gamma,\mathcal{E}}$ for ITE in the attrition group.

Lemma 2. *Under Assumption 2, we have the coverage for the interval of ITE from the attrition group as*

$$\begin{aligned} 1 - \gamma &= \mathbb{P}\left(\mathcal{C} \subset \check{\mathcal{C}}_{\text{ITE}}(X)\right) \\ &= \mathbb{P}\left(V_{\mathcal{E}} < \eta_{\gamma,\mathcal{E}} \mid R = 0\right) \\ &= \mathbb{E}_{X,D} \left[\mathbb{P}\left(V_{\mathcal{E}} < \eta_{\gamma,\mathcal{E}} \mid X, D, R = 1\right) \mid R = 0 \right]. \end{aligned}$$

Proof. See Section C.1 for the proof of Lemma 2. □

Similarly, this identification formula guarantees the constructed prediction intervals $\check{\mathcal{C}}_{\text{ITE}}(X)$ achieve the desired coverage in the attrition group and motivates the EIF for $\eta_{\gamma, \mathcal{E}}$.

Theorem 2. Suppose $\mathbb{E} \left[\frac{(\mathbb{P}(R=0|X,D)^2)}{\mathbb{P}(R=1|X,D)} \right]$ is finite and the density of the conditional distribution of $V_{\mathcal{E}} | R = 0$ at η_{γ} is bounded away from zero. Then under Assumption 2 and 3, the efficient influence function of the conditional quantile $\eta_{\gamma, \mathcal{E}}$ is given up to a proportionality constant by

$$\begin{aligned} \psi_{\mathcal{E}}(\eta_{\gamma, \mathcal{E}}, X; m_{\mathcal{E}}, \pi_R) &= (1 - R) [m_{\mathcal{E}}(\eta_{\gamma, \mathcal{E}}, X, D) - (1 - \gamma)] \\ &\quad + \frac{R}{\pi_R(X, D)} [\mathbb{1}_{\{V_{\mathcal{E}} < \eta_{\gamma, \mathcal{E}}\}} - m_{\mathcal{E}}(\eta_{\gamma, \mathcal{E}}, X, D)], \end{aligned} \quad (10)$$

where

$$\begin{aligned} m_{\mathcal{E}}(\eta_{\gamma, \mathcal{E}}, X, D) &:= \mathbb{E} [\mathbb{1}_{\{V_{\mathcal{E}} < \eta_{\gamma, \mathcal{E}}\}} | X, D, R = 1] \\ \pi_R(X, D) &:= \frac{\mathbb{P}(R = 1 | X, D)}{\mathbb{P}(R = 0 | X, D)}. \end{aligned}$$

Proof. See Section C.3 for the proof of Theorem 2. □

Lemma 2 and Theorem 2 differ from Theorem 4 in Gao et al. (2025) in one key assumption. Under the MAR assumption made by Gao et al. (2025), we do not require the conditional independence $\mathbb{P}(D = d | X, R = 1) = \mathbb{P}(D = d | X, R = 0)$ of the treatment and the missingness pattern.⁹

In practice, we can identify $\eta_{\gamma, \mathcal{E}}$ by finding the smallest value that satisfies the sample moment conditions for the EIF

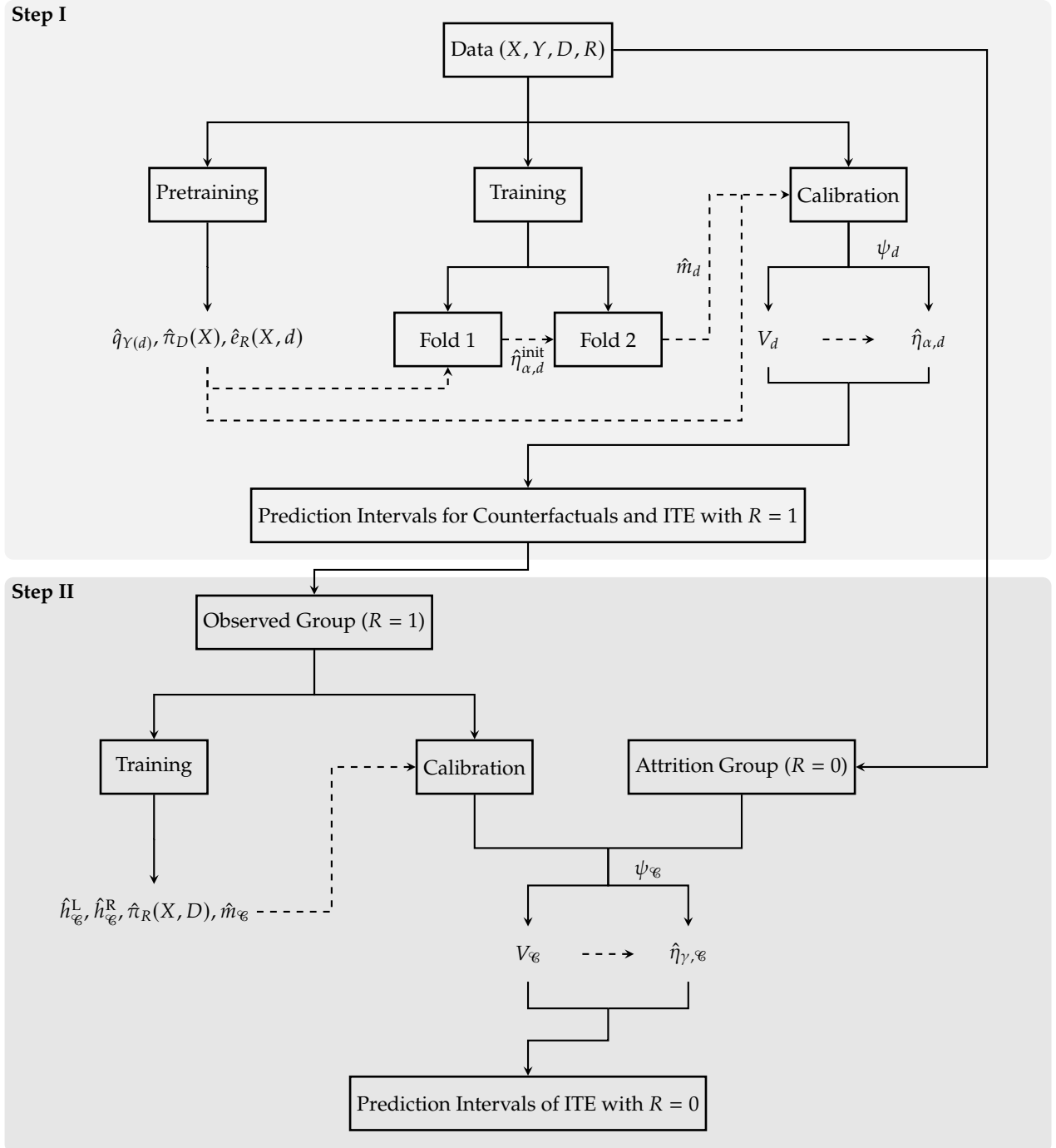
$$\frac{1}{N} \sum_{i=1}^N \psi_{\mathcal{E}}(\hat{\eta}_{\gamma, \mathcal{E}}, X_i; \hat{m}_{\mathcal{E}}, \hat{\pi}_R) \geq 0.$$

6.3 Estimation Algorithm

Now that we have discussed how to obtain the EIFs, we describe the algorithm used. Figure 1 illustrates the overall workflow, and Algorithm D.1 sketches the implementation details. To construct prediction intervals for ITE in the attrition group, we adopt the split conformal inference (Lei and Wasserman, 2014) in combination with the exact nested approach for interval estimation

⁹By contrast, Gao et al. (2025) impose the conditional independence when deriving their identification formula. If $\mathbb{P}(D = d | X, R = 1) = \mathbb{P}(D = d | X, R = 0)$, Lemma 2 reduces to $1 - \gamma = \mathbb{E}_X [\mathbb{P}(V_{\mathcal{E}} < \eta_{\gamma, \mathcal{E}} | X, R = 1) | R = 0]$, which is the result in Gao et al. (2025). However, this requires the stronger assumption that attrition is conditionally independent of treatment status.

FIGURE 1: WORKFLOW OF ALGORITHM



Note: This figure illustrates the overall workflow of the proposed algorithm for constructing prediction intervals for ITE with attrition. The light shaded part represents Step I, which constructs prediction intervals for counterfactuals and ITE within the observed group using semiparametric efficient estimators. The dark shaded part represents Step II, which extrapolates the prediction intervals of ITE to the attrition group using the interval expansion approach with semiparametric efficient estimators.

of ITE (Lei and Candès, 2021). The procedure consists of two main steps. First, following Theorem 1, we use data from the observed group to construct prediction intervals for counterfactuals and ITE. Second, following Theorem 2, we take the interval estimates of the ITE from the first step and use them to construct prediction intervals for the ITE in the attrition group.

We describe the full algorithm as follows. As shown by the light shaded part in Figure 1, Step 1 begins by splitting the data into three folds: (\mathcal{F}_{pr}), training (\mathcal{F}_{tr}), and calibration (\mathcal{F}_{ca}). This differs from the original split conformal inference procedure of Lei and Wasserman (2014) and the method proposed by Gao et al. (2025), which uses a two-fold random split and trains the learner on the first fold. In our setting, identifying the semiparametric efficient estimator $\eta_{\alpha,d}$ using the EIF requires fitting the model on a hold-out fold for nuisance parameter estimation. A two-fold split risks overfitting the nuisance parameter estimators, which undermines both predictive performance and EIF identification.

On \mathcal{F}_{pr} , we train the conditional quantile models $\hat{q}_{\beta}(\cdot)$ and learners for the treatment propensity score $\hat{\pi}_D(X)$ and the attrition propensity score $\hat{e}_R(d, X)$. We then evaluate the nonconformity score V_i for each observation in $\mathcal{F}_{\text{tr}} \cup \mathcal{F}_{\text{ca}}$ following CQR: $V_i = \max \{ \hat{q}_{\alpha_{\text{lo}}}(X_i; \mathcal{F}_{\text{pr}}) - Y_i, Y_i - \hat{q}_{\alpha_{\text{hi}}}(X_i; \mathcal{F}_{\text{pr}}) \}$ to identify $\eta_{\alpha,d}$. Following Gao et al. (2025), we further split the training fold into two subfolds $\mathcal{F}_{\text{tr},1}$ and $\mathcal{F}_{\text{tr},2}$ to reduce the computational burden of estimating the full conditional distribution $m_d(\eta_{\alpha,d}, X)$ for root finding. We also adopt the localized debiased machine learning approach of Kallus et al. (2024): $\mathcal{F}_{\text{tr},1}$ is used to construct an initial estimator $\hat{\eta}_{\alpha,d}^{\text{init}}$ of $\eta_{\alpha,d}$, and $\mathcal{F}_{\text{tr},2}$ is then used to train the learner for $\hat{m}_d(\hat{\eta}_{\alpha,d}^{\text{init}}, X)$.

Then, on \mathcal{F}_{ca} , we identify the semi-parametric efficient estimator $\hat{\eta}_{\alpha,d}$ by finding the smallest values that satisfy

$$\sum_{i \in \mathcal{F}_{\text{ca}}} \psi_d(\hat{\eta}_{\alpha,d}, X_i; \hat{m}_d, \hat{e}_R, \hat{\pi}_D) \geq 0,$$

where \hat{m}_d is trained on $\mathcal{F}_{\text{tr},2}$ and \hat{e}_R and $\hat{\pi}_D$ are trained on \mathcal{F}_{pr} . We then can construct the prediction interval for counterfactuals as

$$\mathcal{C}_d(X) = [\hat{Y}_i^{\text{L}}(d), \hat{Y}_i^{\text{R}}(d)] = [\hat{q}_{\alpha_{\text{lo}}}(X_i; \mathcal{F}_{\text{pr}}) - \hat{\eta}_{\alpha,1-d}, \hat{\eta}_{\alpha,1-d} + \hat{q}_{\alpha_{\text{hi}}}(X_i; \mathcal{F}_{\text{pr}})].$$

Leveraging these prediction intervals for counterfactuals, we can construct the prediction interval

for ITE in the source group as in Equation (6)

$$\mathcal{C}_{\text{ITE}}(X) = \begin{cases} Y^{\text{obs}} - \mathcal{C}_0(X) & \text{if } D = 1 \\ \mathcal{C}_1(X) - Y^{\text{obs}} & \text{if } D = 0 \end{cases}$$

Step 2 shown in the dark shaded area aims to construct the prediction intervals for ITE in the attrition group. We take all observations with observed outcomes and prediction intervals for ITE from $\mathcal{X}_{\text{ca}} \equiv (X_i, Y_i, D_i, R_i, \mathcal{C}_i)$ in Step 1 and treat them as the observed data \mathcal{X}_{obs} . This set is randomly split into a training fold $\mathcal{X}_{\text{obstr}}$ and a calibration fold $\mathcal{X}_{\text{obsca}}$. On $\mathcal{X}_{\text{obstr}}$, we train $\hat{h}^L(\cdot)$ and $\hat{h}^R(\cdot)$ to model the conditional mean of the lower and upper endpoints of \mathcal{C}_i , respectively. We also train the attrition propensity score $\hat{\pi}_R(X, D)$ and the conditional distribution $\hat{m}_{\mathcal{C}}(\eta_{\gamma, \mathcal{C}}, X, D)$. For each observation in \mathcal{C}_{obs} , we compute the nonconformity score $V_{\mathcal{C}} = \max \{ \hat{h}^L(X_i; \mathcal{X}_{\text{obstr}}) - \mathcal{C}_i^L, \mathcal{C}_i^R - \hat{h}^R(X_i, \mathcal{X}_{\text{obstr}}) \}$. Next, we combine the calibration fold $\mathcal{X}_{\text{obsca}}$ with all observations from the attrition group \mathcal{X}_{att} . This combination of $R = 1$ and $R = 0$ explicitly addresses the covariate shift between the observed and attrition groups. Finally, for observations from $\mathcal{X}_{\text{obsca}} \cup \mathcal{X}_{\text{att}}$, we identify the semi-parametric efficient estimator $\hat{\eta}_{\gamma, \mathcal{C}}$ by finding the smallest value that satisfies

$$\sum_{i \in \mathcal{J}_{\text{obsca}} \cup \mathcal{J}_{\text{att}}} \psi_{\mathcal{C}}(\hat{\eta}_{\gamma, \mathcal{C}}, X_i; \hat{m}_{\mathcal{C}}, \hat{\pi}_R) \geq 0,$$

where $\hat{m}_{\mathcal{C}}$ and $\hat{\pi}_R$ are trained on $\mathcal{X}_{\text{obstr}}$. Finally, we can construct the prediction interval for ITE in the target group with attrition as

$$\check{\mathcal{C}}_{\text{ITE}}(x) = \left[\hat{h}^L(x; \mathcal{X}_{\text{obstr}}) - \hat{\eta}_{\gamma, \mathcal{C}}, \hat{h}^R(x; \mathcal{X}_{\text{obstr}}) + \hat{\eta}_{\gamma, \mathcal{C}} \right].$$

6.4 Asymptotic Coverage of the Prediction Interval for ITE with Attrition

Our choice to use semiparametric efficient estimators for constructing prediction intervals for the ITE under attrition is motivated by two considerations. First, the EIF approach allows us to address covariate shift in both steps of the procedure. Second, semiparametric efficiency ensures that the resulting estimator achieves the desired asymptotic coverage for the prediction interval, in contrast to the finite-sample, nonasymptotic coverage guarantees obtained from the weighted split-CQR approach.

To establish the asymptotic coverage of the prediction interval for the ITE under attrition, we must ensure that both semiparametric efficient estimators $\eta_{\alpha,d}$ and $\eta_{\gamma,\mathcal{E}}$ possess the requisite asymptotic properties. These properties guarantee that the constructed prediction intervals achieve the desired asymptotic coverage. Theorem 3 of [Gao et al. \(2025\)](#) formally states the asymptotic properties of $\eta_{\alpha,d}$ and demonstrates the resulting asymptotic coverage of the ITE prediction intervals for the observed group. Following the same reasoning, we establish the asymptotic property of $\eta_{\gamma,\mathcal{E}}$ and the corresponding asymptotic coverage for the ITE prediction intervals in the attrition group. See Appendix B for the regularity conditions, theorem, and technical details.

Theorem B.1 establishes a coverage guarantee for the ITE prediction interval in the attrition group. The deviation from the nominal coverage is governed by the sum of two terms: (i) a term of order $O(N^{-1/2})$ when the data is split into two folds of similar size, and (ii) the product bias from the estimation of nuisance parameters $\pi_R(X, D)$ and $m_{\mathcal{E}}(\eta_{\gamma,\mathcal{E}}, X, D)$, which is negligible if either $\|\hat{\pi}_R(X, D) - \pi_R(X, D)\|_2 = o_p(1)$ or $\|\hat{m}_{\mathcal{E}}(\hat{\eta}_{\gamma,\mathcal{E}}, X, D) - m_{\mathcal{E}}(\hat{\eta}_{\gamma,\mathcal{E}}, X, D)\|_2 = o_p(1)$. The first term comes from approximating $\mathbb{E}[\psi_{\mathcal{E}}]$ with $\mathbb{P}_{\mathcal{J}_2}(\psi_{\mathcal{E}})$. The second term comes from the double robustness property of the EIF $\psi_{\mathcal{E}}$. This rate double robustness property ensures that the asymptotic coverage is robust to small perturbations in the estimation of nuisance parameters, with estimation errors affecting coverage only through second-order terms ([Chernozhukov et al., 2018](#)).

As shown by [Gao et al. \(2025\)](#), prediction intervals of counterfactuals have asymptotic coverage of $(1 - \alpha)$. Also, Theorem B.1 shows that the prediction intervals of ITE in the attrition group have asymptotic coverage of $(1 - \gamma)$. Then, by Bonferroni correction,

$$\begin{aligned} & \mathbb{P}\left(Y_1 - Y_0 \notin \check{\mathcal{C}}_{\text{ITE}}(X) \mid R = 0\right) \\ & \leq \mathbb{P}\left(Y_1 - Y_0 \notin \mathcal{C}_{\text{ITE}} \mid R = 0\right) + \mathbb{P}\left(\mathcal{C}_{\text{ITE}} \not\subset \check{\mathcal{C}}_{\text{ITE}}(X) \mid R = 0\right) \leq \alpha + \gamma + o_p(1), \end{aligned} \tag{11}$$

which shows that the probability of the ITE not being contained in the prediction interval $\check{\mathcal{C}}_{\text{ITE}}(X)$ is bounded above by $(\alpha + \gamma)$ up to a negligible term. This interval expansion function $\check{\mathcal{C}}_{\text{ITE}}$ for ITE prediction intervals in the attrition group is designed to jointly calibrate the upper and lower ends of the interval estimates of ITE \mathcal{C}_{ITE} from the observed group, ensuring that the overall coverage is at least $1 - (\alpha + \gamma)$. Thus, we have

$$\mathbb{P}\left(Y_1 - Y_0 \in \check{\mathcal{C}}_{\text{ITE}}(X) \mid R = 0\right) \geq 1 - (\alpha + \gamma),$$

holds asymptotically, which guarantees the desired coverage.

7 Simulation Studies

In this section, we evaluate the performance of the proposed method through simulation studies. Following [Lei and Candès \(2021\)](#), we adapt a variant of the simulation setting in [Wager and Athey \(2018\)](#). The simulation design assesses the performance of ITE prediction intervals under attrition using two primary metrics. First, we examine the empirical marginal coverage and average length of the ITE prediction intervals in the attrition group across different learning algorithms to identify the best-performing learner. Second, we compare the proposed method against two alternative approaches: a parametric method — multiple imputation using Amelia II — and a nonparametric method — weighted CQR with unweighted nested framework.

The data generating process (DGP) is summarized as follows. The covariate vector $X = (X_1, \dots, X_k)^\top$ is an equicorrelated multivariate Gaussian vector with mean zero and $\text{Var}(X_i) = 1$ and $\text{Cov}(X_i, X_j) = \rho$ for $i \neq j$. When $\rho = 0$, the covariates are independent. When $\rho > 0$, the covariates are positively correlated. The potential outcomes are generated as follows:

$$Y_1 = f(X_1)f(X_2) + \epsilon, \quad Y_0 = \epsilon$$

$$f(x) = \frac{2}{1 + \exp(-12(x - 0.5))}, \quad \epsilon \sim \mathcal{N}(0, 1).$$

The propensity score of treatment $e_D(X)$ is generated as

$$e_D(X) = \frac{1}{4} (1 + \beta_{2,4}(X_1)),$$

where $\beta_{a,b}$ is the CDF of the beta distribution with parameters a and b . According to [Lei and Candès \(2021\)](#), this ensures that $e_D(X) \in [0.25, 0.5]$, thereby providing sufficient overlap between the treatment and control group that satisfies Assumption 3. The propensity score of attrition $e_R(X, D)$ is generated as

$$e_R(X, D) = \text{logit}^{-1}(-0.25 + 0.5D + 0.2X_1 - 0.3X_2),$$

which ensures the MAR assumption that the missingness is correlated with observed covariates. Throughout the simulation, we set the dimension of the covariates $k = 10$. We also consider another more complicated DGP. See Section [E.3](#) for details.

We are interested in evaluating the properties of the ITE prediction intervals in the attrition

group. Corresponding to Table 1, we observe (X, Y, D) in the observed group ($R = 1$) while only observe (X, D) in the attrition group ($R = 0$). The nonconformity scores $V_{\alpha, d}$ and $V_{\gamma, \mathcal{E}}$ are constructed using conformalized quantile residuals from the quantile regression model. We use `quantreg` package in R following [Lei and Candès \(2021\)](#) and set $\alpha_{\text{lo}} = \frac{\alpha}{2}, \alpha_{\text{hi}} = 1 - \frac{\alpha}{2}$ for $V_{\alpha, d}$ and set $\gamma_{\text{lo}} = \frac{\gamma}{2}, \gamma_{\text{hi}} = 1 - \frac{\gamma}{2}$ for $V_{\gamma, \mathcal{E}}$ as the lower and upper quantile for the nonconformity scores. We estimate the propensity scores and other nuisance parameters using Generalized Linear Model (`glm`), Lasso and Elastic-Net Regularized Generalized Linear Model (`glmnet`), Random Forest, Bayesian Additive Regression Trees (BART), and Extreme Gradient Boosting (XGBoost) as base learners via `SuperLearner` package in R. We first split 20% of the data as the pretraining fold, and then use 75% of the remaining data the training fold, as suggested by [Sesia and Candès \(2020\)](#). In the second step, we further split the observed data with prediction interval of ITE from the first step into two folds with the same size for training and calibration.

To evaluate the overall performance of conformal inference for ITE estimation under attrition across different learning algorithms, we conduct 100 Monte Carlo simulations for sample sizes $\{500, 1000, 5000\}$. We compare five different learning algorithms under two levels of covariate correlation: $\rho = 0$ and $\rho = 0.9$. Following [Lei and Candès \(2021\)](#), we set $\alpha = \gamma = 0.025$ to construct ITE prediction intervals for the attrition group with nominal 95% coverage. The empirical marginal coverage of the ITE is then estimated as

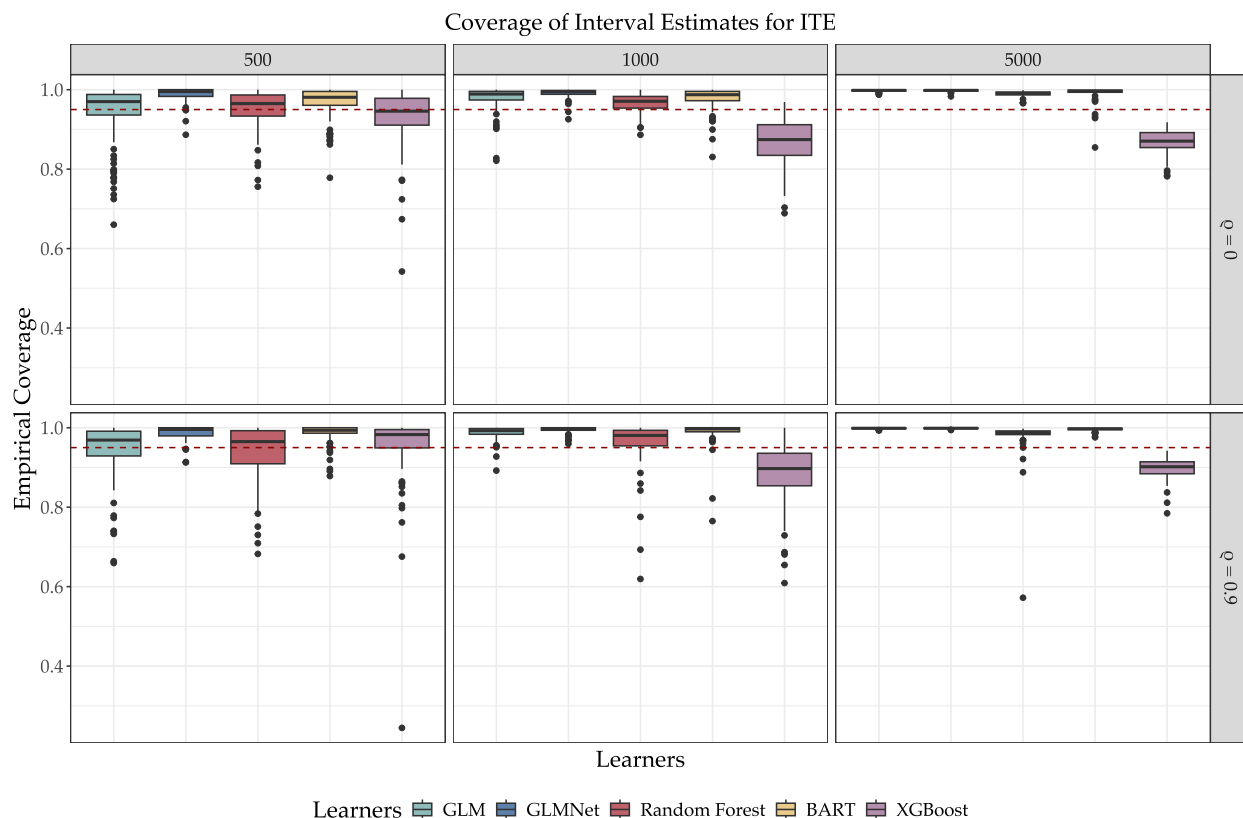
$$\frac{1}{|\mathcal{J}_{R=0}|} \sum_{R=0} \mathbb{1}_{\{Y_i(1) - Y_i(0) \in \check{\mathcal{C}}_{\text{ITE}}(X_i)\}}.$$

As noted by [Lei and Candès \(2021\)](#), a reliable method should, at very least, achieve coverage close to or above the nominal level 0.95. For benchmarking purposes, we also compute the average length of the oracle intervals, defined by the true 0.025th and 0.975th conditional quantiles. In our DGP, the errors are normally distributed, so the expected length is given by $5.54 (\approx 2 \times 1.96 \times \sqrt{2})$.

Figure 2 presents the simulation results for the empirical coverage of ITE prediction intervals in the attrition group, constructed using conformal inference with semiparametric efficient estimator across different learners. XGboost achieves the nominal 95% coverage when the sample size is $N = 500$, but its coverage deteriorates for $N = 1000$ and $N = 5000$. The other four algorithms maintain better coverage than XGBoost and achieve the nominal level across all sample sizes. Among these, attains the highest coverage, reaching nearly 1.0 for $N = 1000$ and $N = 5000$. When the sample size is $N = 5000$, all these four algorithms yield coverage close to 1.0. The empirical

coverage remains stable across different covariate correlations.

FIGURE 2: MC SIMULATION RESULTS OF CONFORMAL INFERENCE FOR ITE WITH ATTRITION

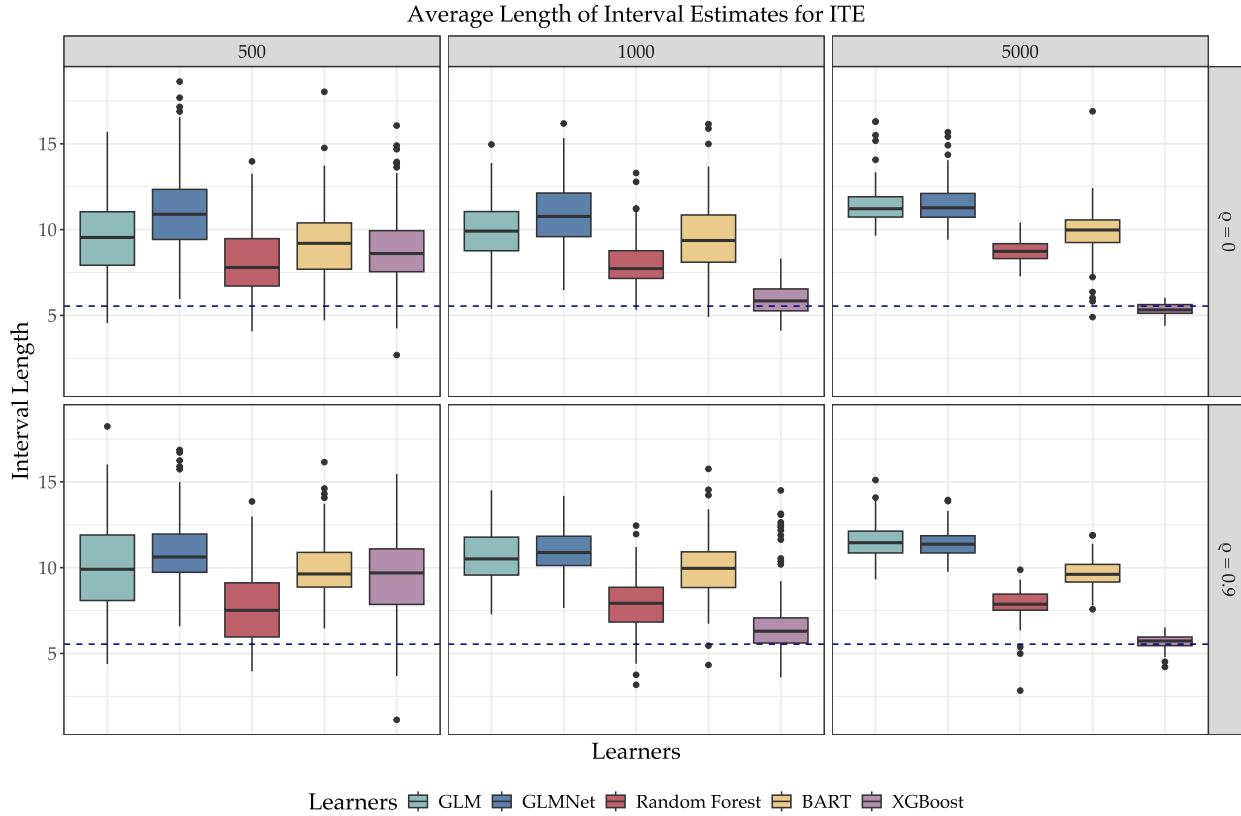


Note: This figure shows the simulation results for the empirical coverage of prediction intervals constructed by semiparametric efficient estimator for ITE of attrition group following DGP1. The red horizontal line corresponds to the target coverage of 95%.

Figure 3 presents the simulation results for the average length of ITE prediction intervals in the attrition group, constructed using conformal inference with semiparametric efficient estimator across different learners. XGBoost produces the shortest intervals with poor empirical coverage. Among the remaining four algorithms, BART yields the longest intervals, consistent with its high empirical coverage. While all four achieve coverage above the nominal level, random forest offers the best balance between coverage and average length: it maintains nominal coverage while producing the shortest average interval length among these methods. Overall, the simulation results indicate that conformal inference with semiparametric efficient estimator yields ITE prediction intervals in the attrition group that achieve the desired empirical coverage and maintain reasonable interval lengths, regardless of whether the covariates are correlated or not.

We further conduct a second simulation study to compare the performance of the proposed conformal inference with semiparametric efficient estimator with multiple imputation, which is

FIGURE 3: MC SIMULATION RESULTS OF CONFORMAL INFERENCE FOR ITE WITH ATTRITION



Note: This figure shows the simulation results for the average length of prediction intervals constructed by semiparametric efficient estimator for ITE of attrition group following DGP1. The blue horizontal line corresponds to the length of oracle intervals.

widely used in political science studies, and the exact method with nested framework of conformal inference for interval outcomes proposed by [Lei and Candès \(2021\)](#). For multiple imputation, we use Amelia II, a fast algorithm using expectation-maximization (EM) with bootstrapping for multiple imputation of missing data ([Honaker et al., 2011](#); [King et al., 2001](#)). Since the missingness induced by fundamental problem of causal inference – only one potential outcome is observed at one time – and the missingness induced by experiment attrition are different theoretically, we use multiple imputation to impute one missingness type at a time. To be specific, we first impute the potential outcomes for the observed group, i.e., we use outcomes of observations from group $D = 1 \ \& \ R = 1$ to impute the counterfactuals $Y(1)$ of observations from group $D = 0 \ \& \ R = 1$. Similarly, we impute the counterfactuals $Y(0)$ of observations from group $D = 1 \ \& \ R = 1$ using outcomes of observations from group $D = 0 \ \& \ R = 1$. Then, we use outcomes of the observed group to impute the attrition group and construct the prediction interval for ITE in the attrition group using the corrected standard error. This procedure corresponds to the logic of the conformal

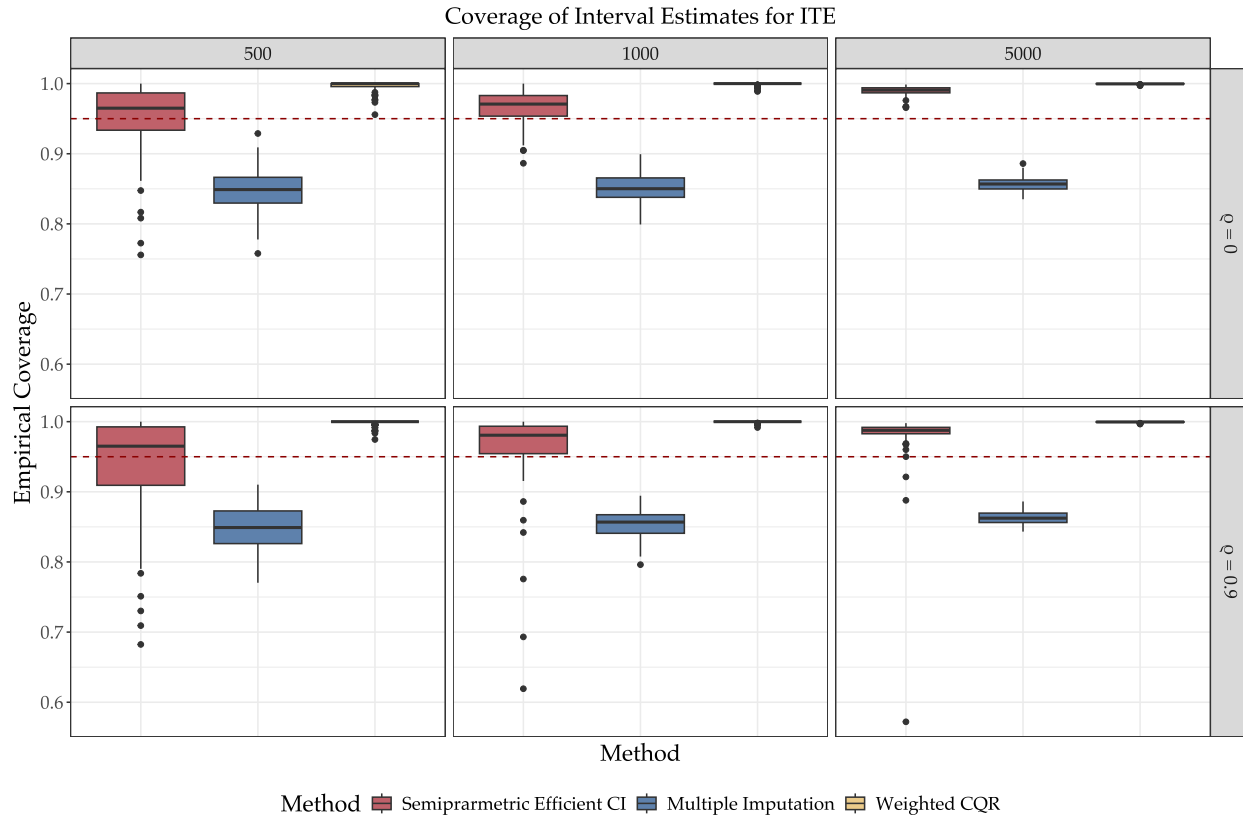
inference algorithm described above. We also conduct two other multiple imputation practice for constructing the prediction interval of ITE with attrition. See Section E.3.2 for the implementation details and simulation results.

In this second simulation study, we choose random forest as the base learner for conformal inference as it performs comparatively the best in the first study, and set $\alpha = \gamma = 0.025$ as well. We conduct 100 MC simulations for sample sizes among $\{500, 1000, 5000\}$ and consider two scenarios of covariate correlation: uncorrelated with $\rho = 0$ and correlated with $\rho = 0.9$ (Lei and Candès, 2021). The empirical marginal coverage of conformal inference prediction interval is evaluated the same as in the first study.

Figure 4 presents the coverage of prediction intervals for ITE with attrition constructed by three different methods. As expected, the weighted CQR with unweighted nested approach for interval estimates by Lei and Candès (2021) has the highest coverage, almost 1 across all sample sizes and covariate correlations. Here we are using the exact method under the nested framework, which has been shown to have larger coverage in Figure E.1. As mentioned above, this high coverage of Lei and Candès (2021) is not surprising since this approach does not assume MAR, which cannot deal with the covariate shift problems from observed group to the attrition group. The multiple imputation method with Amelia has poor coverage across all samples sizes and covariate correlations. There could be several reasons underlying this low coverage. First, the imputation model in Amelia assumes that the complete data are multivariate normal. However, under our DGP, outcomes do not follow a normal distribution. Multiple imputation failed to tackle this distribution, which violates the normality assumption. Second, although Amelia also requires MAR assumption, it does not account for the two different covariate shift problems discussed before. Among all three methods, conformal inference with semiparametric efficient estimator performs the best. Although the coverage is around 95% when the sample size is 500, it goes beyond nominal level when the sample size increases and is stable across different covariate correlations.

Figure 5 presents the average length of prediction intervals for ITE with attrition constructed by three different methods. Among three methods, the weighted CQR with unweighted nested approach has the widest prediction intervals, which is expected since it has the highest empirical coverage. However, such wide intervals are too conservative and not informative enough for inference, as they always cover the true ITE. The average length of intervals constructed by Amelia is the shortest, comparable with the length of oracle confidence intervals. However, this is misleading and not desirable since the empirical coverage is much lower than the nominal level. Notably,

FIGURE 4: COMPARISON OF EMPIRICAL COVERAGE OF PREDICTION INTERVALS FOR ITE WITH ATTRITION

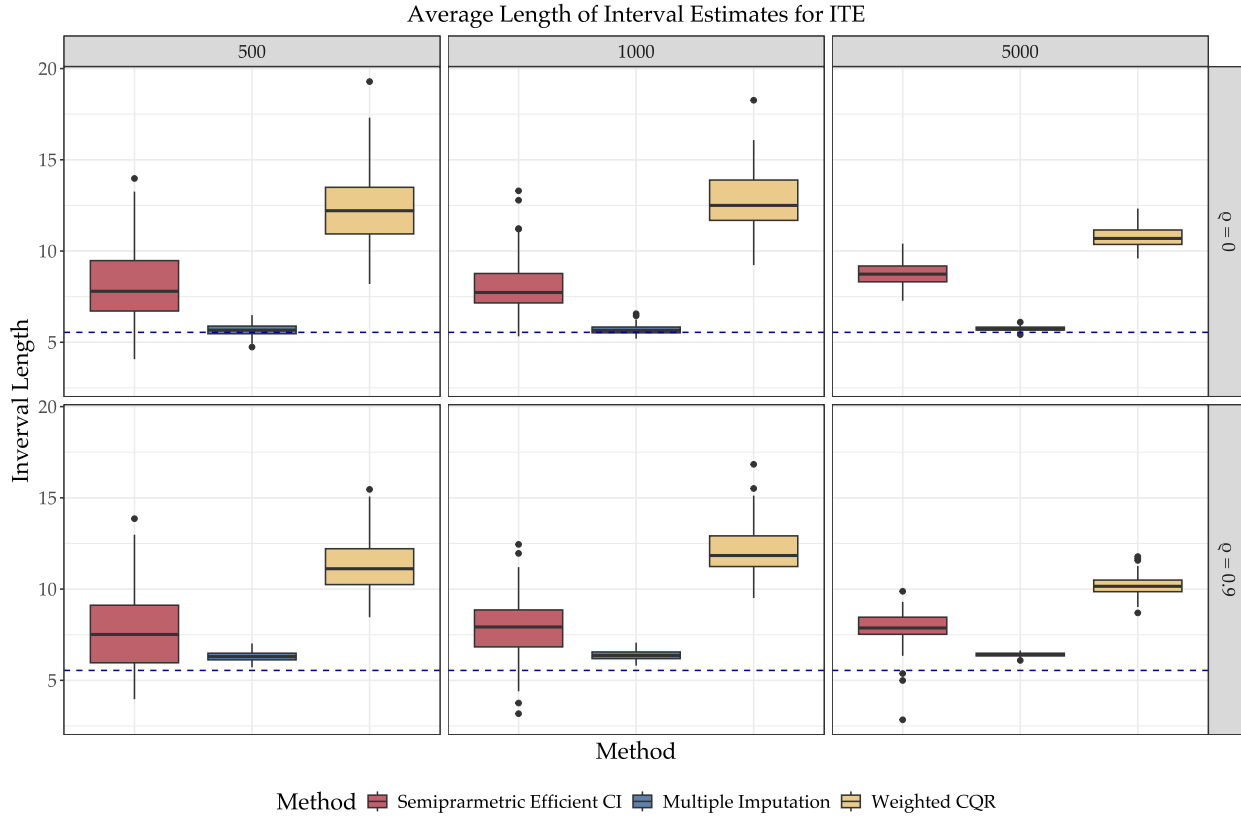


Note: This figure shows the simulation results for the empirical coverage of prediction intervals constructed by conformal inference with semiparametric efficient estimator, multiple imputation with Amelia, and weighted CQR with unweighted nested approach for ITE of attrition group. The red horizontal line corresponds to the target coverage of 95%.

intervals constructed by conformal inference with semiparametric efficient estimator have the best performance across different sample sizes and covariate correlations, corresponding to the empirical coverage.

Based on the simulation results from both studies, conformal inference with semiparametric efficient estimator yields ITE prediction intervals in the attrition group that achieve the desired empirical coverage and maintain reasonable interval lengths across different sample sizes and DGP. Moreover, when compared to current methods like multiple imputation and weighted CQR with unweighted nested approach, the proposed method demonstrates superior performance in terms of both empirical coverage and average interval length across different DGP. These findings highlight the effectiveness of conformal inference with semiparametric efficient estimator for constructing reliable ITE prediction intervals under attrition.

FIGURE 5: COMPARISON OF AVERAGE LENGTH OF PREDICTION INTERVALS FOR ITE WITH ATTRITION



Note: This figure shows the simulation results for the average length of prediction intervals constructed by conformal inference with semiparametric efficient estimator, multiple imputation with Amelia, and weighted CQR with unweighted nested approach for ITE of attrition group. The red horizontal line corresponds to the length of oracle intervals.

8 Empirical Application

In this section, I revisit the study by [Margalit and Shayo \(2021\)](#) and [Finkel et al. \(2024\)](#) to illustrate the proposed method. We show that by using conformal inference with semiparametric efficient estimator, we can construct prediction intervals for ITE in the attrition group with desired coverage. Moreover, we can aggregate ITEs to the ATE of interest for the attrition group and compute the point and interval estimates of ATE for all observations.

8.1 Reanalysis of [Margalit and Shayo \(2021\)](#)

This paper leverages a field experiment to evaluate the impact of financial markets on socioeconomic values and political preferences. In the experiment, the authors designed one asset treatment and three subtreatment within the treatment group. There were 2,183 participants assigned to the treatment group and 521 participants assigned to the control group. The asset treatment required

participants make investment decisions over a period of 6 consecutive weeks. The outcome variable of interest is participants' Socioeconomic values (SEV) measured by a principal component analysis on four items pertaining to issues of personal responsibility, economic fairness, inequality, and redistribution. As mentioned by [Margalit and Shayo \(2021\)](#), the attrition rates are different for different treatments, although they did not find evidence for selective attrition and systematic differences between attrited and non-attrited participants.

Table 2 of [Margalit and Shayo \(2021, 484\)](#) shows the overall treatment effect on SEV, without distinguishing between subtreatments. This reanalysis replicates column (4), which includes pretreatment SEV, political controls, and demographic controls. We consider three methods with 500 MC simulations: conformal inference with semiparametric efficient estimator (CISE), multiple imputation (MI), and weighted CQR (WCQR) with unweighted nested approach for interval estimates. After constructing the prediction intervals for ITE in the attrition group, we aggregate these ITEs to the ATE for the attrition group and compute the standard error across 500 MC simulations. Then we use weighted average of ATE for the observed group and the attrition group to compute the ATE for all observations. The standard error of ATE for all observations is computed as

$$\text{SE}(\text{ATE}_{\text{all}}) = \sqrt{\left(\frac{|\mathcal{J}_{R=1}|}{|\mathcal{J}_{R=1}| + |\mathcal{J}_{R=0}|}\right)^2 \text{SE}(\text{ATE}_{R=1})^2 + \left(\frac{|\mathcal{J}_{R=0}|}{|\mathcal{J}_{R=1}| + |\mathcal{J}_{R=0}|}\right)^2 \text{SE}(\text{ATE}_{R=0})^2},$$

where $\text{SE}(\text{ATE}_{R=1})$ is the standard error of the ATE estimate from the regression model, which is the same as reported by [Margalit and Shayo \(2021\)](#), $\text{SE}(\text{ATE}_{R=0})$ is the standard error of the ATE estimate for the attrition group across 500 MC simulations. We also use IPW to estimate the ATE for the observed group as a comparison to the result reported by [Margalit and Shayo \(2021\)](#).

We also evaluate the average length of the prediction intervals for ATE in the attrition group. Since we do not have the control of the DGP with the real data, we know nothing about the ground truth to evaluate the coverage and the average length as in the simulation studies. Therefore, it is only meaningful to evaluate the average interval length here. The average length of the prediction intervals is computed as

$$\frac{1}{|\mathcal{J}_{R=0}|} \sum_{R=0} \left(\check{\mathcal{C}}_{i, \text{ITE}_{R=0}}^R - \check{\mathcal{C}}_{i, \text{ITE}_{R=0}}^L \right),$$

where $\check{\mathcal{C}}_{i, \text{ITE}_{R=0}}^R$ and $\check{\mathcal{C}}_{i, \text{ITE}_{R=0}}^L$ are the upper and lower bounds of the prediction interval for ITE

TABLE 2: REANALYSIS OF **MARGALIT AND SHAYO (2021)** TABLE 2 COLUMN (4)

	(1)	(2)	(3)	(4)
Method	ATER1	ATER0	ATEall	Length
CISE	0.098 (0.052)	0.190 (0.180)	0.114 (0.054)	6.894 (0.860)
MI	0.098 (0.052)	0.129 (0.040)	0.103 (0.044)	5.668 (0.079)
WCQR	0.098 (0.052)	0.205 (0.109)	0.117 (0.047)	10.495 (0.830)
IPW	0.110 (0.053)			
Observations	2,223	480	2,703	

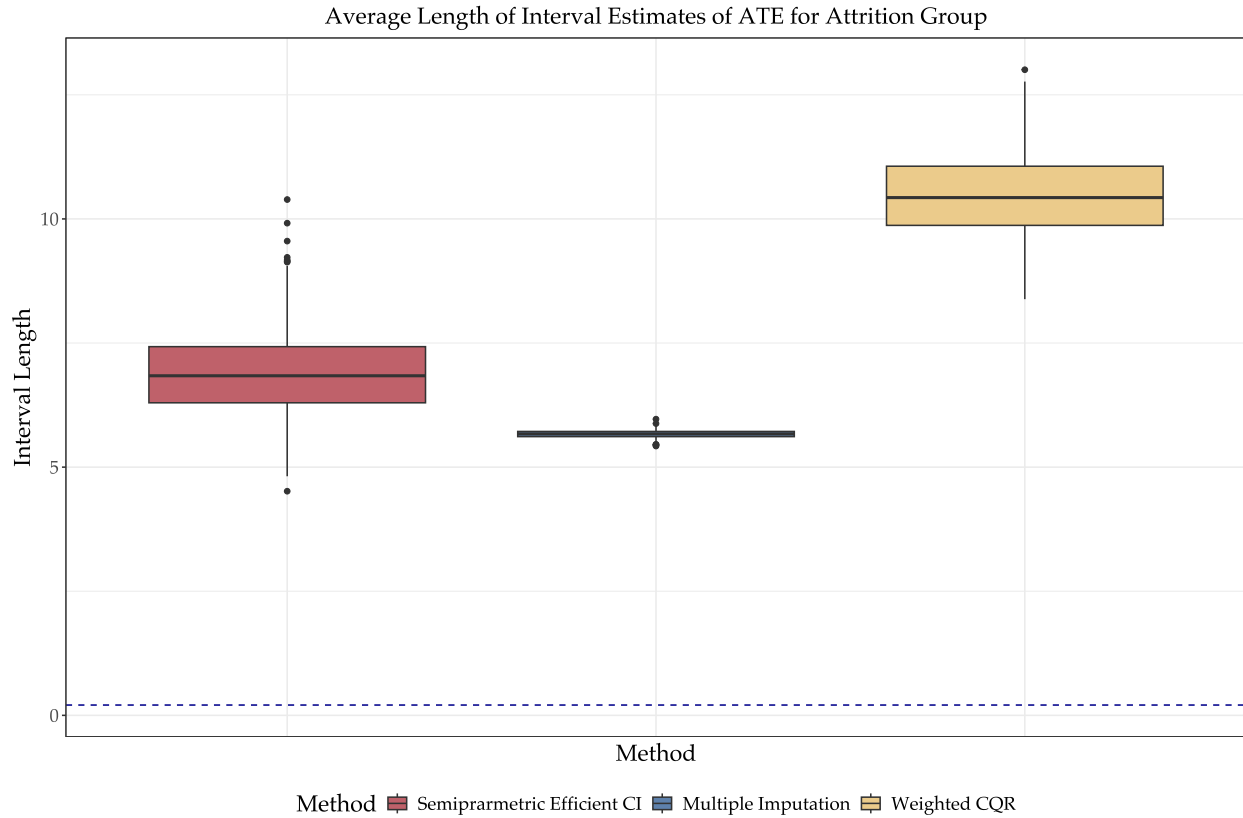
Note: This tables presents the replication results for **Margalit and Shayo (2021)** Table 2 column (4). Column (1) - (3) report point and interval estimates of ATE for observed group (ATER1), attrition group (ATER0), and all observations (ATEall) using conformal inference with semiparametric efficient estimator (CISE), multiple imputation (MI), weighted CQR (WCQR) with unweighted nested approach for interval estimates, and IPW. Column (4) reports the average length of prediction intervals of ATE for the attrition group. The standard errors are reported in parentheses.

in the attrition group. Similarly, we compute the standard error for the empirical coverage and average length of the prediction intervals for ATE in the attrition group across 500 MC simulations.

Table 2 presents the reanalysis results for **Margalit and Shayo (2021)** Table 2 column (4). Among 2,703 participants, 480 participants are in the attrition group, which is 17.8% of the total sample size. As column (4) shows, different from the common knowledge that prediction intervals constructed by conformal inference is much wider than any alternative methods, the average length of the prediction intervals by CISE and MI are comparable, while the average length of the prediction intervals by WCQR is much wider. Although in the simulation studies in the previous section, we show that CISE has the best performance in terms of empirical coverage and average length, we are considering the extreme DGP which violates the normality assumption. However, in this empirical application with real data, MI performs better than simulation studies. This may because the real data is not as extreme as the simulation DGP, and the normality assumption is more likely to hold. Another note is that ATE estimate from IPW is almost the same as the result reported by **Margalit and Shayo (2021)**. However, such an estimate is only for the observed group, which may lead to biased estimates of the overall ATE when there is attrition. Figure 6 shows the simulation results for the average length of prediction intervals constructed by three methods.

ATE estimates are different between groups. For the attrition group, as column (2) shows, the

FIGURE 6: COMPARISON OF AVERAGE LENGTH OF PREDICTION INTERVALS



Note: This figure shows the simulation results for the average length of prediction intervals constructed by conformal inference with semiparametric efficient estimator, multiple imputation with Amelia, and weighted CQR with unweighted nested approach for ITE of attrition group. The blue horizontal line corresponds to the length of oracle intervals.

point estimate by CISE is 0.19, which is almost twice the ATE of the observed group. However, the point estimate of ATE for all observations slightly increases to 0.114 and remains significant at 5% level, which does not change the substantive conclusion when only using the observed group. This may be because that although the attrition group has a larger ATE, it only accounts for 17.8% of the total sample size and the point estimate is not significant at the conventional level.

8.2 Reanalysis of Finkel et al. (2024)

This paper studies how the online civic education induces democratic values and behaviors in new democracies by designing and testing three civic education interventions and using Tunisia as a case study. The authors recruited young Tunisians between 18 and 35 through paid advertisements via the online platforms Facebook and Instagram. In total, 5,069 participants started a baseline survey and 2,073 finished the first and last question of the survey, which leads to a completion

rate of 45.5%. The authors designed three different treatments through exposing participants to different videos emphasizing democracy frames: democracy gain frame, democracy loss frame, and democratic self-efficacy frame, as well as a control group. The outcome variables include evaluations of political regimes and political engagement, broadly. In our empirical application, we focus on the results from Table 2 of [Finkel et al. \(2024, 623\)](#), which compares all treatment groups versus the control group on regime evaluations. The authors considered four measures related to evaluations: democratic regime rating (M1), Ben Ali regime rating (M2), non-democratic regime alternatives (M3), and regime democratic performance (M4).

Table 2 of [Finkel et al. \(2024\)](#) presents estimates of all treatment groups pooled together versus the control group. This reanalysis replicates column (2) - (5), which considers four different measures of regime evaluations with pre-treatment controls: gender, age, education, employment status, prior registration status, prior support for democracy, interest in political matters, and animal-related matters. Similar to the first application, we consider three methods with 500 MC simulations and construct the prediction intervals for ITE in the attrition group. We also aggregate these ITEs to the ATE for the attrition group and compute the standard errors. Similarly, we compute ATE estimates by IPW as a comparison to the estimates reported in their paper. The evaluation of the average length of the prediction intervals for ATE in the attrition group and their standard errors follows the same logic as in the first application.

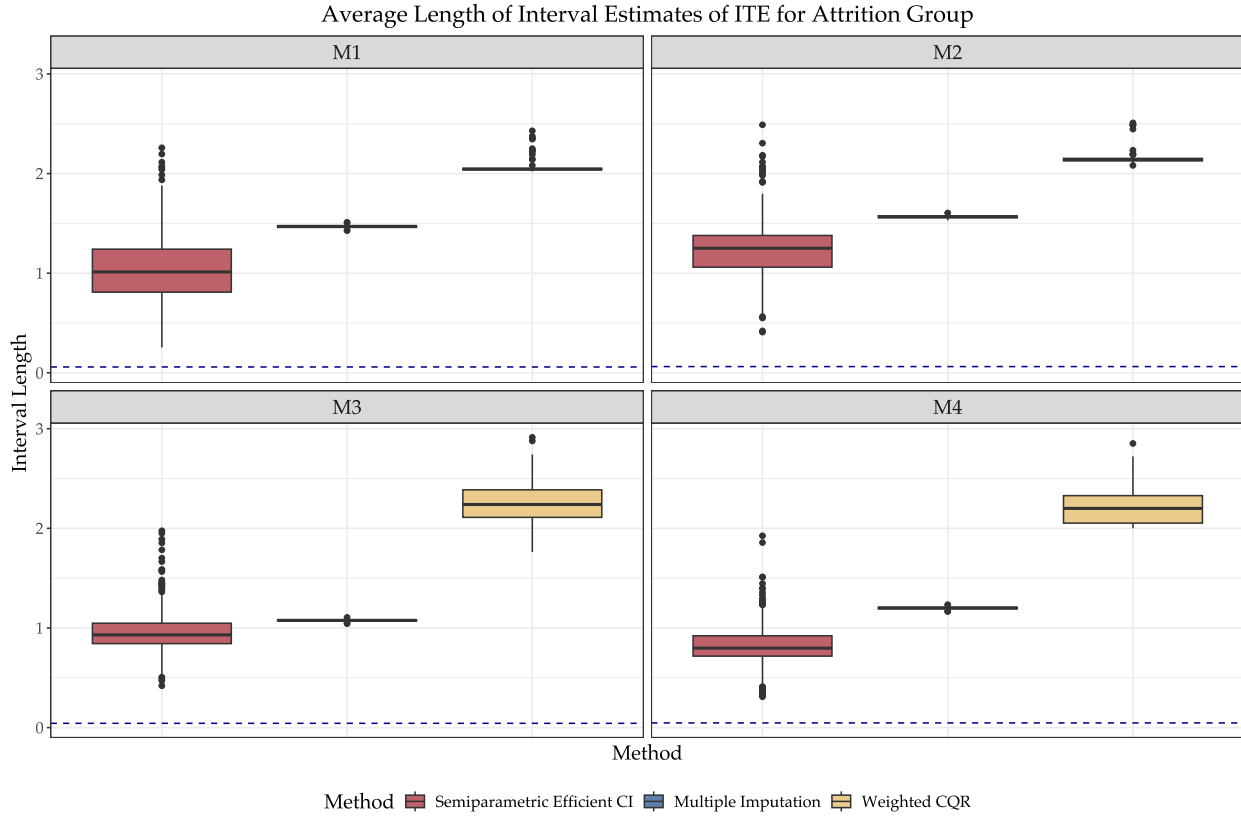
Table 3 presents the reanalysis results for [Finkel et al. \(2024\)](#) Table 2 column (2) - (5). The attrition rates are different for different measures of regime evaluations, which is 36.4% for M1, 40.8% for M2, 40.7% for M3, and 36.8% for M4. As column (4) shows, the average length of the prediction intervals by CISE is shorter than that by MI for all four outcomes in this practice. The average length of the prediction intervals by WCQR is almost twice the length of that by CISE, which is consistent with the simulation results in the previous section. IPW still reports similar ATE estimates for the observed group, but fail to provide estimates for the attrition group and all observations. Figure 7 shows the simulation results for the average length of prediction intervals constructed by three methods. Overall, CISE has the best performance both in terms of empirical coverage and average length.

For ATE estimates, the results for M1 and M4 remain unchanged in both substantive conclusions and significance levels. In contrast, for M2, the ATE estimate for all observations becomes significant at the 1% level, while the ATE for the observed group is only significant at the 5% level. For M3, the ATE for all observations reaches significance at the 5% level, changing the orig-

TABLE 3: REANALYSIS OF FINKEL ET AL. (2024) TABLE 2 COLUMN (2) - (5)

M1 Democratic Regime Rating				
Method	(1) ATER1	(2) ATER0	(3) ATEall	(4) Length
CISE	0.014 (0.015)	0.012 (0.021)	0.013 (0.012)	1.030 (0.333)
MI	0.014 (0.015)	0.005 (0.007)	0.010 (0.009)	1.469 (0.013)
WCQR	0.014 (0.015)	0.018 (0.006)	0.016 (0.009)	2.051 (0.040)
IPW	0.009 (0.015)			
Observations	2,190	1,254	3,444	
M2 Ben Ali Regime Rating				
Method	(1) ATER1	(2) ATER0	(3) ATEall	(4) Length
CISE	-0.041 (0.016)	-0.059 (0.021)	-0.048 (0.013)	1.241 (0.281)
MI	-0.041 (0.016)	-0.035 (0.008)	-0.039 (0.010)	1.566 (0.013)
WCQR	-0.041 (0.016)	-0.069 (0.011)	-0.053 (0.011)	2.143 (0.039)
IPW	-0.037 (0.017)			
Observations	2,197	1,517	3,714	
M3 Non-democratic Regime Alternatives				
Method	(1) ATER1	(2) ATER0	(3) ATEall	(4) Length
CISE	-0.004 (0.011)	-0.078 (0.033)	-0.034 (0.015)	0.963 (0.206)
MI	-0.004 (0.011)	0.003 (0.005)	-0.001 (0.007)	1.076 (0.011)
WCQR	-0.004 (0.011)	-0.064 (0.016)	-0.028 (0.009)	2.249 (0.200)
IPW	-0.004 (0.011)			
Observations	2,203	1,511	3714	
M4 Regime Democratic Performance				
Method	(1) ATER1	(2) ATER0	(3) ATEall	(4) Length
CISE	0.040 (0.012)	0.048 (0.017)	0.043 (0.010)	0.819 (0.219)
MI	0.040 (0.012)	0.039 (0.006)	0.040 (0.008)	1.200 (0.012)
WCQR	0.040 (0.012)	0.024 (0.018)	0.034 (0.010)	2.208 (0.161)
IPW	0.041 (0.013)			
Observations	2,346	1,368	3,714	

FIGURE 7: COMPARISON OF AVERAGE LENGTH OF PREDICTION INTERVALS

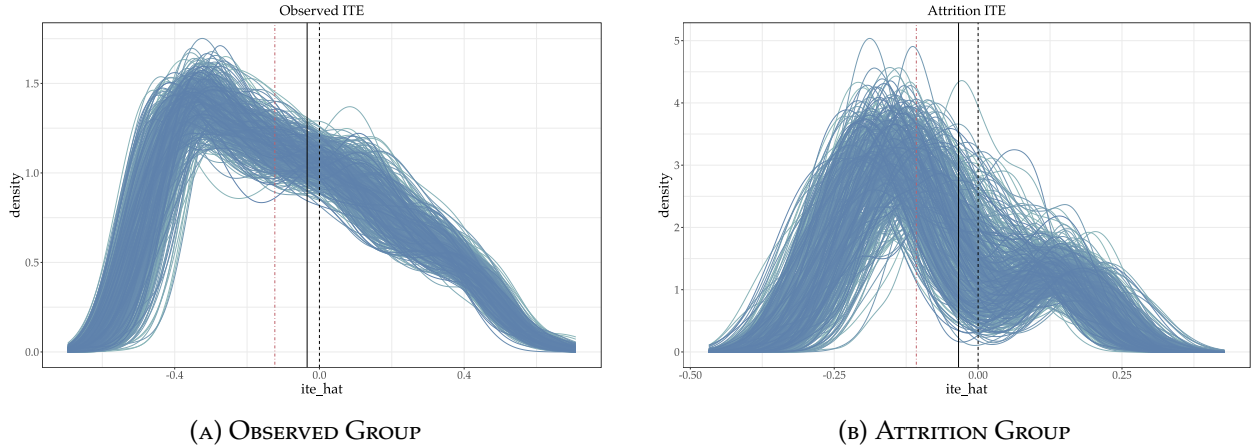


Note: This figure shows the simulation results for the average length of prediction intervals constructed by conformal inference with semiparametric efficient estimator, multiple imputation with Amelia, and weighted QOR with unweighted nested approach for ITE of attrition group. The blue horizontal line corresponds to the length of oracle intervals.

inal substantive conclusion reported by the authors. This shift likely occurs because the ATE for the attrition group is not only statistically significant at conventional levels but also substantially different from that of the observed group.

To understand the heterogeneous ATE estimates for the observed group and the attrition group for M3, we take a step back to analyze the ITEs instead of the ATE. Figure 8 shows the density of ITE estimates for the observed and attrition group across 500 MC simulations. As Panel (B) shows, the ITE estimates for the attrition groups indicate the presence of heterogeneous effects, resulting in a different aggregated ATE. To discover the potential source, we interact the pretreatment covariates with the treatment indicator. Table F.1 shows that those that have expressed a lot of interest in politics experience a larger treatment effect. However, as the regression results in Table F.2 show, we fail to discover a negative interaction term as expected. This may suggest that there are other unobserved confounders leading to the heterogeneous ATE between the observed and the attrition group.

FIGURE 8: ITE ESTIMATES FOR OBSERVED AND ATTRITION GROUPS



Note: These two plots exhibit the density of ITE estimates for the observed and attrition group across 500 MC simulations. The red dotted line denotes the median of the ITE estimates, the black dotted line denotes the ATE estimate for the attrition group (-0.034), and the black solid line denotes.

Overall, these two empirical applications illustrate that the proposed conformal inference with semiparametric efficient estimator can construct prediction intervals for ITE in the attrition group with desired coverage and narrower width, and can easily be aggregated to the ATE of interest for the attrition group. The point and interval estimates of ATE for all observations can be computed as well. The application results also serve as a cautionary note that simply ignoring the attrition group and only using observed group may lead to biased estimates and different substantive conclusions, especially when the attrition rate is high. However, there are also limitations of the proposed method. First, given that the DGP of the real data may satisfy the normality assumption, conformal inference with semiparametric efficient estimator may not always outperform the multiple imputation in interval length. Second, the attrition rate can largely influence both the point and interval estimates of ATE of the attrition group and all observations. When the attrition rate is really high, everything may become noisier for inference. Third, the proposed method can only provide the prediction intervals of ITE for part of the observed group because some data needs to be excluded for the model training and evaluation purpose. Therefore, it is hard to evaluate the coverage and average length of the prediction intervals of ITE or ATE for all observations.

9 Concluding Remarks

Attrition in survey and field experiment is a common problem in political science research. Simply ignoring the missing data induced by attrition and perform complete case analysis may lead to biased and inconsistent estimates, potentially resulting in misleading substantive conclusions. While existing methods such as multiple imputation, inverse probability weighting, and partial identification offer tools to address attrition, they often rely on additional assumptions and typically do not account for the covariate shift between observed and missing data. Employing the conformal inference framework, I identify three primary challenges when the outcomes are missing at random (MAR): (1) the covariate shift problems between treatment groups in observed data, as well as between the observed the attrition group; (2) prediction intervals that are both valid and sufficiently narrow to be practically useful; and (3) the extension of conformal inference to ensure asymptotic properties. This paper addresses these challenges by employing a nonparametric conformal inference approach augmented with a semiparametric efficient estimator to construct valid prediction intervals for causal estimands in the presence of attrition.

Through extensive Monte Carlo simulation studies and empirical applications, I demonstrate that the proposed method can construct prediction intervals for the estimands of interest in the attrition group with both valid coverage and narrower widths. It also outperforms the existing methods like multiple imputation with Amelia II and weighted CQR in terms of empirical coverage and average length. In addition, researchers can easily aggregate the individual-level estimates to the group level and compare the treatment effects among observed, attrited, and all observations. Nevertheless, the approach has several limitations. First, while the method does not require the assumption of ignorability of missingness, it still requires the MAR assumption. Second, when the attrition rate is high, the point and interval estimates could become noisy. Third, due to the data-splitting procedure required for model training and evaluation, it is challenging to construct prediction intervals for all the units in the observed group.

This paper also suggests several avenues for future research. First, extending the conformal inference framework to the missing not at random (MNAR) setting would enhance its robustness and applicability, particularly in cases where attrition is correlated with unobserved confounders (Huber, 2012; Jin et al., 2023). Second, integrating conformal inference with double machine learning could yield a more flexible and robust framework for estimating treatment effects, especially in the presence of high-dimensional nuisance parameters and the need for cross-fitting procedures

(Chernozhukov et al., 2018; Kennedy, 2023). Finally, adapting conformal inference methods to panel data structures would expand their utility for analyzing dynamic processes and handling attrition in longitudinal studies (Chernozhukov et al., 2021).

References

- ANGELOPOULOS, A. N., R. F. BARBER, AND S. BATES (2024): “Theoretical foundations of conformal prediction,” *arXiv preprint arXiv:2411.11824*.
- ANGELOPOULOS, A. N. AND S. BATES (2022): “A gentle introduction to conformal prediction and distribution-free uncertainty quantification,” *arXiv preprint arXiv:2107.07511*.
- ATHEY, S., R. CHETTY, AND G. IMBENS (2020): “Combining Experimental and Observational Data to Estimate Treatment Effects on Long Term Outcomes,” *arXiv preprint arXiv:2006.09676*.
- CHERNOZHUKOV, V., D. CHETVERIKOV, M. DEMIRER, E. DUFLO, C. HANSEN, W. NEWEY, AND J. ROBINS (2018): “Double/Debiased Machine Learning for Treatment and Structural Parameters,” *The Econometrics Journal*, 21, C1–C68.
- CHERNOZHUKOV, V., K. WÜTHRICH, AND Y. ZHU (2021): “An Exact and Robust Conformal Inference Method for Counterfactual and Synthetic Controls,” *Journal of the American Statistical Association*, 116, 1849–1864.
- COPPOCK, A., A. S. GERBER, D. P. GREEN, AND H. L. KERN (2017): “Combining Double Sampling and Bounds to Address Nonignorable Missing Outcomes in Randomized Experiments,” *Political Analysis*, 25, 188–206.
- EGAMI, N. AND E. HARTMAN (2023): “Elements of External Validity: Framework, Design, and Analysis,” *American Political Science Review*, 117, 1070–1088.
- FINKEL, S. E., A. NEUNDORF, AND E. RASCÓN RAMÍREZ (2024): “Can Online Civic Education Induce Democratic Citizenship? Experimental Evidence from a New Democracy,” *American Journal of Political Science*, 68, 613–630.
- FISHER, R. A. (1937): *The Design of Experiments.*, Oliver & Boyd, Edinburgh & London.
- FUKUMOTO, K. (2022): “Nonignorable Attrition in Pairwise Randomized Experiments,” *Political Analysis*, 30, 132–141.
- GAO, C., P. B. GILBERT, AND L. HAN (2025): “On the Role of Surrogates in Conformal Inference of Individual Causal Effects,” *arXiv preprint arXiv:2412.12365*.

- GERBER, A. AND D. GREEN (2012): *Field Experiments: Design, Analysis, and Interpretation*, W. W. Norton.
- GOHDES, A. R. (2020): "Repression Technology: Internet Accessibility and State Violence," *American Journal of Political Science*, 64, 488–503.
- HAUSMAN, J. A. AND D. A. WISE (1979): "Attrition Bias in Experimental and Panel Data: The Gary Income Maintenance Experiment," *Econometrica*, 47, 455–473.
- HECKMAN, J. J. (1979): "Sample Selection Bias as a Specification Error," *Econometrica*, 47, 153–161.
- HOLLAND, P. W. (1986): "Statistics and Causal Inference," *Journal of the American Statistical Association*, 81, 945–960.
- HONAKER, J., G. KING, AND M. BLACKWELL (2011): "Amelia II: A Program for Missing Data," *Journal of Statistical Software*, 45, 1–47.
- HOROWITZ, J. L. AND C. F. MANSKI (1998): "Censoring of Outcomes and Regressors Due to Survey Nonresponse: Identification and Estimation Using Weights and Imputations," *Journal of Econometrics*, 84, 37–58.
- (2000): "Nonparametric Analysis of Randomized Experiments with Missing Covariate and Outcome Data," *Journal of the American Statistical Association*, 95, 77–84.
- HORVITZ, D. G. AND D. J. AND THOMPSON (1952): "A Generalization of Sampling Without Replacement from a Finite Universe," *Journal of the American Statistical Association*, 47, 663–685.
- HUBER, M. (2012): "Identification of Average Treatment Effects in Social Experiments Under Alternative Forms of Attrition," *Journal of Educational and Behavioral Statistics*, 37, 443–474.
- IMAI, K. AND A. STRAUSS (2011): "Estimation of Heterogeneous Treatment Effects from Randomized Experiments, with Application to the Optimal Planning of the Get-Out-the-Vote Campaign," *Political Analysis*, 19, 1–19.
- IMBENS, G. W. (2024): "Causal Inference in the Social Sciences," *Annual Review of Statistics and Its Application*, 11, 123–152.
- IMBENS, G. W. AND D. B. RUBIN (2015): *Causal Inference in Statistics, Social, and Biomedical Sciences*, Cambridge university press.

- JIN, Y., Z. REN, AND E. J. CANDÈS (2023): "Sensitivity Analysis of Individual Treatment Effects: A Robust Conformal Inference Approach," *Proceedings of the National Academy of Sciences*, 120, e2214889120.
- KALLA, J. L. AND D. E. BROCKMAN (2018): "The Minimal Persuasive Effects of Campaign Contact in General Elections: Evidence from 49 Field Experiments," *American Political Science Review*, 112, 148–166.
- KALLUS, N., X. MAO, AND M. UEHARA (2024): "Localized Debiased Machine Learning: Efficient Inference on Quantile Treatment Effects and Beyond," *Journal of Machine Learning Research*, 25, 1–59.
- KENNEDY, E. H. (2023): "Semiparametric Doubly Robust Targeted Double Machine Learning: A Review," *arXiv preprint arXiv:2203.06469*.
- KING, G., J. HONAKER, A. JOSEPH, AND K. SCHEVE (2001): "Analyzing Incomplete Political Science Data: An Alternative Algorithm for Multiple Imputation," *American Political Science Review*, 95, 49–69.
- KOENKER, R. AND G. BASSETT (1978): "Regression Quantiles," *Econometrica*, 46, 33–50.
- KOENKER, R. AND K. F. HALLOCK (2001): "Quantile Regression," *Journal of Economic Perspectives*, 15, 143–156.
- LALONDE, R. J. (1986): "Evaluating the Econometric Evaluations of Training Programs with Experimental Data," *The American Economic Review*, 76, 604–620.
- LEE, D. S. (2009): "Training, Wages, and Sample Selection: Estimating Sharp Bounds on Treatment Effects," *The Review of Economic Studies*, 76, 1071–1102.
- LEI, J., M. G'SELL, A. RINALDO, R. J. TIBSHIRANI, AND L. WASSERMAN (2018): "Distribution-Free Predictive Inference for Regression," *Journal of the American Statistical Association*, 113, 1094–1111.
- LEI, J., J. ROBINS, AND L. WASSERMAN (2013): "Distribution-Free Prediction Sets," *Journal of the American Statistical Association*, 108, 278–287.
- LEI, J. AND L. WASSERMAN (2014): "Distribution-Free Prediction Bands for Non-parametric Regression," *Journal of the Royal Statistical Society Series B: Statistical Methodology*, 76, 71–96.

- LEI, L. AND E. J. CANDÈS (2021): “Conformal Inference of Counterfactuals and Individual Treatment Effects,” *Journal of the Royal Statistical Society Series B: Statistical Methodology*, 83, 911–938.
- MARGALIT, Y. AND M. SHAYO (2021): “How Markets Shape Values and Political Preferences: A Field Experiment,” *American Journal of Political Science*, 65, 473–492.
- MUELLER, L. (2024): “Crowd Cohesion and Protest Outcomes,” *American Journal of Political Science*, 68, 42–57.
- NEWBY, W. K. (1994): “The Asymptotic Variance of Semiparametric Estimators,” *Econometrica*, 62, 1349–1382.
- ROMANO, Y., E. PATTERSON, AND E. CANDÈS (2019): “Conformalized Quantile Regression,” in *Advances in Neural Information Processing Systems*, Curran Associates, Inc., vol. 32.
- ROMANO, Y., M. SESIA, AND E. J. CANDÈS (2020): “Classification with Valid and Adaptive Coverage,” in *Proceedings of the 34th International Conference on Neural Information Processing Systems*, Red Hook, NY, USA: Curran Associates Inc., NIPS ’20, 3581–3591.
- ROSENBAUM, P. R. AND D. B. RUBIN (1983): “The Central Role of the Propensity Score in Observational Studies for Causal Effects,” *Biometrika*.
- RUBIN, D. B. (1974): “Estimating Causal Effects of Treatments in Randomized and Nonrandomized Studies,” *Journal of Educational Psychology*, 66, 688–701.
- (1976): “Inference and Missing Data,” *Biometrika*, 63, 581–592.
- SADINLE, M., J. LEI, AND L. WASSERMAN (2019): “Least Ambiguous Set-Valued Classifiers With Bounded Error Levels,” *Journal of the American Statistical Association*, 114, 223–234.
- SEZIA, M. AND E. J. CANDÈS (2020): “A Comparison of Some Conformal Quantile Regression Methods,” *Stat*, 9, e261.
- SHIMODAIRA, H. (2000): “Improving Predictive Inference under Covariate Shift by Weighting the Log-Likelihood Function,” *Journal of Statistical Planning and Inference*, 90, 227–244.
- SHIN, S. (2024): “Difference-in-Differences Design with Outcomes Missing Not at Random,” *arXiv preprint arXiv:2411.18772*.

- SPLAWA-NEYMAN, J. (1990(1923)): "On the Application of Probability Theory to Agricultural Experiments. Essay on Principles. Section 9, transl. by D. M. Dabrowska and T. P. Speed," *Statistical Science*, 5, 465–472.
- TIBSHIRANI, R. J., R. FOYCEL BARBER, E. CANDES, AND A. RAMDAS (2019): "Conformal Prediction Under Covariate Shift," in *Advances in Neural Information Processing Systems*, Curran Associates, Inc., vol. 32.
- VOVK, V., A. GAMMERMAN, AND C. SAUNDERS (1999): "Machine-Learning Applications of Algorithmic Randomness," in *Proceedings of the Sixteenth International Conference on Machine Learning*, San Francisco, CA, USA: Morgan Kaufmann Publishers Inc., ICML '99, 444–453.
- VOVK, V., I. NOURETDINOV, AND A. GAMMERMAN (2009): "On-Line Predictive Linear Regression," *The Annals of Statistics*, 37, 1566–1590.
- VOVK, V., J. SHEN, V. MANOKHIN, AND M.-G. XIE (2019): "Nonparametric Predictive Distributions Based on Conformal Prediction," *Machine Learning*, 108, 445–474.
- WAGER, S. AND S. ATHEY (2018): "Estimation and Inference of Heterogeneous Treatment Effects Using Random Forests," *Journal of the American Statistical Association*, 113, 1228–1242.
- YANG, Y., A. K. KUCHIBHOTLA, AND E. TCHETGEN TCHETGEN (2024): "Doubly Robust Calibration of Prediction Sets under Covariate Shift," *Journal of the Royal Statistical Society Series B: Statistical Methodology*, 86, 943–965.

Appendix

A Conformal Inference

A.1 Marginal Coverage

Theorem A.1. *Suppose that $(X_1, Y_1), \dots, (X_{n+1}, Y_{n+1})$ are exchangeable and s is a symmetric conformal score function. Then, the prediction interval $\mathcal{C}(X_{n+1})$ satisfies the marginal coverage guarantee,*

$$\mathbb{P}(Y_{n+1} \in \mathcal{C}(X_{n+1})) \geq 1 - \alpha.$$

A.2 Exchangeability

Definition A.1 (Exchangeability). Let $Z_1, \dots, Z_n \in \mathcal{X}$ be random variables with a joint distribution. We say that the random vector (Z_1, \dots, Z_n) is exchangeable if, for every permutation $\sigma \in \mathcal{S}_n$,

$$(Z_1, \dots, Z_n) \stackrel{d}{=} (Z_{\sigma(1)}, \dots, Z_{\sigma(n)}),$$

where $\stackrel{d}{=}$ denotes equality in distribution, and \mathcal{S}_n is the set of all permutations on $[n] := \{1, \dots, n\}$.

Similarly, let $Z_1, Z_2, \dots \in \mathcal{X}$ be an infinite sequence of random variables with joint distribution. We say that this infinite sequence is exchangeable if (Z_1, \dots, Z_n) is exchangeable for every $n \geq 1$.

B Asymptotic Coverage of the Prediction Interval for ITE with Attrition

In line with [Yang et al. \(2024\)](#), we connect the target coverage level $(1 - \gamma)$ and the EIF for $\eta_{\gamma, \mathcal{E}}$.

Lemma B.1. *Let $\pi_R : \{0, 1\} \times \mathcal{X} \rightarrow \mathbb{R}^+$ and $m_{\mathcal{E}} : \{0, 1\} \times \mathcal{X} \times \mathbb{R} \rightarrow [0, 1]$ be any two functions. Then, under Assumption 2 and 3, the following coverage for the EIF $\psi_{\mathcal{E}}(\eta_{\gamma, \mathcal{E}}, X)$.*

$$\mathbb{P}(V_{\mathcal{E}} < \eta_{\gamma, \mathcal{E}} \mid R = 0) = 1 - \gamma + \frac{\mathbb{E}[\psi_{\mathcal{E}}(\eta_{\gamma, \mathcal{E}}, X; m_{\mathcal{E}}, \pi_R)]}{\mathbb{P}(R = 0)},$$

holds true whenever either of the following holds true:

1. $\pi_R(X, D)$ is estimated consistently or
2. $m_{\mathcal{E}}(\eta_{\gamma, \mathcal{E}}, X, D)$ is estimated consistently.

Proof. See Section C.5.1 for the proof of Lemma B.1. □

Lemma B.1 states that the asymptotic coverage of the ITE prediction interval for the attrition group deviates from the nominal level $1 - \gamma$ by a term that is proportional to the expectation of the EIF. It further establishes the double robustness of both the influence function and the resulting coverage: as long as either π_R or $m_{\mathcal{E}}$ is consistently estimated, the desired coverage can be achieved. We have a set of regularity conditions required to ensure the asymptotic coverage of the estimator $\eta_{\gamma, \mathcal{E}}$.

- (A1) The function $(\eta, x) \mapsto \hat{m}_{\mathcal{E}}(\eta, X, D)$ is bounded, i.e., there exists m_0 such that for all $\eta \in \mathbb{R}$ and $x \in \mathbb{R}^d$, $|\hat{m}(\eta, x, d)| \leq m_0$. The function $x \mapsto \hat{\pi}_R(x, d)$ is bounded from below by a positive constant, i.e., there exists $\pi_0 > 0$ such that for all $x \in \mathbb{R}^d$, $|\hat{\pi}_R(x, d)| \geq \pi_0$.
- (A2) The estimator $\hat{m}_{\mathcal{E}}(\eta, x, d)$ is a non-decreasing function of η .

Following the two-step conformal inference framework for constructing interval estimates of the ITE under attrition, Theorem B.1 establishes that the proposed method attains the desired asymptotic coverage for the ITE prediction intervals in the attrition group.

Theorem B.1. *Under Assumption 1 to 3 and regularity conditions (A1) and (A2), there exists some*

universal constants C_0 and C_1 such that for any $\delta > 0$,

$$\begin{aligned} \mathbb{P}(V_{\mathfrak{E}} < \hat{\eta}_{\gamma, \mathfrak{E}} \mid R = 0) &\geq 1 - \gamma \\ &- C_0 \frac{\pi_0^{-1}(1 + m_0)}{\mathbb{P}(R = 0)} \sqrt{\frac{\log(1/\delta) + 1}{|\mathcal{J}_2|}} \\ &- C_1 \frac{\|\hat{\pi}_R(X, D) - \pi_R(X, D)\|_2}{\mathbb{P}(R = 0)} \cdot \sup_{\eta} \|\hat{m}_{\mathfrak{E}}(\hat{\eta}_{\gamma, \mathfrak{E}}, X, D) - m_{\mathfrak{E}}(\hat{\eta}_{\gamma, \mathfrak{E}}, X, D)\|_2 \end{aligned}$$

holds with probability at least $1 - \delta$, where $|\mathcal{J}_2|$ is the Lebesgue measure of the calibration data when conducting conformal inference on the interval estimates of ITE with attrition.

Proof. See Section C.4 for the proof of Theorem B.1. □

C Technical Proofs

C.1 Proof of Lemma 1 and 2

Proof of Lemma 1. The result is immediate following the law of iterated expectations and the unconfoundedness. \square

Proof of Lemma 2. The result is immediate following the law of iterated expectations and the MAR assumption. \square

C.2 Proof of Theorem 1

Proof of Theorem 1. To prove Theorem 1 and derive the EIF, we leverage Gateaux derivatives (directional derivatives) and the Riesz representation theorem.

Define $\mathbb{O} := (X, Y, D, R)$. The efficient influence function is defined as the unique mean-zero function ψ such that the pathwise derivative of the target parameter $\eta_{\alpha,1}$ satisfies:

$$\frac{\partial}{\partial t} \eta_{\alpha,1}(P_t) \Big|_{t=0} = \mathbb{E} [\psi(\mathbb{O}) \cdot s(\mathbb{O})], \quad (\text{C1})$$

where P_t is a perturbation of the true distribution P along a score function $s(\mathbb{O})$, and $s(\mathbb{O})$ is any valid score function. According to [Kennedy \(2023\)](#), the influence function ψ has been referred to as pathwise derivative, gradient, and Neyman orthogonal score (e.g., [Chernozhukov et al., 2018](#); [Newey, 1994](#)).

Define the functional

$$\begin{aligned} \Psi(\mathbb{O}) &:= \mathbb{E} [m_1(\eta_{\alpha,1}, X) \mid D = 0, R = 1] - (1 - \alpha) \\ &= \frac{\mathbb{E} [(m_1(\eta_{\alpha,1}, X) - (1 - \alpha)) \cdot \mathbb{1}_{\{D=0, R=1\}}]}{\mathbb{E} [\mathbb{1}_{\{D=0, R=1\}}]} \\ &= \mathbb{E} [R(1 - D) (m_1(\eta_{\alpha,1}, X) - (1 - \alpha))]. \end{aligned}$$

Then, the parameter $\eta_{\alpha,1}$, which is the $(1 - \alpha)$ -quantile of the nonconformity score $V_1 = V(X, Y(1))$ given $D = 0, R = 1$, is identified by the moment condition

$$\Psi(\mathbb{O}) = \mathbb{E} [R(1 - D) (m_1(\eta_{\alpha,1}, X) - (1 - \alpha))] = 0.$$

Consider a pathwise perturbation of the true distribution P along a score function $s(\mathbb{G})$, where $s(\mathbb{G})$ satisfies:

$$\mathbb{E}[s(\mathbb{G})] = 0, \quad \mathbb{E}[s(\mathbb{G})^2] < \infty.$$

The perturbed distribution is:

$$P_t(\mathbb{G}) = (1 + t \cdot s(\mathbb{G}))P(\mathbb{G}),$$

for small t , ensuring P_t remains a valid probability distribution.

The perturbed parameter $\eta_{\alpha,1}(P_t)$ satisfies the perturbed moment condition:

$$\mathbb{E}_t \left[R(1 - D) \left(m_{1,t}(\eta_{\alpha,1}(P_t), X) - (1 - \alpha) \right) \right] = 0 \quad (\text{C2})$$

To find how $\eta_{\alpha,1}(P_t)$ changes with t , we take the total derivative of the perturbed moment condition at w.r.t. t at $t = 0$:

$$\left. \frac{\partial}{\partial t} \mathbb{E}_t \left[R(1 - D) \left(m_{1,t}(\eta_{\alpha,1}(P_t), X) - (1 - \alpha) \right) \right] \right|_{t=0} = 0. \quad (\text{C3})$$

We have the result that the expectation under P_t of any function $g(\mathbb{G})$ is

$$\begin{aligned} \mathbb{E}_t[g(\mathbb{G})] &= \int g(\mathbb{G})P_t(\mathbb{G})d\mathbb{G} = \int g(\mathbb{G})(1 + t \cdot s(\mathbb{G}))P(\mathbb{G})d\mathbb{G} \\ &= \mathbb{E}[g(\mathbb{G})] + t\mathbb{E}[g(\mathbb{G}) \cdot s(\mathbb{G})]. \end{aligned}$$

Then, for the function $g(\mathbb{G}) = R(1 - D) \left(m_{1,t}(\eta_{\alpha,1}(P_t), X) - (1 - \alpha) \right)$, the perturbed moment condition is

$$\begin{aligned} \mathbb{E}_t \left[R(1 - D) \left(m_{1,t}(\eta_{\alpha,1}(P_t), X) - (1 - \alpha) \right) \right] &= \mathbb{E} \left[R(1 - D) \left(m_1(\eta_{\alpha,1}, X) - (1 - \alpha) \right) \right] \\ &\quad + t\mathbb{E} \left[s(\mathbb{G}) \cdot R(1 - D) \left(m_1(\eta_{\alpha,1}, X) - (1 - \alpha) \right) \right]. \end{aligned}$$

By the chain rule, the derivative of the perturbed moment condition at $t = 0$ has three components: the perturbation of the expectation \mathbb{E} , the perturbation of the conditional probability m_1 , and the perturbation of the quantile $\eta_{\alpha,1}$. So, we can write the total derivatives explicitly. By the

result above, the perturbation of the expectation \mathbb{E} gives

$$\begin{aligned} \text{I} &= \frac{\partial}{\partial t} \mathbb{E}_t \left[R(1-D) (m_{1,t}(\eta_{\alpha,1}(P_t), X) - (1-\alpha)) \right] \Big|_{t=0} \\ &= \mathbb{E} \left[s(\odot) \cdot R(1-D) (m_1(\eta_{\alpha,1}, X) - (1-\alpha)) \right]. \end{aligned}$$

The perturbation of the conditional probability m_1 gives

$$\text{II} = \mathbb{E} \left[R(1-D) \frac{\partial m_{1,t}(\eta_{\alpha,1}, X)}{\partial t} \Big|_{t=0} \right]$$

Under the perturbed distribution P_t , by Bayes' rule, the conditional probability becomes

$$\begin{aligned} m_{1,t}(\eta_{\alpha,1}, X) &= P_t(V_1 < \eta_{\alpha,1} \mid X, D = 1, R = 1) \\ &= \frac{P_t(V_1 < \eta_{\alpha,1}, D = 1, R = 1 \mid X)}{P_t(D = 1, R = 1 \mid X)} \\ &= \frac{\mathbb{E}_t \left[\mathbb{1}_{\{V_1 < \eta_{\alpha,1}\}} DR \mid X \right]}{\mathbb{E}_t [DR \mid X]} \\ &= \frac{\mathbb{E} \left[\mathbb{1}_{\{V_1 < \eta_{\alpha,1}\}} DR \mid X \right] + t \mathbb{E} \left[s(\odot) \cdot \mathbb{1}_{\{V_1 < \eta_{\alpha,1}\}} DR \mid X \right]}{\mathbb{E} [DR \mid X] + t \mathbb{E} [s(\odot) \cdot DR \mid X]} \\ &\approx m_1(\eta_{\alpha,1}, X) + t \left(\frac{\mathbb{E} \left[s(\odot) \cdot \mathbb{1}_{\{V_1 < \eta_{\alpha,1}\}} DR \mid X \right]}{\mathbb{E} [DR \mid X]} - m_1(\eta_{\alpha,1}, X) \cdot \frac{\mathbb{E} [s(\odot) \cdot DR \mid X]}{\mathbb{E} [DR \mid X]} \right), \end{aligned}$$

where the last approximation comes from the first-order Taylor expansion. Then, we take the derivative of $m_{1,t}(\eta_{\alpha,1}, X)$ w.r.t. t at $t = 0$:

$$\begin{aligned} \frac{\partial m_{1,t}(\eta_{\alpha,1}, X)}{\partial t} \Big|_{t=0} &= \frac{\mathbb{E} \left[s(\odot) \cdot \mathbb{1}_{\{V_1 < \eta_{\alpha,1}\}} DR \mid X \right]}{\mathbb{E} [DR \mid X]} - m_1(\eta_{\alpha,1}, X) \cdot \frac{\mathbb{E} [s(\odot) \cdot DR \mid X]}{\mathbb{E} [DR \mid X]} \\ &= \mathbb{E} \left[s(\odot) \cdot \left(\frac{\mathbb{1}_{\{V_1 < \eta_{\alpha,1}\}} DR}{\mathbb{E} [DR \mid X]} - m_1(\eta_{\alpha,1}, X) \cdot \frac{DR}{\mathbb{E} [DR \mid X]} \right) \mid X \right] \\ &= \mathbb{E} \left[s(\odot) \cdot \left(\mathbb{1}_{\{V_1 < \eta_{\alpha,1}\}} - m_1(\eta_{\alpha,1}, X) \right) \cdot \frac{DR}{P(D = 1, R = 1 \mid X)} \mid X \right]. \end{aligned}$$

Then, plug in to Π , we have

$$\begin{aligned}
\Pi &= \mathbb{E} \cdot \left[R(1 - D) \mathbb{E} \left[s(\odot) \cdot \left(\mathbb{1}_{\{V_1 < \eta_{\alpha,1}\}} - m_1(\eta_{\alpha,1}, X) \right) \cdot \frac{DR}{P(D = 1, R = 1 | X)} \mid X \right] \right] \\
&= \mathbb{E} \left[s(\odot) \cdot DR \cdot \frac{P(D = 0, R = 1 | X)}{P(D = 1, R = 1 | X)} \cdot \left(\mathbb{1}_{\{V_1 < \eta_{\alpha,1}\}} - m_1(\eta_{\alpha,1}, X) \right) \right] \\
&= \mathbb{E} \left[s(\odot) \cdot DR \cdot \frac{(1 - e_D(X))e_R(X, 0)}{e_D(X)e_R(X, 1)} \cdot \left(\mathbb{1}_{\{V_1 < \eta_{\alpha,1}\}} - m_1(\eta_{\alpha,1}, X) \right) \right] \\
&= \mathbb{E} \left[s(\odot) \cdot DR \cdot \frac{e_R(X, 0)}{\pi_D(X)e_R(X, 1)} \cdot \left(\mathbb{1}_{\{V_1 < \eta_{\alpha,1}\}} - m_1(\eta_{\alpha,1}, X) \right) \right].
\end{aligned}$$

The perturbation of the quantile $\eta_{\alpha,1}$ gives

$$\begin{aligned}
\text{III} &= \mathbb{E} \left[R(1 - D) \frac{\partial m_1(\eta_{\alpha,1}, X)}{\partial \eta} \cdot \frac{\partial \eta_{\alpha,1}(P_t)}{\partial t} \Big|_{t=0} \right] \\
&\propto \frac{\partial}{\partial t} \eta_{\alpha,1}(P_t).
\end{aligned}$$

Therefore, the total derivative of the perturbed moment condition at $t = 0$ is

$$\frac{\partial}{\partial t} \mathbb{E}_t \left[R(1 - D) (m_{1,t}(\eta_{\alpha,1}(P_t), X) - (1 - \alpha)) \right] \Big|_{t=0} = 0 = \text{I} + \text{II} + \text{III}.$$

Then,

$$\begin{aligned}
&\frac{\partial}{\partial t} \eta_{\alpha,1}(P_t) \propto \\
&-\mathbb{E} \left[s(\odot) \cdot \left\{ R(1 - D) (m_1(\eta_{\alpha,1}, X) - (1 - \alpha)) + \frac{DR e_R(X, 0)}{\pi_D(X) e_R(X, 1)} \cdot \left(\mathbb{1}_{\{V_1 < \eta_{\alpha,1}\}} - m_1(\eta_{\alpha,1}, X) \right) \right\} \right]
\end{aligned}$$

By the Riesz representation theorem and Equation **C1**, the efficient influence function ψ is given by

$$\begin{aligned}
\psi(\eta_{\alpha,1}, X; m, e_R, \pi_D) &= \\
&R(1 - D) (m_1(\eta_{\alpha,1}, X) - (1 - \alpha)) + \frac{DR e_R(X, 0)}{\pi_D(X) e_R(X, 1)} \cdot \left(\mathbb{1}_{\{V_1 < \eta_{\alpha,1}\}} - m_1(\eta_{\alpha,1}, X) \right).
\end{aligned}$$

The EIF under $D = 0$ follows the same derivation. There are other ways to derive the EIF. See [Gao et al. \(2025\)](#) for a proof using parametric submodels and tangent spaces from a Hilbert space perspective. \square

C.3 Proof of Theorem 2

Proof of Theorem 2. The proof follows the same steps as in Theorem 1.

The $(1 - \gamma)$ -quantile of the nonconformity score $V_{\mathfrak{E}} = V(X, \mathfrak{E}_i)$ for the attrition group $R = 0$ is identified by the moment condition

$$\begin{aligned} \mathbb{E} \left[m_{\mathfrak{E}}(\eta_{\gamma, \mathfrak{E}}, X, D) \mid R = 0 \right] - (1 - \gamma) &= 0 \\ \Rightarrow \mathbb{E} \left[(1 - R) \left(m_{\mathfrak{E}}(\eta_{\gamma, \mathfrak{E}}, X, D) - (1 - \gamma) \right) \right] &= 0. \end{aligned}$$

Consider a pathwise perturbation of the true distribution P along a score function $s(\mathfrak{G})$, where $s(\mathfrak{G})$ satisfies:

$$\mathbb{E}[s(\mathfrak{G})] = 0, \quad \mathbb{E} \left[s(\mathfrak{G})^2 \right] < \infty.$$

The perturbed distribution is:

$$P_t(\mathfrak{G}) = (1 + t \cdot s(\mathfrak{G}))P(\mathfrak{G}),$$

for small t , ensuring P_t remains a valid probability distribution.

Under P_t , the moment condition becomes

$$\mathbb{E}_t \left[(1 - R) \left(m_{\mathfrak{E}, t}(\eta_{\gamma, \mathfrak{E}}(P_t), X, D) - (1 - \gamma) \right) \right] = 0.$$

To find how $\eta_{\gamma, \mathfrak{E}}(P_t)$ changes with t , we take the total derivative of the perturbed moment condition at w.r.t. t at $t = 0$:

$$\left. \frac{\partial}{\partial t} \mathbb{E}_t \left[(1 - R) \left(m_{\mathfrak{E}, t}(\eta_{\gamma, \mathfrak{E}}(P_t), X, D) - (1 - \gamma) \right) \right] \right|_{t=0} = 0.$$

By the results shown in Theorem 1, we have

$$\begin{aligned} \mathbb{E}_t \left[(1 - R) \left(m_{\mathfrak{E}, t}(\eta_{\gamma, \mathfrak{E}}(P_t), X, D) - (1 - \gamma) \right) \right] &= \mathbb{E} \left[(1 - R) \left(m_{\mathfrak{E}}(\eta_{\gamma, \mathfrak{E}}, X, D) - (1 - \gamma) \right) \right] \\ &\quad + t \mathbb{E} \left[s(\mathfrak{G}) \cdot (1 - R) \left(m_{\mathfrak{E}}(\eta_{\gamma, \mathfrak{E}}, X, D) - (1 - \gamma) \right) \right]. \end{aligned}$$

Then, by the chain rule, the derivative of the perturbed moment condition at $t = 0$ has three components: the perturbation of the expectation \mathbb{E} , the perturbation of the conditional probability $m_{\mathfrak{E}}$, and the perturbation of the quantile $\eta_{\gamma, \mathfrak{E}}$. So, we can write the total derivatives explicitly.

By the result above, the perturbation of the expectation \mathbb{E} gives

$$\begin{aligned} \text{I} &= \frac{\partial}{\partial t} \mathbb{E}_t \left[(1-R) (m_{\mathcal{G}}(\eta_{\gamma, \mathcal{G}}, X, D) - (1-\gamma)) \right] \Big|_{t=0} \\ &= \mathbb{E} \left[s(\mathcal{G}) \cdot (1-R) (m_{\mathcal{G}}(\eta_{\gamma, \mathcal{G}}, X, D) - (1-\gamma)) \right]. \end{aligned}$$

Then perturbation of the conditional probability $m_{\mathcal{G}}$ gives

$$\text{II} = \mathbb{E} \left[(1-R) \frac{\partial m_{\mathcal{G},t}(\eta_{\gamma, \mathcal{G}}, X, D)}{\partial t} \Big|_{t=0} \right].$$

Under the perturbed distribution P_t , by Bayes' rule, the conditional probability becomes

$$\begin{aligned} m_{\mathcal{G},t}(\eta_{\gamma, \mathcal{G}}, X, D) &= P_t(V_{\mathcal{G}} < \eta_{\gamma, \mathcal{G}} \mid X, D, R = 1) \\ &= \frac{P_t(V_{\mathcal{G}} < \eta_{\gamma, \mathcal{G}}, R = 1)}{P_t(R = 1 \mid X, D)} \\ &= \frac{\mathbb{E}_t \left[\mathbf{1}_{\{V_{\mathcal{G}} < \eta_{\gamma, \mathcal{G}}\}} R \mid X, D \right]}{\mathbb{E}_t [R \mid X, D]} \\ &= \frac{\mathbb{E} \left[\mathbf{1}_{\{V_{\mathcal{G}} < \eta_{\gamma, \mathcal{G}}\}} R \mid X, D \right] + t \mathbb{E} \left[s(\mathcal{G}) \cdot \mathbf{1}_{\{V_{\mathcal{G}} < \eta_{\gamma, \mathcal{G}}\}} R \mid X, D \right]}{\mathbb{E}[R \mid X, D] + t \mathbb{E}[s(\mathcal{G}) \cdot R \mid X, D]} \\ &\approx m_{\mathcal{G}}(\eta_{\gamma, \mathcal{G}}, X, D) + t \left(\frac{\mathbb{E} \left[s(\mathcal{G}) \cdot \mathbf{1}_{\{V_{\mathcal{G}} < \eta_{\gamma, \mathcal{G}}\}} R \mid X, D \right]}{\mathbb{E}[R \mid X, D]} - m_{\mathcal{G}}(\eta_{\gamma, \mathcal{G}}, X, D) \cdot \frac{\mathbb{E}[s(\mathcal{G}) \cdot R \mid X, D]}{\mathbb{E}[R \mid X, D]} \right), \end{aligned}$$

where the last approximation comes from the first-order Taylor expansion. Then, taking the derivative of $m_{\mathcal{G},t}(\eta_{\gamma, \mathcal{G}}, X, D)$ w.r.t. t at $t = 0$:

$$\begin{aligned} \frac{\partial m_{\mathcal{G},t}(\eta_{\gamma, \mathcal{G}}, X, D)}{\partial t} \Big|_{t=0} &= \frac{\mathbb{E} \left[s(\mathcal{G}) \cdot R \left(\mathbf{1}_{\{V_{\mathcal{G}} < \eta_{\gamma, \mathcal{G}}\}} - m_{\mathcal{G}}(\eta_{\gamma, \mathcal{G}}, X, D) \right) \mid X, D \right]}{\mathbb{E}[R \mid X, D]} \\ &= \mathbb{E} \left[s(\mathcal{G}) \cdot \frac{R}{e_R(X, D)} \left(\mathbf{1}_{\{V_{\mathcal{G}} < \eta_{\gamma, \mathcal{G}}\}} - m_{\mathcal{G}}(\eta_{\gamma, \mathcal{G}}, X, D) \right) \mid X \right]. \end{aligned}$$

Plug into II, we have

$$\begin{aligned}
\Pi &= \mathbb{E} \left[(1 - R) \mathbb{E} \left[s(\mathbb{G}) \cdot \frac{R}{e_R(X, D)} \left(\mathbb{1}_{\{V_{\mathbb{G}} < \eta_{\gamma, \mathbb{G}}\}} - m_{\mathbb{G}}(\eta_{\gamma, \mathbb{G}}, X, D) \right) \mid X, D \right] \right] \\
&= \mathbb{E} \left[s(\mathbb{G}) \cdot R \frac{1 - e_R(X, D)}{e_R(X, D)} \left(\mathbb{1}_{\{V_{\mathbb{G}} < \eta_{\gamma, \mathbb{G}}\}} - m_{\mathbb{G}}(\eta_{\gamma, \mathbb{G}}, X, D) \right) \right] \\
&= \mathbb{E} \left[s(\mathbb{G}) \cdot \frac{R}{\pi_R(X, D)} \left(\mathbb{1}_{\{V_{\mathbb{G}} < \eta_{\gamma, \mathbb{G}}\}} - m_{\mathbb{G}}(\eta_{\gamma, \mathbb{G}}, X, D) \right) \right]
\end{aligned}$$

The perturbation of the quantile $\eta_{\gamma, \mathbb{G}}$ gives

$$\begin{aligned}
\text{III} &= \mathbb{E} \left[R \frac{\partial m_{\mathbb{G}}(\eta_{\gamma, \mathbb{G}}, X, D)}{\partial \eta} \frac{\partial \eta_{\gamma, \mathbb{G}}(P_t)}{\partial t} \Bigg|_{t=0} \right] \\
&\propto \frac{\partial}{\partial t} \eta_{\gamma, \mathbb{G}}(P_t).
\end{aligned}$$

Therefore, the total derivative of the perturbed moment condition at $t = 0$ is

$$\frac{\partial}{\partial t} \mathbb{E}_t \left[(1 - R) (m_{\mathbb{G}, t}(\eta_{\gamma, \mathbb{G}}(P_t), X, D) - (1 - \gamma)) \right] \Bigg|_{t=0} = 0 = \text{I} + \text{II} + \text{III}.$$

Then,

$$\begin{aligned}
&\frac{\partial}{\partial t} \eta_{\gamma, \mathbb{G}}(P_t) \\
&\propto -\mathbb{E} \left[s(\mathbb{G}) \cdot \left\{ (1 - R) (m_{\mathbb{G}}(\eta_{\gamma, \mathbb{G}}, X, D) - (1 - \gamma)) + \frac{R}{\pi_R(X, D)} \cdot \left(\mathbb{1}_{\{V_{\mathbb{G}} < \eta_{\gamma, \mathbb{G}}\}} - m_{\mathbb{G}}(\eta_{\gamma, \mathbb{G}}, X, D) \right) \right\} \right].
\end{aligned}$$

By the Riesz representation theorem, the efficient influence function $\psi_{\mathbb{G}}$ is given by

$$\begin{aligned}
\psi_{\mathbb{G}}(\eta_{\gamma, \mathbb{G}}, X; m_{\mathbb{G}}, e_R, \pi_R) &= (1 - R) (m_{\mathbb{G}}(\eta_{\gamma, \mathbb{G}}, X, D) - (1 - \gamma)) \\
&\quad + \frac{R}{\pi_R(X, D)} \cdot \left(\mathbb{1}_{\{V_{\mathbb{G}} < \eta_{\gamma, \mathbb{G}}\}} - m_{\mathbb{G}}(\eta_{\gamma, \mathbb{G}}, X, D) \right).
\end{aligned}$$

□

C.4 Proof of Theorem B.1

Proof of Theorem B.1. By Lemma B.1, we can obtain that for the empirically estimated $\hat{\eta}_{\gamma, \mathcal{E}}$ using the calibration data \mathcal{J}_2 for conducting conformal inference on the attrition group,

$$\begin{aligned} \mathbb{P}(V_{\mathcal{E}} < \hat{\eta}_{\gamma, \mathcal{E}} \mid R = 0) - (1 - \gamma) &= \frac{\mathbb{P}_{\mathcal{J}_2} [\psi_{\mathcal{E}}(\hat{\eta}_{\gamma, \mathcal{E}}, X; \hat{m}_{\mathcal{E}}, \hat{\pi}_R)]}{\mathbb{P}(R = 0)} \\ &+ \frac{\mathbb{E} [\psi_{\mathcal{E}}(\hat{\eta}_{\gamma, \mathcal{E}}, X; \hat{m}_{\mathcal{E}}, \hat{\pi}_R)] - \mathbb{P}_{\mathcal{J}_2} [\psi_{\mathcal{E}}(\hat{\eta}_{\gamma, \mathcal{E}}, X; \hat{m}_{\mathcal{E}}, \hat{\pi}_R)]}{\mathbb{P}(R = 0)} \\ &+ \frac{\mathbb{E} [\psi(\hat{\eta}_{\gamma, \mathcal{E}}, X; m_{\mathcal{E}}, \pi_R)] - \mathbb{E} [\psi_{\mathcal{E}}(\hat{\eta}_{\gamma, \mathcal{E}}, X; \hat{m}_{\mathcal{E}}, \hat{\pi}_R)]}{\mathbb{P}(R = 0)} \\ &\geq 0 + \text{I} + \text{II}, \end{aligned}$$

where $\mathbb{P}_{\mathcal{J}_2}[\cdot]$ denotes the sample mean over the calibration data. Here, $\mathbb{P}_{\mathcal{J}_2} [\psi_{\mathcal{E}}(\hat{\eta}_{\gamma, \mathcal{E}}, X; \hat{m}_{\mathcal{E}}, \hat{\pi}_R)] \geq 0$ by definition. Term I is negligible if $\psi_{\mathcal{E}}(\eta_{\gamma, \mathcal{E}}, X; m_{\mathcal{E}}, \pi_R)$ belongs to a Donsker class. If the Donsker condition is not satisfied, the sample splitting procedure proposed by Chernozhukov et al. (2018) can be used to ensure that I is negligible, i.e., use \mathcal{J}_1 for estimation and \mathcal{J}_2 for estimation of $\eta_{\gamma, \mathcal{E}}$. See Lemma C.1 for more details on the bound of I.

Term II is the second-order remainder term, which is negligible if the s $m_{\mathcal{E}}(\eta_{\gamma, \mathcal{E}}, X, D)$ and $\pi_R(X, D)$ are estimated consistently.

$$\begin{aligned} &\mathbb{E} [\psi_{\mathcal{E}}(\hat{\eta}_{\gamma, \mathcal{E}}, X; \hat{m}_{\mathcal{E}}, \hat{\pi}_R)] - \mathbb{E} [\psi(\hat{\eta}_{\gamma, \mathcal{E}}, X; m_{\mathcal{E}}, \pi_R)] \\ &= \mathbb{E} [\mathbb{P}(R = 0 \mid X, D) [\hat{m}_{\mathcal{E}}(\hat{\eta}_{\gamma, \mathcal{E}}, X, D) - m_{\mathcal{E}}(\hat{\eta}_{\gamma, \mathcal{E}}, X, D)]] \\ &+ \mathbb{E} \left[\mathbb{P}(R = 1 \mid X, D) \cdot \frac{1}{\pi_R(X, D)} (m_{\mathcal{E}}(\hat{\eta}_{\gamma, \mathcal{E}}, X, D) - \hat{m}_{\mathcal{E}}(\hat{\eta}_{\gamma, \mathcal{E}}, X, D)) \right] \\ &+ \mathbb{E} \left[\mathbb{P}(R = 1 \mid X, D) \cdot \left(\frac{1}{\hat{\pi}_R(X, D)} - \frac{1}{\pi_R(X, D)} \right) \left(\mathbb{1}_{\{V_{\mathcal{E}} < \hat{\eta}_{\gamma, \mathcal{E}}\}} - \hat{m}_{\mathcal{E}}(\hat{\eta}_{\gamma, \mathcal{E}}, X, D) \right) \right] \\ &= \mathbb{E} \left[\mathbb{P}(R = 1 \mid X, D) \cdot \left(\frac{1}{\hat{\pi}_R(X, D)} - \frac{1}{\pi_R(X, D)} \right) (m_{\mathcal{E}}(\hat{\eta}_{\gamma, \mathcal{E}}, X, D) - \hat{m}_{\mathcal{E}}(\hat{\eta}_{\gamma, \mathcal{E}}, X, D)) \right]. \end{aligned}$$

Therefore,

$$\begin{aligned}
& \sup_{\eta_{\gamma, \mathfrak{E}} \in \mathbb{R}} \left| \mathbb{E} \left[\psi_{\mathfrak{E}}(\hat{\eta}_{\gamma, \mathfrak{E}}, X; \hat{m}_{\mathfrak{E}}, \hat{\pi}_R) \right] - \mathbb{E} \left[\psi(\hat{\eta}_{\gamma, \mathfrak{E}}, X; m_{\mathfrak{E}}, \pi_R) \right] \right| \\
&= \sup_{\eta_{\gamma, \mathfrak{E}} \in \mathbb{R}} \left| \mathbb{E} \left[\mathbb{P}(R = 1 \mid X, D) \cdot \left(\frac{1}{\hat{\pi}_R(X, D)} - \frac{1}{\pi_R(X, D)} \right) (m_{\mathfrak{E}}(\hat{\eta}_{\gamma, \mathfrak{E}}, X, D) - \hat{m}_{\mathfrak{E}}(\hat{\eta}_{\gamma, \mathfrak{E}}, X, D)) \right] \right| \\
&\lesssim \|\hat{\pi}_R(X, D) - \pi_R(X, D)\|_2 \cdot \sup_{\eta_{\gamma, \mathfrak{E}}} \|\hat{m}_{\mathfrak{E}}(\hat{\eta}_{\gamma, \mathfrak{E}}, X, D) - m_{\mathfrak{E}}(\hat{\eta}_{\gamma, \mathfrak{E}}, X, D)\|_2,
\end{aligned}$$

where the last inequality follows from the Mean Value Theorem and the Hölder's inequality.

Combining the bounds for I and II, we have

$$\begin{aligned}
\mathbb{P}(V_{\mathfrak{E}} < \hat{\eta}_{\gamma, \mathfrak{E}} \mid R = 0) &\geq 1 - \gamma \\
&- C_0 \frac{\pi_0^{-1}(1 + m_0)}{\mathbb{P}(R = 0)} \sqrt{\frac{\log(1/\delta) + 1}{|\mathcal{J}_2|}} \\
&- C_1 \frac{\|\hat{\pi}_R(X, D) - \pi_R(X, D)\|_2}{\mathbb{P}(R = 0)} \cdot \sup_{\eta} \|\hat{m}_{\mathfrak{E}}(\hat{\eta}_{\gamma, \mathfrak{E}}, X, D) - m_{\mathfrak{E}}(\hat{\eta}_{\gamma, \mathfrak{E}}, X, D)\|_2
\end{aligned}$$

with probability at least $1 - \delta$.

□

C.5 Additional Technical Details

C.5.1 Proof of Lemma B.1

Firstly, we can show that

$$\begin{aligned}
\mathbb{P}(V_{\mathfrak{E}} < \eta_{\gamma, \mathfrak{E}} \mid R = 0) &= \mathbb{E} \left[\mathbb{E} [V_{\mathfrak{E}} < \eta_{\gamma, \mathfrak{E}} \mid X, D, R = 0] \mid R = 0 \right] \\
&\stackrel{\text{Assumption 2}}{=} \mathbb{E} \left[\mathbb{E} [V_{\mathfrak{E}} < \eta_{\gamma, \mathfrak{E}} \mid X, D, R = 1] \mid R = 0 \right] \\
&= \int \int_{-\infty}^{\eta_{\gamma, \mathfrak{E}}} f(\eta_{\mathfrak{E}} \mid x, d, R = 1) d\eta_{\mathfrak{E}} dP_{X, D \mid R=0}(x, d) \\
&= \int \int_{-\infty}^{\eta_{\gamma, \mathfrak{E}}} \frac{f(x, d \mid R = 0)}{f(x, d \mid R = 1)} f(\eta_{\mathfrak{E}} \mid x, d, R = 1) d\eta_{\mathfrak{E}} dP_{X, D \mid R=1}(x, d) \\
&= \mathbb{E} \left[\frac{f(X, D \mid R = 0)}{f(X, D \mid R = 1)} \cdot \mathbb{1}_{\{V_{\mathfrak{E}} < \eta_{\gamma, \mathfrak{E}}\}} \mid R = 1 \right].
\end{aligned} \tag{C4}$$

On the other hand, we can show that

$$\mathbb{E} [\psi_{\mathcal{E}} (\eta_{\gamma, \mathcal{E}}, X; m_{\mathcal{E}}, \pi_R)] = \mathbb{P}(R = 0) \cdot \left\{ \mathbb{E} \left[\frac{f(X, D | R = 0)}{f(X, D | R = 1)} \cdot \mathbb{1}_{\{V_{\mathcal{E}} < \eta_{\gamma, \mathcal{E}}\}} \mid R = 1 \right] - (1 - \gamma) \right\}. \quad (\text{C5})$$

Combining Equation (C4) and (C5) completes the proof. We prove Equation (C5) in two steps.

$$\mathbb{E} [\psi_{\mathcal{E}} (\eta_{\gamma, \mathcal{E}}, X; m_{\mathcal{E}}, \pi_R)] = \mathbb{E} [\mathbb{P}(R = 0 | X, D) (\mathbb{P}(V_{\mathcal{E}} < \eta_{\gamma, \mathcal{E}} | X, D, R = 1) - (1 - \gamma))], \quad (\text{C5.1})$$

and

$$\begin{aligned} & \mathbb{E} [\mathbb{P}(R = 0 | X, D) (\mathbb{P}(V_{\mathcal{E}} < \eta_{\gamma, \mathcal{E}} | X, D, R = 1) - (1 - \gamma))] \\ &= \mathbb{P}(R = 0) \cdot \left\{ \mathbb{E} \left[\frac{f(X, D | R = 0)}{f(X, D | R = 1)} \cdot \mathbb{1}_{\{V_{\mathcal{E}} < \eta_{\gamma, \mathcal{E}}\}} \mid R = 1 \right] - (1 - \gamma) \right\} \end{aligned} \quad (\text{C5.2})$$

For Equation (C5.1), if $\pi_R(X, D) = \frac{\mathbb{P}(R=1|X,D)}{\mathbb{P}(R=0|X,D)}$ is correct, then we have

$$\mathbb{E} \left[\frac{R}{\pi_R(X, D)} \mid X, D \right] = \mathbb{P}(R = 1 | X, D) \cdot \frac{\mathbb{P}(R = 0 | X, D)}{\mathbb{P}(R = 1 | X, D)} = \mathbb{P}(R = 0 | X, D).$$

This implies that

$$\begin{aligned} & \mathbb{E} \left[\frac{R}{\pi_R(X, D)} \left[\mathbb{1}_{\{V_{\mathcal{E}} < \eta_{\gamma, \mathcal{E}}\}} - m_{\mathcal{E}}(\eta_{\gamma, \mathcal{E}}, X, D) \right] \right] \\ &= \mathbb{E} [\mathbb{P}(R = 0 | X, D) [\mathbb{P}(V_{\mathcal{E}} < \eta_{\gamma, \mathcal{E}} | X, D, R = 1) - m_{\mathcal{E}}(\eta_{\gamma, \mathcal{E}}, X, D)]]]. \end{aligned}$$

Similarly,

$$\mathbb{E} [(1 - R) [m_{\mathcal{E}}(\eta_{\gamma, \mathcal{E}}, X, D) - (1 - \gamma)]] = \mathbb{E} [\mathbb{P}(R = 0 | X, D) [m_{\mathcal{E}}(\eta_{\gamma, \mathcal{E}}, X, D) - (1 - \gamma)]].$$

Hence, if $\pi_R(\cdot)$ is the true density ratio, we have

$$\mathbb{E} [\psi_{\mathcal{E}} (\eta_{\gamma, \mathcal{E}}, X; m_{\mathcal{E}}, \pi_R)] = \mathbb{E} [\mathbb{P}(R = 0 | X, D) (\mathbb{P}(V_{\mathcal{E}} < \eta_{\gamma, \mathcal{E}} | X, D, R = 1) - (1 - \gamma))].$$

This completes the proof of Equation (C5.1) when $\pi_R(\cdot)$ is estimated correctly.

If the conditional mean $m_{\mathcal{E}}(\eta_{\gamma, \mathcal{E}}, X, D) = \mathbb{E} [\mathbb{1}_{\{V_{\mathcal{E}} < \eta_{\gamma, \mathcal{E}}\}} \mid X, D, R = 1]$ is correct, then we have

$$\mathbb{E} \left[\frac{R}{\pi_R(X, D)} \left[\mathbb{1}_{\{V_{\mathcal{E}} < \eta_{\gamma, \mathcal{E}}\}} - m_{\mathcal{E}}(\eta_{\gamma, \mathcal{E}}, X, D) \right] \right] = 0$$

Hence,

$$\begin{aligned}\mathbb{E} [\psi_{\mathfrak{E}} (\eta_{\gamma, \mathfrak{E}}, X; m_{\mathfrak{E}}, \pi_R)] &= \mathbb{E} [(1 - R) [m_{\mathfrak{E}} (\eta_{\gamma, \mathfrak{E}}, X, D) - (1 - \gamma)]] \\ &= \mathbb{E} [\mathbb{P}(R = 0 | X, D) [\mathbb{P}(V_{\mathfrak{E}} < \eta_{\gamma, \mathfrak{E}} | X, D, R = 1) - (1 - \gamma)]] .\end{aligned}$$

This completes the proof of Equation (C5.1) when $m_{\mathfrak{E}}(\cdot)$ is estimated correctly.

Then, for Equation (C5.2), we can show that

$$\begin{aligned}& \mathbb{E} [\mathbb{P}(R = 0 | X, D) [\mathbb{P}(V_{\mathfrak{E}} < \eta_{\gamma, \mathfrak{E}} | X, D, R = 1) - (1 - \gamma)]] \\ &= \mathbb{E} \left[R \cdot \frac{\mathbb{P}(R = 0 | X, D)}{\mathbb{P}(R = 1 | X, D)} \cdot \mathbb{P}(V_{\mathfrak{E}} < \eta_{\gamma, \mathfrak{E}} | X, D, R = 1) \right] - \mathbb{P}(R = 0) \cdot (1 - \gamma) \\ &= \frac{\mathbb{P}(R = 0)}{\mathbb{P}(R = 1)} \mathbb{E} \left[R \cdot \frac{f(X, D | R = 0)}{f(X, D | R = 1)} \cdot \mathbb{1}_{\{V_{\mathfrak{E}} < \eta_{\gamma, \mathfrak{E}}\}} \right] - \mathbb{P}(R = 0) \cdot (1 - \gamma) \tag{C6} \\ &= \frac{\mathbb{P}(R = 0)}{\mathbb{P}(R = 1)} \cdot \mathbb{P}(R = 1) \cdot \mathbb{E} \left[\frac{f(X, D | R = 0)}{f(X, D | R = 1)} \cdot \mathbb{1}_{\{V_{\mathfrak{E}} < \eta_{\gamma, \mathfrak{E}}\}} | R = 1 \right] - \mathbb{P}(R = 0) \cdot (1 - \gamma) \\ &= \mathbb{P}(R = 0) \cdot \mathbb{E} \left[\frac{f(X, D | R = 0)}{f(X, D | R = 1)} \cdot \mathbb{1}_{\{V_{\mathfrak{E}} < \eta_{\gamma, \mathfrak{E}}\}} | R = 1 \right] - \mathbb{P}(R = 0) \cdot (1 - \gamma).\end{aligned}$$

This completes the proof of Equation (C5.2).

Thus, we have

$$\mathbb{P}(V_{\mathfrak{E}} < \eta_{\gamma, \mathfrak{E}} | R = 0) = 1 - \gamma + \frac{\mathbb{E} [\psi_{\mathfrak{E}} (\eta_{\gamma, \mathfrak{E}}, X; m_{\mathfrak{E}}, \pi_R)]}{\mathbb{P}(R = 0)}.$$

C.5.2 Proof of Lemma C.1

Lemma C.1. *Under regularity conditions (A1) and (A2), there exists a universal constant C_0 such that for any $\delta > 0$,*

$$\mathbb{P} \left(|\mathbb{I}| \leq C_0 \frac{\pi_0^{-1}(1 + m_0)}{\mathbb{P}(R = 0)} \sqrt{\frac{\log(1/\delta) + 1}{|\mathcal{J}_2|}} \mid \mathcal{J}_1 \right) \geq 1 - \delta.$$

Proof of Lemma C.1. The proof is adapted from Theorem 3 of Yang et al. (2024) and Lemma A.1 from Gao et al. (2025). Without loss of generality, assume the indexes in \mathcal{J}_2 is $1, \dots, N$, with $N := |\mathcal{J}_2|$.

We can expand $\mathbb{P}_{\mathcal{J}_2} [\psi_{\mathfrak{C}}(\hat{\eta}_{\gamma, \mathfrak{C}}, X; \hat{m}_{\mathfrak{C}}, \hat{\pi}_R)] - \mathbb{E} [\psi_{\mathfrak{C}}(\hat{\eta}_{\gamma, \mathfrak{C}}, X; \hat{m}_{\mathfrak{C}}, \hat{\pi}_R)]$ into three parts.

$$\begin{aligned}
& \mathbb{P}_{\mathcal{J}_2} [\psi_{\mathfrak{C}}(\hat{\eta}_{\gamma, \mathfrak{C}}, X; \hat{m}_{\mathfrak{C}}, \hat{\pi}_R)] - \mathbb{E} [\psi_{\mathfrak{C}}(\hat{\eta}_{\gamma, \mathfrak{C}}, X; \hat{m}_{\mathfrak{C}}, \hat{\pi}_R)] \\
&= \frac{1}{N} \sum_{i=1}^N \frac{R}{\hat{\pi}_R(X_i, D_i)} \mathbb{1}_{\{V_{\mathfrak{C}, i} < \eta_{\gamma, \mathfrak{C}}\}} - \mathbb{E} \left[\frac{R}{\hat{\pi}_R(X_i, D_i)} \mathbb{1}_{\{V_{\mathfrak{C}, i} < \eta_{\gamma, \mathfrak{C}}\}} \right] \\
&+ \frac{1}{N} \sum_{i=1}^N \left((1-R) - \frac{R}{\hat{\pi}_R(X_i, D_i)} \hat{m}_{\mathfrak{C}}(\eta_{\gamma, \mathfrak{C}}, X_i, D_i) \right) - \mathbb{E} \left[(1-R) - \frac{R}{\hat{\pi}_R(X_i, D_i)} \hat{m}_{\mathfrak{C}}(\eta_{\gamma, \mathfrak{C}}, X_i, D_i) \right] \\
&+ (1-\gamma) \left[\frac{1}{N} \sum_{i=1}^N (1-R) - \mathbb{P}(R=0) \right] \\
&=: \mathfrak{R}_1(\eta_{\gamma, \mathfrak{C}}) + \mathfrak{R}_2(\eta_{\gamma, \mathfrak{C}}) + \mathfrak{R}_3(\eta_{\gamma, \mathfrak{C}}),
\end{aligned}$$

where these three terms will be controlled separately. For $\mathfrak{O}_i = (X_i, Y_i, D_i, R_i)$, $i \in \mathcal{J}_2$ and any function $f : \mathbb{R}^{d+3} \rightarrow \mathbb{R}$, define

$$\mathbb{G}_N f = \frac{1}{\sqrt{N}} \sum_{i=1}^N [f(\mathfrak{O}_i) - \mathbb{E}[f(\mathfrak{O}_i)]]$$

Bound on $\sup_{\eta_{\gamma, \mathfrak{C}}} |\mathfrak{R}_1(\eta_{\gamma, \mathfrak{C}})|$: We define a class of functions \mathfrak{F}_1 :

$$\mathfrak{F} := \left\{ f : f_{\eta} = \frac{R}{\pi_R(X, D)} \mathbb{1}_{\{V_{\mathfrak{C}} < \eta_{\gamma, \mathfrak{C}}\}}, \forall \eta \in \mathbb{R} \right\}.$$

Notice that $\forall f_{\eta} \in \mathfrak{F}$, we have $|f_{\eta}| \leq R\pi_0^{-1} \mathbb{1}_{\{V_{\mathfrak{C}} < \eta_{\gamma, \mathfrak{C}}\}}$. Therefore, $F(w) := R\pi_0^{-1}$ is an envelope function of \mathfrak{F} . Let $\|\cdot\|_{\mathfrak{F}}$ denote the supremum norm over the class \mathfrak{F} , i.e., $\|z\|_{\mathfrak{F}} = \sup_{f \in \mathfrak{F}} |z(f)|$.

Applying Lemma C.2 with $s(r, x) = \frac{R}{\hat{\pi}_R(X, D)}$ and $h(x, y) = V_{\mathfrak{C}}$ gives

$$\mathbb{E} \|\mathbb{G}_N\|_{\mathfrak{F}} \leq \mathfrak{C}_1 \pi_0^{-1},$$

where \mathfrak{C}_1 is a universal constant. Applying McDiarmid's inequality, we have

$$\mathbb{P}(\|\mathbb{G}_N\|_{\mathfrak{F}} - \mathbb{E}\|\mathbb{G}_N\|_{\mathfrak{F}} \geq t) \leq 2 \exp\left(-\frac{2t^2}{\sum_{i=1}^N c_i^2}\right) \leq 2 \exp\left(-\frac{2t^2}{\sum_{i=1}^N 4\pi_0^{-2}/N}\right) = \exp\left(-\frac{t^2}{2\pi_0^{-2}}\right), \quad (\text{C7})$$

where

$$c_i \leq \sup_{\theta, \theta'} \sup_{\eta} \sqrt{N} \left| \frac{1}{N} \frac{R_i}{\hat{\pi}_R(X_i, D_i)} \mathbb{1}_{\{V_{\mathbb{E}, i} < \eta\}} - \frac{1}{N} \frac{R'_i}{\hat{\pi}_R(X'_i, D'_i)} \mathbb{1}_{\{V_{\mathbb{E}, i'} < \eta\}} \right| \leq \frac{2\pi_0^{-1}}{\sqrt{N}}$$

Substituting into Equation (C7), we have

$$\mathbb{P} \left(\|\mathbb{G}_N\|_{\mathcal{F}} \geq C_2 \pi_0^{-1} \sqrt{1 + \log \left(\frac{1}{\delta} \right)} \right) \leq \delta, \quad (\text{C8})$$

for an absolute constant C_2 .

Bound on $\sup_{\eta_{\gamma, \mathbb{E}}} |\mathcal{R}_2(\eta_{\gamma, \mathbb{E}})|$: similar to the above, we define a class of functions \mathcal{F} : $\mathcal{F} := \left\{ f_{\eta} : f_{\eta} = \left[(1 - R) - \frac{R}{\hat{\pi}_R(X, D)} \right] \right\}$ where

$$\begin{aligned} f_{\eta} &= \left[(1 - R) - \frac{R}{\hat{\pi}_R(X, D)} \right] \cdot \hat{m}_{\mathbb{E}}(\eta_{\gamma, \mathbb{E}}, X, D) \\ &= \left[(1 - R) - \frac{R}{\hat{\pi}_R(X, D)} \right] \int_0^{m_0} \mathbb{1}_{\{\hat{m}_{\mathbb{E}}(\eta_{\gamma, \mathbb{E}}, X, D) \geq u\}} du \\ &= \int_0^{m_0} \left[(1 - R) - \frac{R}{\hat{\pi}_R(X, D)} \right] \mathbb{1}_{\{\eta_{\gamma, \mathbb{E}} \geq h(X, u)\}} du, \end{aligned}$$

where the second equality is from the monotonicity of $\hat{m}_{\mathbb{E}}(\eta_{\gamma, \mathbb{E}}, X, D)$ in $\eta_{\gamma, \mathbb{E}}$. Then,

$$\begin{aligned} \sup_{\eta} |\mathbb{G}_N f| &= \sup_{\eta} \left| \mathbb{G}_N \left[\int_0^{m_0} \left[(1 - R) - \frac{R}{\hat{\pi}_R(X, D)} \right] \mathbb{1}_{\{\eta_{\gamma, \mathbb{E}} \geq h(X, u)\}} du \right] \right| \\ &\leq \int_0^{m_0} \sup_{\eta} \left| \mathbb{G}_N \left[\left[(1 - R) - \frac{R}{\hat{\pi}_R(X, D)} \right] \mathbb{1}_{\{\eta_{\gamma, \mathbb{E}} \geq h(X, u)\}} \right] \right| du \end{aligned}$$

Therefore, taking expectation on both sides and applying Lemma C.2, we have

$$\mathbb{E} \|\mathbb{G}_N\|_{\mathcal{F}} \lesssim \int_0^{m_0} \mathfrak{C}_2 \pi_0^{-1} du \lesssim \mathfrak{C}_2 m_0 \pi_0^{-1}.$$

By McDiarmid's inequality, we have

$$\mathbb{P} (\|\mathbb{G}_N\|_{\mathcal{F}} - \mathbb{E} \|\mathbb{G}_N\|_{\mathcal{F}} \geq t) \leq \exp \left(-\frac{2t^2}{\sum_{i=1}^N c_i^2} \right) \leq \exp \left(-\frac{2t^2}{\sum_{i=1}^N 4\pi_0^{-2} m_0^2 / N} \right) = \exp \left(\frac{-t^2}{2\pi_0^{-2} m_0^2} \right), \quad (\text{C9})$$

where

$$c_i := \sup_{\theta, \theta'} \sup_{\eta} \sqrt{N} \left| \frac{1}{N} \left[(1 - R_i) - \frac{R_i}{\hat{\pi}_R(X_i, D_i)} \right] \hat{m}_{\mathcal{E}}(\eta, X_i, D_i) - \frac{1}{N} \left[(1 - R'_i) - \frac{R'_i}{\hat{\pi}_R(X'_i, D'_i)} \right] \hat{m}_{\mathcal{E}}(\eta, X'_i, D'_i) \right|$$

$$\leq \frac{2m_0\pi_0^{-1}}{\sqrt{N}}.$$

Substituting into Equation (C9), we have

$$\mathbb{P} \left(\|\mathbb{G}_N\|_{\mathcal{F}} \geq C_3 m_0 \pi_0^{-1} \sqrt{1 + \log \left(\frac{1}{\delta} \right)} \right) \leq \delta, \quad (\text{C10})$$

for an absolute constant C_3 .

Bound on $\sup_{\eta_{\gamma, \mathcal{E}}} |\mathcal{R}_3(\eta_{\gamma, \mathcal{E}})|$: Since the random variables R_i is i.i.d, applying Hoeffding's inequality gives

$$\mathbb{P} \left(\frac{1}{N} \sum_{i=1}^N (1 - R_i) - \mathbb{P}(R_i = 0) \geq t \right) \leq \exp \left(-\frac{2t^2}{N} \right),$$

which implies that

$$\mathbb{P} \left(\mathcal{R}_3 \geq (1 - \gamma) \sqrt{\frac{1}{2N} \log \left(\frac{1}{\delta} \right)} \right) \leq \delta. \quad (\text{C11})$$

Combining the bounds in Equations (C8), (C10) and (C11) using the union bound, we have that for $\delta > 0$, there exists a universal constant C_0 such that

$$\sup_{\eta} |\mathcal{R}_1(\eta_{\gamma, \mathcal{E}}) + \mathcal{R}_2(\eta_{\gamma, \mathcal{E}}) + \mathcal{R}_3(\eta_{\gamma, \mathcal{E}})| \lesssim C_0 \pi_0^{-1} (1 + m_0) \sqrt{\frac{\log(1/\delta) + 1}{|\mathcal{J}_2|}}$$

with probability at least $1 - \delta$.

□

C.5.3 Additional Lemmas

Lemma C.2 (Lemma 8 of [Yang et al. \(2024\)](#)). *There exists a universal constant $\mathfrak{C} < \infty$ such that for any functions $s(t, x) \in [-\kappa_0, \kappa_0]$ and $h(x, y)$.*

$$\mathbb{E} \left[\sup_{\eta} |\mathbb{G}_N \left[s(r, x) \mathbb{1}_{\{h(x, y) \leq \eta\}} \right]| \right] \leq \mathfrak{C} \kappa_0.$$

D Algorithms

D.1 Interval Estimates for ITE with Attrition by Semiparametric Efficient Estimator

Algorithm D.1 Interval Estimates for ITE with Attrition by Semiparametric Efficient Estimator

Input: Level α , level γ , data $\mathcal{F} \equiv (X_i, Y_i, D_i, R_i)_{i=1}^n$, function $\hat{q}_\beta(x; \mathcal{D})$ to fit β -th conditional quantile, functions $\hat{\pi}_D(x; \mathcal{D})$, $\hat{e}_R(x, d; \mathcal{D})$, and $\hat{\pi}_R(x, d; \mathcal{D})$ to fit the propensity score at x (and d), function $\hat{m}(t, W; \mathcal{D})$ to fit the conditional CDF at t , $\hat{h}^L(x; \mathcal{D})$, $\hat{h}^R(x; \mathcal{D})$ to fit the conditional mean using \mathcal{D} as data, efficient influence functions ψ_d and $\psi_{\mathcal{C}}$ to identify the threshold of nonconformity score.

Step I: Data splitting

- 1: Split the data into three folds: a pretraining fold \mathcal{F}_{pr} , a training fold \mathcal{F}_{tr} , and a calibration fold \mathcal{F}_{ca} .
- 2: Split the training fold into two subfolds $\mathcal{F}_{\text{tr},1}$ and $\mathcal{F}_{\text{tr},2}$.

Step II: Conformal Inference for Counterfactuals

- 1: For each $i \in \mathcal{F}_{\text{tr}} \cup \mathcal{F}_{\text{ca}}$ with $R_i = 1$, compute the nonconformity score following CQR: $V_i = \max \{ \hat{q}_{\alpha_{\text{lo}}}(X_i; \mathcal{F}_{\text{pr}}) - Y_i, Y_i - \hat{q}_{\alpha_{\text{hi}}}(X_i; \mathcal{F}_{\text{pr}}) \}$.
- 2: For each $i \in \mathcal{F}_{\text{tr},1}$, obtain an initial estimator of the threshold $\hat{\eta}_{\alpha,d}^{\text{init}}$.
- 3: For each $i \in \mathcal{F}_{\text{tr},2}$, train the conditional CDF $\hat{m}(\hat{\eta}_{\alpha,d}^{\text{init}}, X)$.
- 4: **for** $i \in \mathcal{F}_{\text{ca}}$ with $D_i = 1$ **do**
- 5: Identify $\hat{\eta}_{\alpha,0}$ by solving the eif ψ_0 using $\hat{\pi}_D(X_i; \mathcal{F}_{\text{pr}})$, $\hat{e}_R(X_i, D_i = 1; \mathcal{F}_{\text{pr}})$, and $\hat{m}(\hat{\eta}_{\alpha,1}^{\text{init}}, X_i, R_i = 1, D_i = 1; \mathcal{F}_{\text{tr},2})$ as s.
- 6: Construct $\mathcal{C}_0(x) = [\hat{Y}_i^L(0), \hat{Y}_i^R(0)] = [\hat{q}_{\alpha_{\text{lo}}}(X_i; \mathcal{F}_{\text{pr}}) - \hat{\eta}_{\alpha,0}, \hat{\eta}_{\alpha,0} - \hat{q}_{\alpha_{\text{hi}}}(X_i; \mathcal{F}_{\text{pr}})]$.
- 7: Compute $\mathcal{C}_{\text{ITE}} = [Y_i(1) - \hat{Y}_i^R(0), Y_i(1) - \hat{Y}_i^L(0)]$.
- 8: **end for**
- 9: **for** $i \in \mathcal{F}_{\text{ca}}$ with $D_i = 0$ **do**
- 10: Identify $\hat{\eta}_{\alpha,1}$ by solving the eif ψ_1 using $\hat{\pi}_D(X_i; \mathcal{F}_{\text{pr}})$, $\hat{e}_R(X_i, D_i = 0; \mathcal{F}_{\text{pr}})$, and $\hat{m}(\hat{\eta}_{\alpha,0}^{\text{init}}, X_i, R_i = 1, D_i = 0; \mathcal{F}_{\text{tr},2})$ as s.
- 11: Construct $\mathcal{C}_1(x) = [\hat{Y}_i^L(1), \hat{Y}_i^R(1)] = [\hat{q}_{\alpha_{\text{lo}}}(X_i; \mathcal{F}_{\text{pr}}) - \hat{\eta}_{\alpha,1}, \hat{\eta}_{\alpha,1} - \hat{q}_{\alpha_{\text{hi}}}(X_i; \mathcal{F}_{\text{pr}})]$.
- 12: Compute $\mathcal{C}_{\text{ITE}} = [\hat{Y}_i^L(1) - Y_i(0), \hat{Y}_i^R(1) - Y_i(0)]$.
- 13: **end for**

Step III: Interval estimates of ITE on the target data with attrition.

- 1: Take $\mathcal{F}_{\text{ca}} \equiv (X_i, Y_i, D_i, R_i, \mathcal{C}_i)$ with $R_i = 1$ and $\mathcal{C}_i = [\mathcal{C}_i^L, \mathcal{C}_i^R]$ as the observed data. Take \mathcal{F}_{att} from \mathcal{F} with $R_i = 0$ as the attrition data.
- 2: Split $\mathcal{F}_{\text{ca}} \equiv \mathcal{F}_{\text{obs}}$ into two folds $\mathcal{F}_{\text{obstr}}$ and $\mathcal{F}_{\text{obsca}}$.
- 3: For each $i \in \mathcal{F}_{\text{obs}}$, compute score $V_i = \max \{ \hat{h}^L(X_i; \mathcal{F}_{\text{obstr}}) - \mathcal{C}_i^L, \mathcal{C}_i^R - \hat{h}^R(X_i; \mathcal{F}_{\text{obstr}}) \}$.
- 4: For each $i \in \mathcal{F}_{\text{obsca}} \cup \mathcal{F}_{\text{att}}$, identify $\hat{\eta}_{\gamma,\mathcal{C}}$ by solving the eif $\psi_{\mathcal{C}}$ using $\hat{\pi}_R(X_i, D_i; \mathcal{F}_{\text{obstr}})$, and $\hat{m}_{\mathcal{C}}(\hat{\eta}_{\gamma,\mathcal{C}}, X_i, D_i; \mathcal{F}_{\text{obstr}})$ as s.

Output: $\check{\mathcal{C}}_{\text{ITE}}(x) = [\hat{h}^L(x; \mathcal{F}_{\text{obstr}}) - \hat{\eta}_{\gamma,\mathcal{C}}, \hat{h}^R(x; \mathcal{F}_{\text{obstr}}) + \hat{\eta}_{\gamma,\mathcal{C}}]$.

D.2 Weighted Split Conformalized Quantile Regression

Algorithm D.2 Weighted Split CQR

Input: Level α , data $\mathcal{D} \equiv (X_i, Y_i)_{i \in \mathcal{J}}$, testing point x , function $\hat{q}_\tau(x; \mathcal{D})$ to estimate the conditional quantile τ and function $w(x; \mathcal{D})$ to estimate the weight at x using \mathcal{D} as the data.

Procedure:

- 1: Split the data \mathcal{D} into a training set $\mathcal{D}_{\text{tr}} \equiv (X_i, Y_i)_{i \in \mathcal{J}_{\text{tr}}}$ and a calibration set $\mathcal{D}_{\text{ca}} \equiv (X_i, Y_i)_{i \in \mathcal{J}_{\text{ca}}}$.
- 2: For each $i \in \mathcal{J}_{\text{ca}}$, compute the score $S_i = \max \{ \hat{q}_{\alpha_{\text{lo}}}(X_i; \mathcal{D}_{\text{tr}}) - Y_i, Y_i - \hat{q}_{\alpha_{\text{hi}}}(X_i; \mathcal{D}_{\text{tr}}) \}$.
- 3: For each $i \in \mathcal{J}_{\text{ca}}$, compute the weight $W_i = \hat{w}(X_i, \mathcal{D}_{\text{tr}})$.
- 4: Compute the normalized weights $\hat{p}_i(x) = \frac{W_i}{\sum_{i \in \mathcal{J}_{\text{ca}}} W_i + \hat{w}(x; \mathcal{D}_{\text{tr}})}$ and $\hat{p}_\infty(x) = \frac{\hat{w}(x; \mathcal{D}_{\text{tr}})}{\sum_{i \in \mathcal{J}_{\text{ca}}} W_i + \hat{w}(x; \mathcal{D}_{\text{tr}})}$.
- 5: Compute $\eta(x)$ as the $\left[(1 - \alpha) \frac{|\mathcal{J}_{\text{ca}}| + 1}{|\mathcal{J}_{\text{ca}}|} \right]$ -th quantile of the distribution $\sum_{i \in \mathcal{J}_{\text{ca}}} \hat{p}_i(x) \delta_{S_i} + \hat{p}_\infty(x) \delta_\infty$.

Output: Prediction interval $\mathcal{C}(x) = [\hat{q}_{\alpha_{\text{lo}}}(x; \mathcal{D}_{\text{tr}}) - \eta(x), \hat{q}_{\alpha_{\text{hi}}}(x; \mathcal{D}_{\text{tr}}) + \eta(x)]$.

D.3 Unweighted Conformal Inference for Interval Outcomes

Algorithm D.3 Unweighted Conformal Inference for Interval Outcomes

Input: Level γ , data $\mathcal{D} \equiv (X_i, \mathcal{C}_i)_{i \in \mathcal{J}}$ where $\mathcal{C}_i = [\mathcal{C}_i^L, \mathcal{C}_i^R]$, testing point x , functions $\hat{m}^L(x; \mathcal{D})$ and $\hat{m}^R(x; \mathcal{D})$ to fit the conditional mean/median of $\mathcal{C}_i^L, \mathcal{C}_i^R$ using \mathcal{D} as the data.

Procedure:

- 1: Split the data \mathcal{D} into a training set $\mathcal{D}_{\text{tr}} \equiv (X_i, \mathcal{C}_i)_{i \in \mathcal{J}_{\text{tr}}}$ and a calibration set $\mathcal{D}_{\text{ca}} \equiv (X_i, \mathcal{C}_i)_{i \in \mathcal{J}_{\text{ca}}}$.
- 2: For each $i \in \mathcal{J}_{\text{ca}}$, compute the score $S_i = \max \{ \hat{m}^L(x; \mathcal{D}_{\text{tr}}) - \mathcal{C}_i^L, \mathcal{C}_i^R - \hat{m}^R(x; \mathcal{D}_{\text{tr}}) \}$.
- 3: Compute η as the $\left[(1 - \gamma) \frac{|\mathcal{J}_{\text{ca}}| + 1}{|\mathcal{J}_{\text{ca}}|} \right]$ -th quantile of the empirical distribution $\{S_i : i \in \mathcal{J}_{\text{ca}}\}$.

Output: $\check{\mathcal{C}}_{\text{ITE}} = [\hat{m}^L(x; \mathcal{D}_{\text{tr}}) - \eta, \hat{m}^R(x; \mathcal{D}_{\text{tr}}) + \eta]$.

D.4 Interval Estimates for ITE with Attrition

Algorithm D.4 Interval Estimates for ITE with Attrition

Input: Level α , level γ (only for the exact version), source data $\mathcal{X} \equiv (X_i, Y_i, D_i)_{i=1}^n$ without attrition, target data point x with attrition.

Step I: Data splitting

- 1: Split the source data into two folds \mathcal{X}_1 and \mathcal{X}_2 .
- 2: Estimate the propensity score $\hat{e}_D(x)$ on \mathcal{X}_1 .

Step II: Counterfactual Inference on \mathcal{X}_2 .

- 1: **for** i in \mathcal{X}_2 with $D_i = 1$ **do**
- 2: Compute $[\hat{Y}_i^L(0), \hat{Y}_i^R(0)]$ in Algorithm D.2 on \mathcal{X}_1 with level α and $w_0(x) = \frac{\hat{e}_D(x)}{1-\hat{e}_D(x)}$.
- 3: Compute $\mathcal{C}_i = [Y_i(1) - \hat{Y}_i^R(0), Y_i(1) - \hat{Y}_i^L(0)]$.
- 4: **end for**
- 5: **for** i in \mathcal{X}_2 with $D_i = 0$ **do**
- 6: Compute $[\hat{Y}_i^L(1), \hat{Y}_i^R(1)]$ in Algorithm D.2 on \mathcal{X}_1 with level α and $w_1(x) = \frac{1-\hat{e}_D(x)}{\hat{e}_D(x)}$.
- 7: Compute $\mathcal{C}_i = [\hat{Y}_i^L(1) - Y_i(0), \hat{Y}_i^R(1) - Y_i(0)]$.
- 8: **end for**

Step III: Interval estimates of ITE on the target data with attrition.

- 1: (Exact version) Apply Algorithm D.3 on $(X_i, \mathcal{C}_i)_{i \in \mathcal{X}_2}$ with level γ , yielding an interval $\check{\mathcal{C}}_{\text{ITE}}(x)$.
- 2: (Inexact version) Fit conditional quantiles of \mathcal{C}_i^L and \mathcal{C}_i^R , yielding an interval $\check{\mathcal{C}}_{\text{ITE}}(x)$.

Output: $\check{\mathcal{C}}_{\text{ITE}}(x)$.

E Additional Simulation Results

E.1 Simulation Results for Unweighted Conformal Inference for ITE with Attrition

This section provides the simulation results for the unweighted conformal inference for interval outcomes with attrition proposed by (Lei and Candès, 2021).

We use the exact nested method and consider two scenarios with different missingness patterns induced by the attrition: MCAR and MAR. The data generating process (DGP) is as follows: covariate vector $X_i = (X_{i1}, \dots, X_{id})^\top \sim \mathcal{N}(0, \mathbb{I}_d)$ with $d = 5$, independent across i . Given a covariate vector X_i , I generate the potential outcomes as

$$Y_i(1) = X_i^\top \beta + \varepsilon_{i1}, \quad Y_i(0) = \varepsilon_{i0}, \quad \varepsilon_{i1}, \varepsilon_{i0} \stackrel{\text{i.i.d.}}{\sim} \mathcal{N}(0, 1),$$

where $\beta = \mathbf{1}_d$. The treatment assignment is generated following nonlinear propensity score,

$$e_D(X_i) = \Phi(X_{i1}), \quad D_i = \mathbf{1}_{e_D(X_i) < U_i}, \quad U_i \sim \text{UNIF}(0, 1).$$

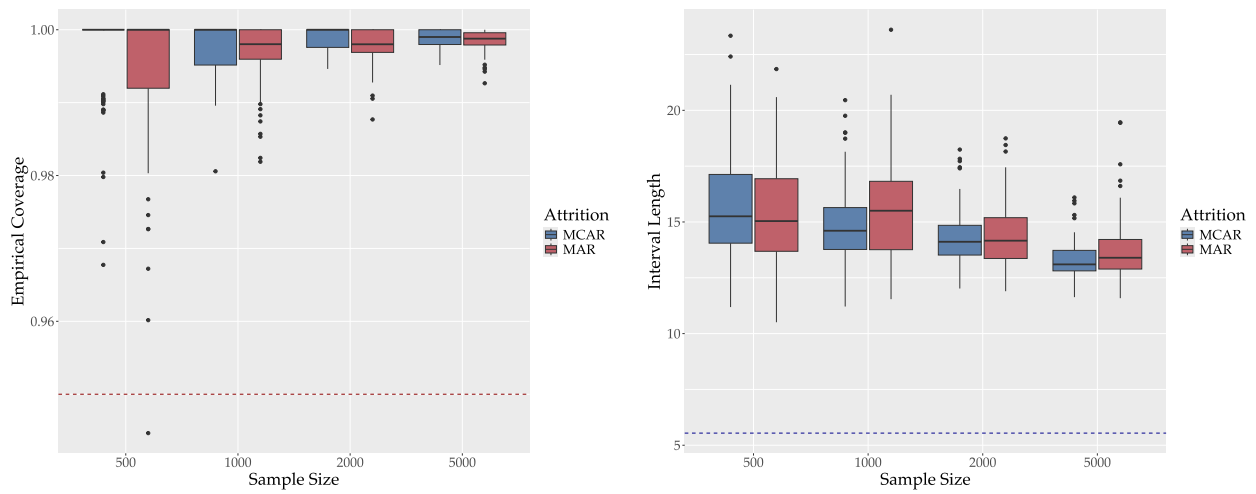
Also, I generate the missingness indicator R separately for two missingness patterns. For MCAR, $R_i \stackrel{\text{i.i.d.}}{\sim} \text{BERN}(p)$ with $p = 0.8$. For MAR, following Assumption 2, R is generated as

$$\text{logit}(P(R_i = 1 \mid D_i, X_i)) = \kappa_0 + \kappa_1 D_i + \kappa_2 X_{i1} + \kappa_3 X_{i2},$$

with parameters set to $(\kappa_0, \kappa_1, \kappa_2, \kappa_3) = (-0.2, 0.5, 0.2, -0.3)$. Following this DGP, the observations are given by the tuple $(X_i, D_i, R_i, R_i \cdot Y_i)$.

I conduct simulations with sample size $n \in \{500, 1000, 2000, 5000\}$ and 100 MC iterations. I compute the average empirical coverage and average interval length of the prediction intervals for ITE in the target group with attrition. The target coverage is set to be 95%. To fit the conditional quantiles, I use the quantile random forest.

FIGURE E.1: UNWEIGHTED CONFORMAL INFERENCE FOR INTERVAL ESTIMATES OF ITE WITH ATTRITION



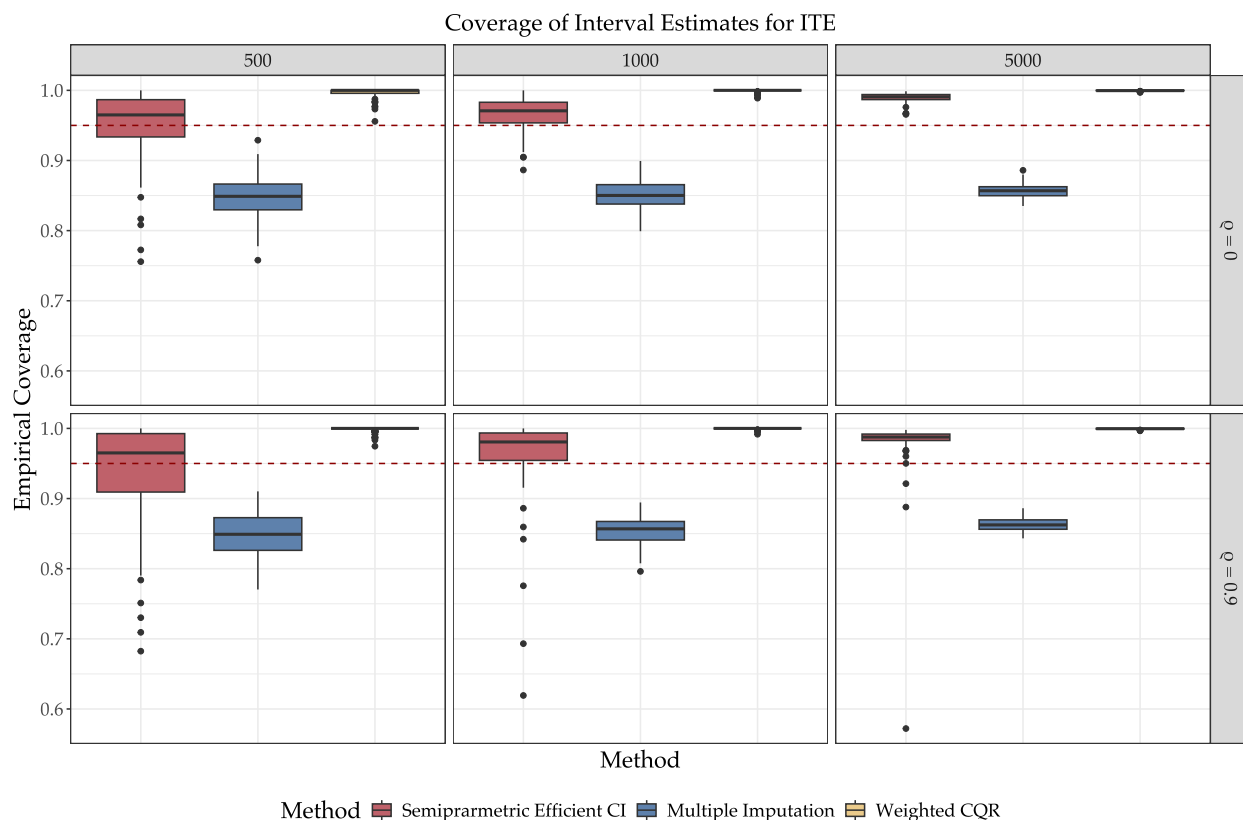
Note: This figure shows the simulation results of Exact method. The left panel shows the average empirical coverage and the right panel shows the average interval length of the prediction intervals for ITE in the target group with attrition. The red horizontal line corresponds to the target coverage of 95% and the blue horizontal line corresponds to the average length of oracle intervals.

E.2 Comparison with Different Multiple Imputation Procedures

Here, we consider two other multiple imputation procedures. The first one still follows the working flow of conformal inference. First, we impute the potential outcomes for the observed group, i.e., use $D = 1 \& R = 1$ to impute the counterfactuals of $D = 0 \& R = 1$, and vice versa. Second, we compute the ITE for the observed group. Third, we impute the ITE for the attrition group. The second one follows a reverse order. First, we impute the attrition group using observed group, i.e., use $D = 1 \& R = 1$ to impute $D = 1 \& R = 0$, and use $D = 0 \& R = 1$ to impute $D = 0 \& R = 0$. Then, we use the treatment group to impute the counterfactuals of the control group, and vice versa.

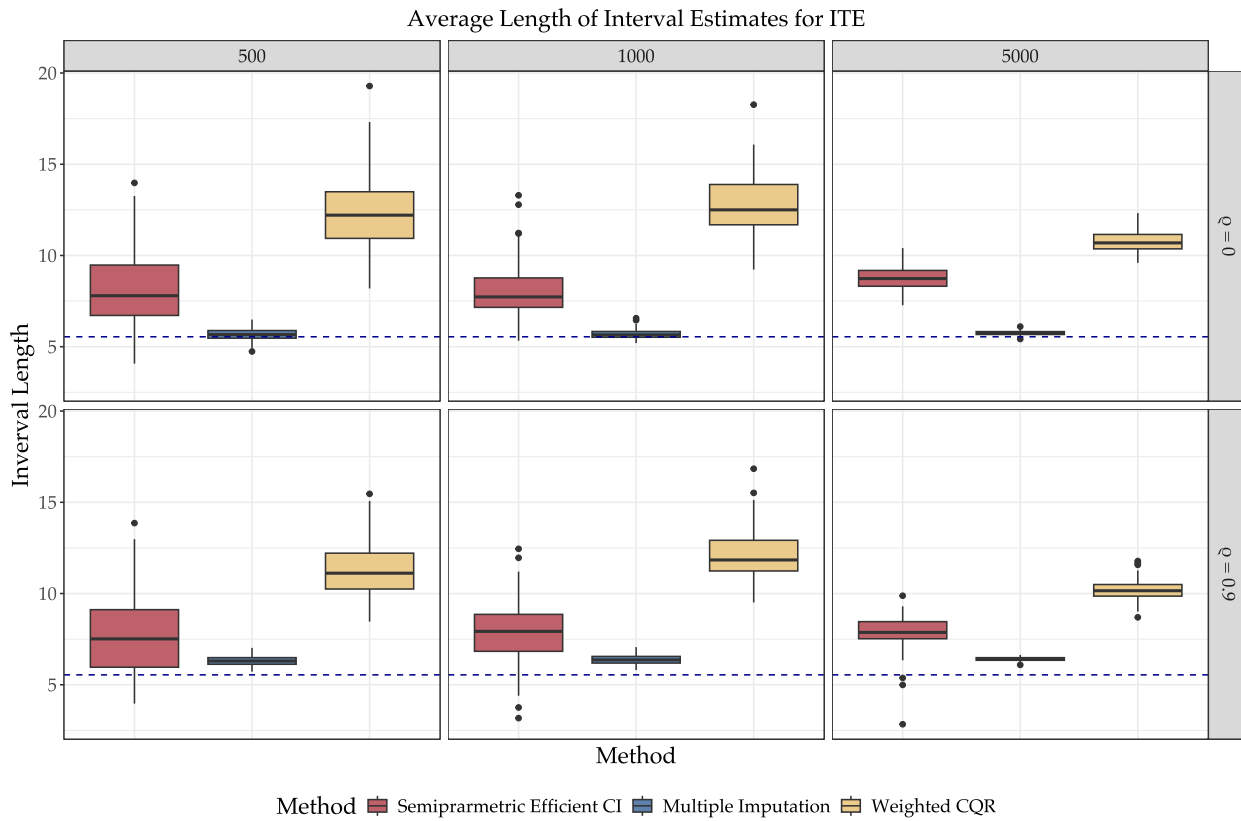
Figure E.2 and Figure E.3 show the comparison among three methods with the second procedure of multiple imputation.

FIGURE E.2: COMPARISON OF EMPIRICAL COVERAGE OF PREDICTION INTERVALS FOR ITE WITH ATTRITION



Note: This figure shows the simulation results for the empirical coverage of prediction intervals constructed by conformal inference with semiparametric efficient estimator, multiple imputation with Amelia, and weighted CQR with unweighted nested approach for ITE of attrition group. The red horizontal line corresponds to the target coverage of 95%.

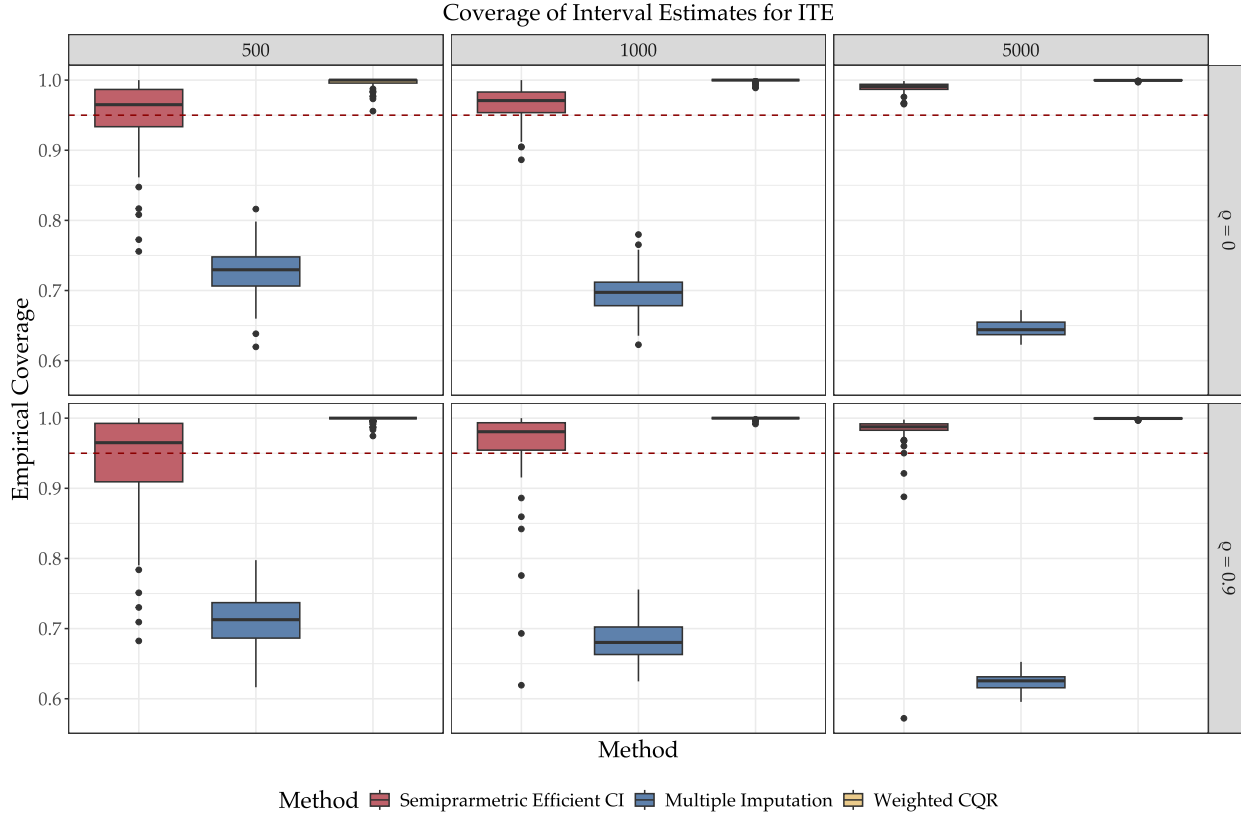
FIGURE E.3: COMPARISON OF AVERAGE LENGTH OF PREDICTION INTERVALS FOR ITE WITH ATTRITION



Note: This figure shows the simulation results for the average length of prediction intervals constructed by conformal inference with semiparametric efficient estimator, multiple imputation with Amelia, and weighted CQR with unweighted nested approach for ITE of attrition group. The red horizontal line corresponds to the length of oracle intervals.

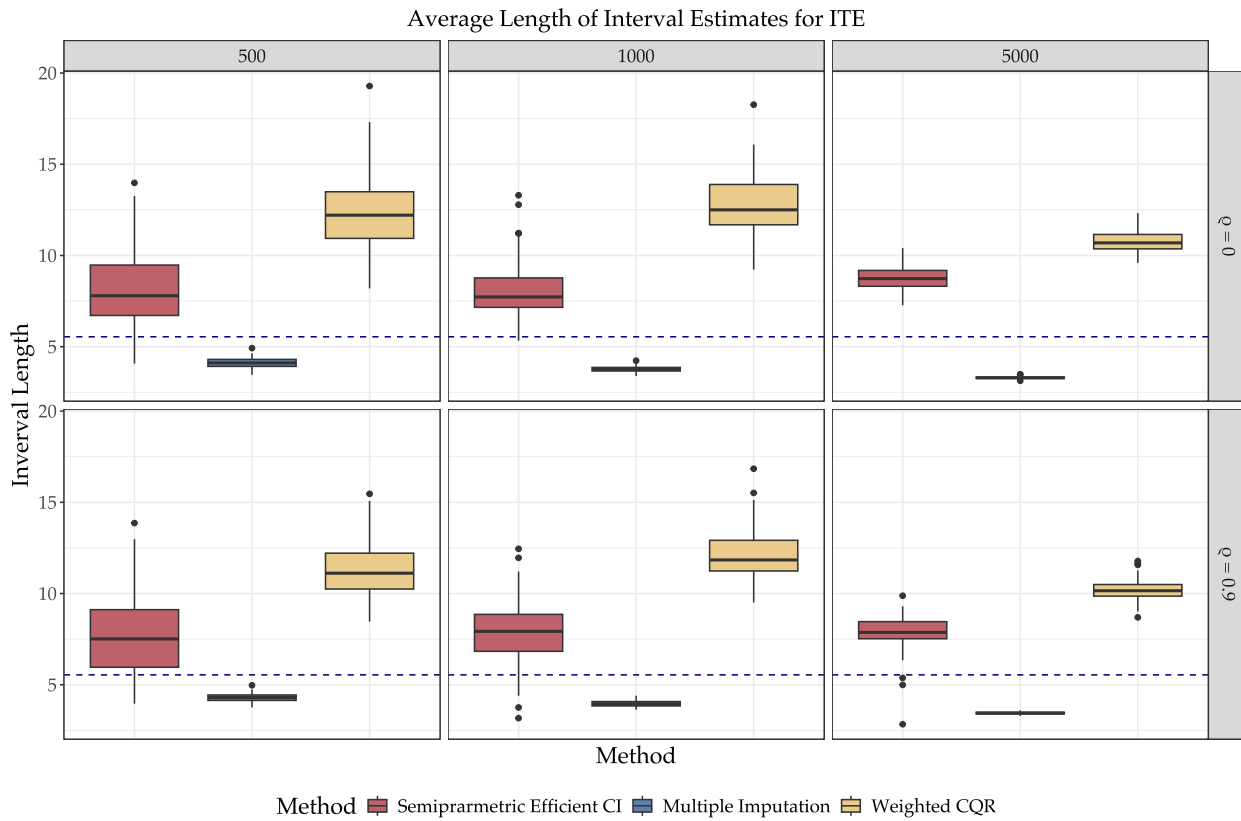
Figure E.4 and Figure E.5 show the comparison among three methods with the third procedure of multiple imputation.

FIGURE E.4: COMPARISON OF EMPIRICAL COVERAGE OF PREDICTION INTERVALS FOR ITE WITH ATTRITION



Note: This figure shows the simulation results for the empirical coverage of prediction intervals constructed by conformal inference with semiparametric efficient estimator, multiple imputation with Amelia, and weighted CQR with unweighted nested approach for ITE of attrition group. The red horizontal line corresponds to the target coverage of 95%.

FIGURE E.5: COMPARISON OF AVERAGE LENGTH OF PREDICTION INTERVALS FOR ITE WITH ATTRITION



Note: This figure shows the simulation results for the average length of prediction intervals constructed by conformal inference with semiparametric efficient estimator, multiple imputation with Amelia, and weighted CQR with unweighted nested approach for ITE of attrition group. The red horizontal line corresponds to the length of oracle intervals.

E.3 Simulation Results with Different DGP

In this section, I consider a different data generating process (DGP) to evaluate the performance of the proposed method. The covariate vector $X = (X_1, \dots, X_d)^\top$ is an equicorrelated multivariate Gaussian vector with mean zero and $\text{Var}(X_i) = 1$ and $\text{Cov}(X_i, X_j) = \rho$ for $i \neq j$. When $\rho = 0$, the covariates are independent. When $\rho > 0$, the covariates are positively correlated. The potential outcomes are generated as follows:

$$\begin{aligned} Y_1 &= X_1^2 + 0.2X_2 + 1/\log(1 + \exp(X_3)) + 0.8\exp(X_4) + \epsilon \\ Y_0 &= 1/\log(1 + \exp(X_3)) + \epsilon, \quad \epsilon \sim \mathcal{N}(0, 1). \end{aligned}$$

We still consider homoscedastic noise. The propensity score of treatment $e_D(X)$ is generated as

$$e_D(X) = \text{logit}^{-1}(-0.5X_1 - 0.3X_2 + 0.2X_3).$$

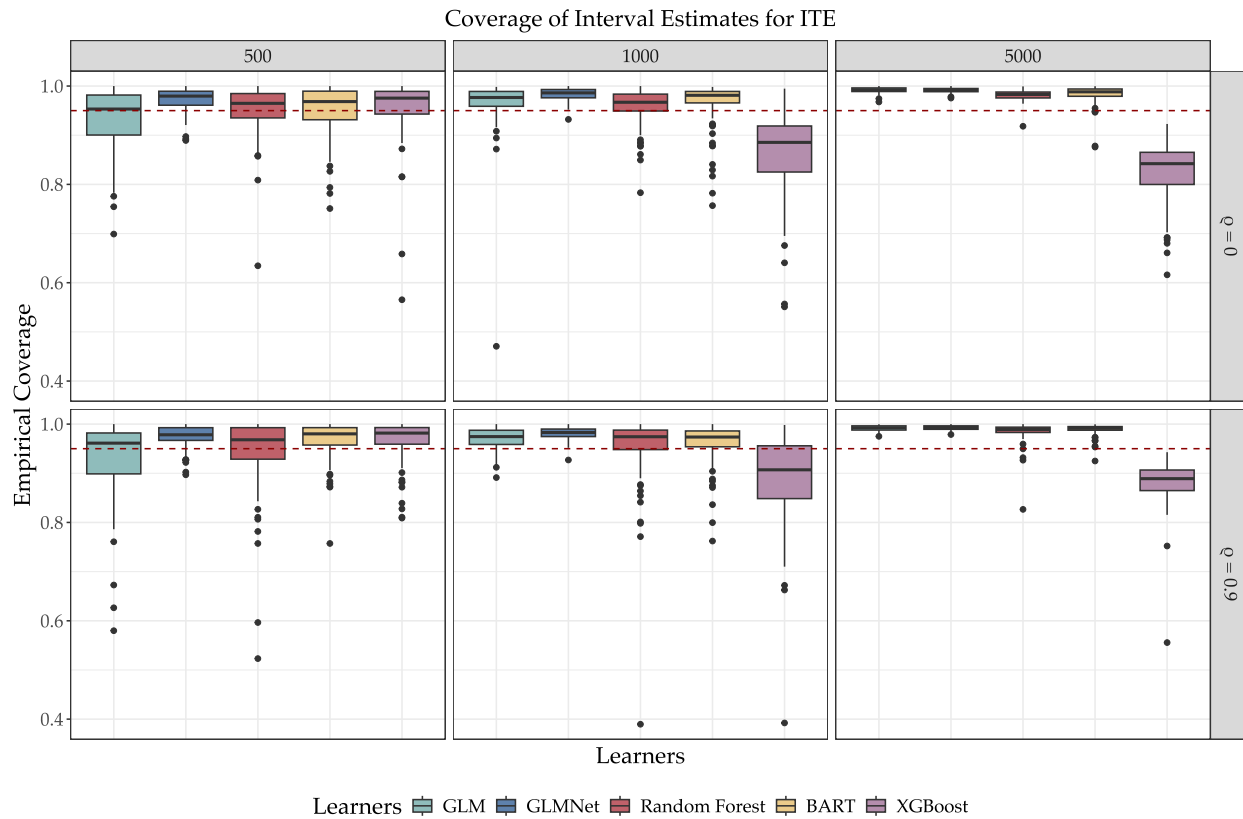
The propensity score of attrition $e_R(X, D)$ is generated as

$$e_R(X, D) = \text{logit}^{-1}(-1 + 0.3D + 0.5X_1 - 0.4X_2),$$

which ensures the MAR assumption. Throughout the simulation, we set the dimension of the covariates $d = 10$.

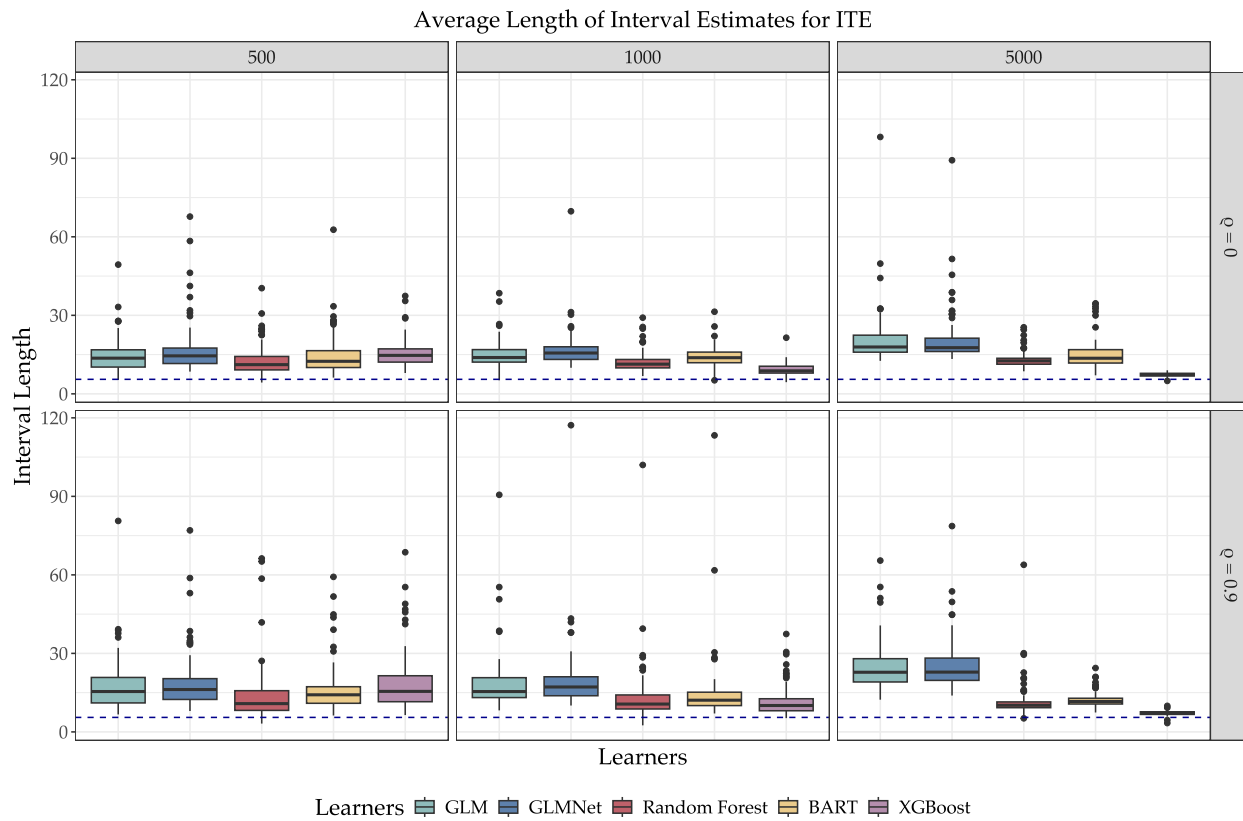
E.3.1 Simulation Results for Conformal Inference with Semiparametric Efficient Estimator

FIGURE E.6: MC SIMULATION RESULTS OF CONFORMAL INFERENCE FOR ITE WITH ATTRITION



Note: This figure shows the simulation results for the empirical coverage of prediction intervals constructed by semi-parametric efficient estimator for ITE of attrition group following DGP2. The red horizontal line corresponds to the target coverage of 95%.

FIGURE E.7: MC SIMULATION RESULTS OF CONFORMAL INFERENCE FOR ITE WITH ATTRITION



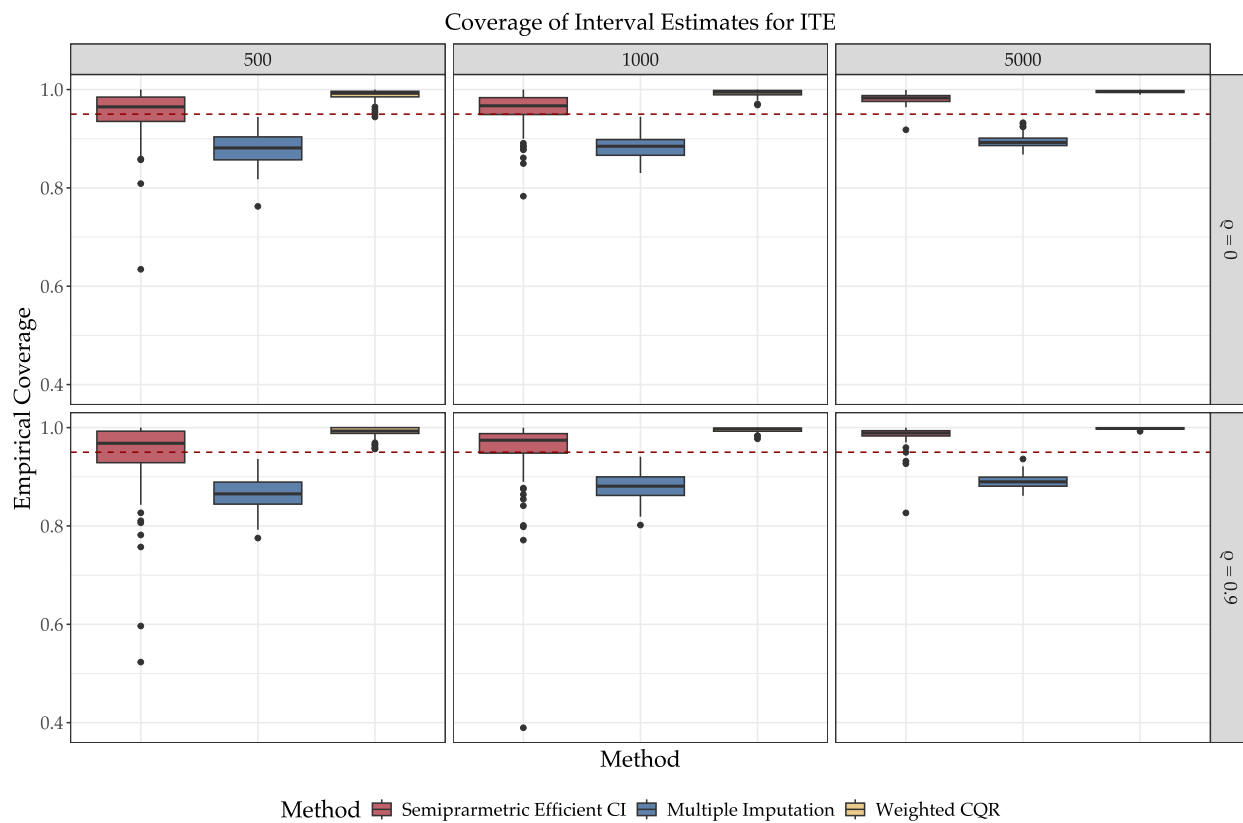
Note: This figure shows the simulation results for the average length of prediction intervals constructed by semiparametric efficient estimator for ITE of attrition group following DGP2. The blue horizontal line corresponds to the length of oracle intervals.

E.3.2 Simulation Results for Comparison with Other Methods

Similar to the second study of Section 7, we compare the empirical coverage and average length of the prediction intervals for ITE with attrition using conformal inference with semiparametric efficient estimator, multiple imputation with Amelia, and weighted CQR with unweighted and nested approach proposed by [Lei and Candès \(2021\)](#).

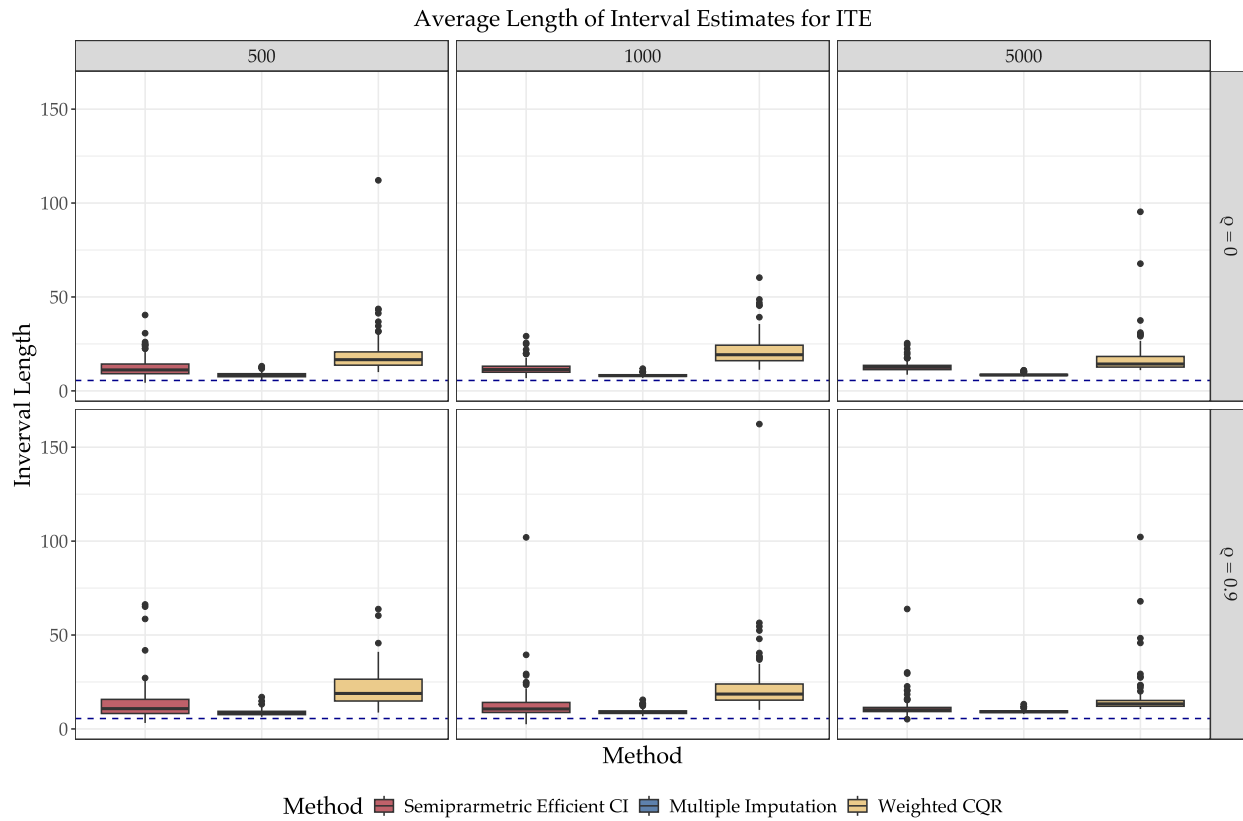
Figure E.10 and Figure E.11 show the comparison among three methods with the first procedure of multiple imputation under the second DGP.

FIGURE E.8: COMPARISON OF EMPIRICAL COVERAGE OF PREDICTION INTERVALS FOR ITE WITH ATTRITION



Note: This figure shows the simulation results for the empirical coverage of prediction intervals constructed by conformal inference with semiparametric efficient estimator, multiple imputation with Amelia, and weighted CQR with unweighted nested approach for ITE of attrition group. The red horizontal line corresponds to the target coverage of 95%.

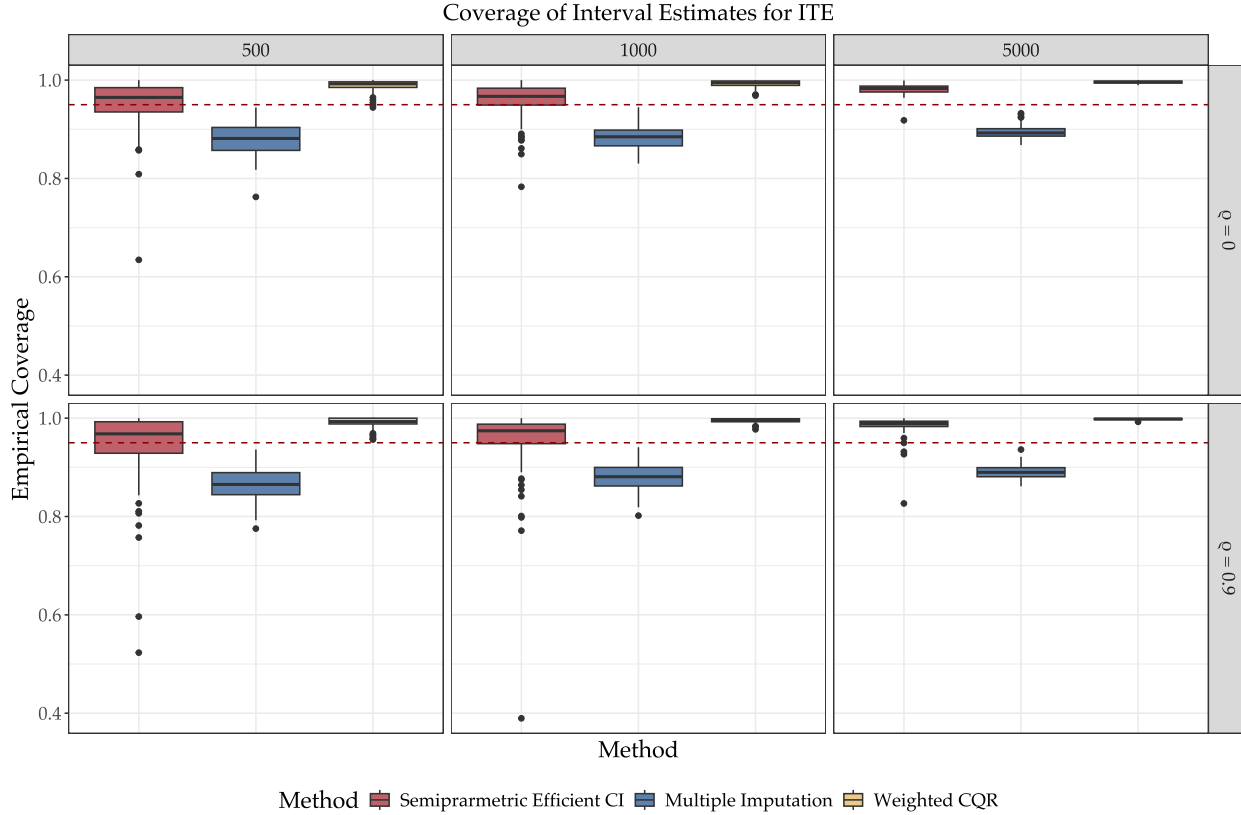
FIGURE E.9: COMPARISON OF AVERAGE LENGTH OF PREDICTION INTERVALS FOR ITE WITH ATTRITION



Note: This figure shows the simulation results for the average length of prediction intervals constructed by conformal inference with semiparametric efficient estimator, multiple imputation with Amelia, and weighted CQR with unweighted nested approach for ITE of attrition group. The red horizontal line corresponds to the length of oracle intervals.

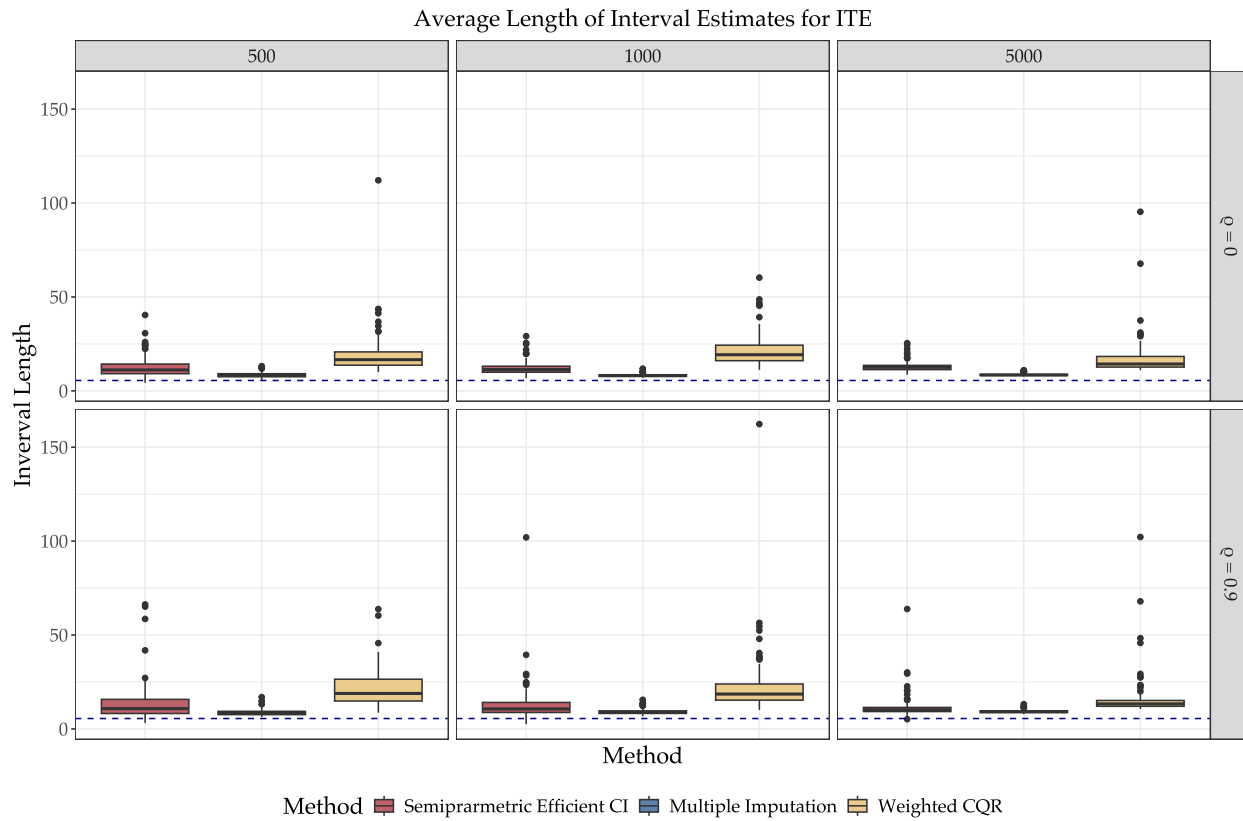
Figure E.10 and Figure E.11 show the comparison among three methods with the second procedure of multiple imputation under the second DGP.

FIGURE E.10: COMPARISON OF EMPIRICAL COVERAGE OF PREDICTION INTERVALS FOR ITE WITH ATTRITION



Note: This figure shows the simulation results for the empirical coverage of prediction intervals constructed by conformal inference with semiparametric efficient estimator, multiple imputation with Amelia, and weighted CQR with unweighted nested approach for ITE of attrition group. The red horizontal line corresponds to the target coverage of 95%.

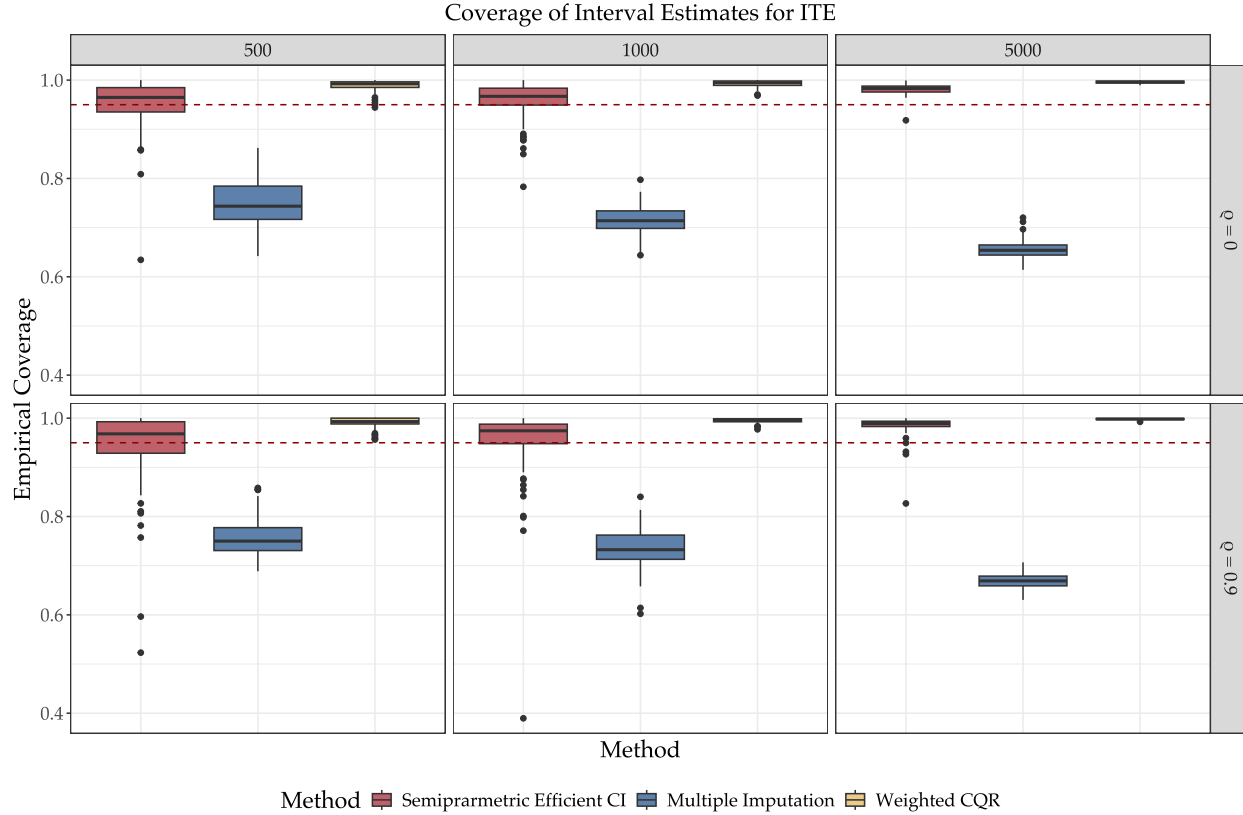
FIGURE E.11: COMPARISON OF AVERAGE LENGTH OF PREDICTION INTERVALS FOR ITE WITH ATTRITION



Note: This figure shows the simulation results for the average length of prediction intervals constructed by conformal inference with semiparametric efficient estimator, multiple imputation with Amelia, and weighted CQR with unweighted nested approach for ITE of attrition group. The red horizontal line corresponds to the length of oracle intervals.

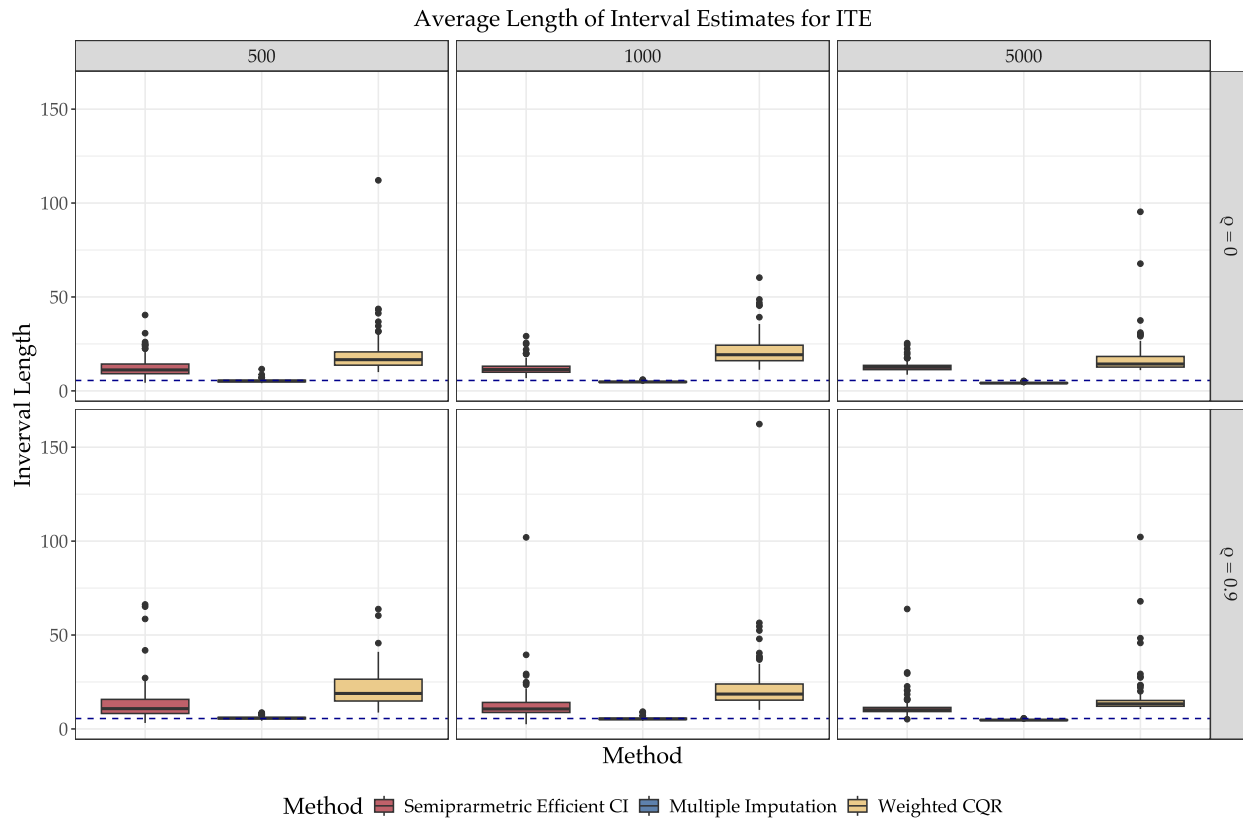
Figure E.12 and Figure E.13 show the comparison among three methods with the third procedure of multiple imputation under the second DGP.

FIGURE E.12: COMPARISON OF EMPIRICAL COVERAGE OF PREDICTION INTERVALS FOR ITE WITH ATTRITION



Note: This figure shows the simulation results for the empirical coverage of prediction intervals constructed by conformal inference with semiparametric efficient estimator, multiple imputation with Amelia, and weighted CQR with unweighted nested approach for ITE of attrition group. The red horizontal line corresponds to the target coverage of 95%.

FIGURE E.13: COMPARISON OF AVERAGE LENGTH OF PREDICTION INTERVALS FOR ITE WITH ATTRITION



Note: This figure shows the simulation results for the average length of prediction intervals constructed by conformal inference with semiparametric efficient estimator, multiple imputation with Amelia, and weighted CQR with unweighted nested approach for ITE of attrition group. The red horizontal line corresponds to the length of oracle intervals.

F Discussion on Replication Results

F.1 Reanalysis of Finkel et al. (2024)

TABLE F.1: BALANCE TEST: OBSERVED VS. ATTRITION GROUPS

Variable	Observed (R = 1)			Attrition (R = 0)			p_value
	Mean_Observed	SD_Observed	N_Observed	Mean_Attrition	SD_Attrition	N_Attrition	
D	0.760	0.427	2203	0.761	0.427	1511	0.932
age	21.529	3.877	2203	21.635	4.131	1511	0.429
ani_2	0.068	0.252	2203	0.082	0.275	1511	0.115
ani_3	0.230	0.421	2203	0.197	0.398	1511	0.015
ani_4	0.326	0.469	2203	0.298	0.457	1511	0.064
ani_5	0.268	0.443	2203	0.289	0.454	1511	0.154
autoc_pref	0.236	0.425	2203	0.255	0.436	1511	0.189
dem_pref	0.585	0.493	2203	0.512	0.500	1511	0.000
educ_new_2	0.108	0.310	2203	0.134	0.341	1511	0.017
educ_new_3	0.245	0.430	2203	0.269	0.443	1511	0.101
educ_new_4	0.393	0.488	2203	0.307	0.461	1511	0.000
educ_new_5	0.213	0.410	2203	0.208	0.406	1511	0.684
employed	0.298	0.458	2203	0.347	0.476	1511	0.002
f_ani_2	0.030	0.171	2203	0.050	0.219	1511	0.002
f_educ_new_2	0.025	0.155	2203	0.034	0.181	1511	0.105
f_polint_new_2	0.044	0.206	2203	0.063	0.243	1511	0.016
female	0.326	0.469	2203	0.361	0.480	1511	0.031
polint_new_2	0.284	0.451	2203	0.249	0.432	1511	0.016
polint_new_3	0.379	0.485	2203	0.349	0.477	1511	0.061
polint_new_4	0.125	0.331	2203	0.156	0.363	1511	0.010
regis_dnw	0.128	0.334	2203	0.162	0.369	1511	0.004
regis_no	0.277	0.448	2203	0.273	0.445	1511	0.754

TABLE F.2: HTE REGRESSION: POLITICAL INTEREST INTERACTIONS

	Authoritarian Support
D	-0.024 (0.024)
polint_new_2	-0.077*** (0.028)
polint_new_3	-0.091*** (0.026)
polint_new_4	-0.087** (0.035)
D × polint_new_2	0.027 (0.032)
D × polint_new_3	0.013 (0.030)
D × polint_new_4	0.088** (0.040)
Intercept	0.324*** (0.021)
Observations	2,203

Note: Standard errors in parentheses. * $p < 0.1$; ** $p < 0.05$; *** $p < 0.01$.